Title
Development of a Simulation Tool to Evaluate the Performance of Radia nt Cooling Ceilings

Authors
Stetiu, C.
Feustel, H.E.
Winkelmann, F.C.

Publication Date
1995-06-01

LBL-37300
UC-1600

Lawrence Berkeley Laboratory
UNIVERSITY OF CALIFORNIA

ENERGY & ENVIRONMENT DIVISION

Development of a Simulation Tool to Evaluate the Performance of Radiant Cooling Ceilings

C. Stetiu, H.E. Feustel, and F.C. Winkelmann

June 1995

ENERGY AND ENVIRONMENT DIVISION

Prepared for the U.S. Department of Energy under Contract Number DE-AC03-76SF00098

Available to DOE and DOE Contractors
from the Office of Scientific and Technical Information
P.O. Box 62, Oak Ridge, TN 37831
Prices available from (615) 576-8401

Available to the public from the
National Technical Information Service
U.S. Department of Commerce
5285 Port Royal Road, Springfield, VA 22161

DISCLAIMER

LBL-37300
UC-1600

Development of a Simulation Tool to Evaluate the Performance of Radiant Cooling Ceilings

Corina Stetiu
Helmut E. Feustel
Frederick C. Winkelmann

Energy and Environment Division
Lawrence Berkeley Laboratory
University of California, Berkeley
Berkeley, CA 94720

CIEE Report, June 1995

This work was funded by the California Institute for Energy Efficiency (CIEE), a research unit of the University of California. Publication of research results does not imply CIEE endorsement or, or agreement with, these findings, nor that of any CIEE sponsor. This work was also supported by the Assistant Secretary for Energy Efficiency and Renewable Energy, Office of Building Technologies, Building Systems Division of the Department of Energy, under contract No. DE-AC03-76SF00098.

Table of Contents

Abstract 1

1. Introduction 2

1.1 Disadvantages of All-Air Systems 2

1.2 The radiant cooling alternative 3

2. Background 4

2.1 Historical Development of Radiant Cooling 4

2.2 Thermal Comfort 5

2.3 Cooling Power 7

2.4 Cooling Performance 8

2.5 Energy Savings 12

2.6 Peak-Power Requirement 13

2.7 Economics 15

2.8 System types 17

2.8.1 The panel system 17

2.8.2 The cooling grid system 19

2.8.3 The core cooling system 22

2.8.4 The raised floor cooling system 23

2.9 Control Issues 23

2.10 Summary 24

3. Problems to be solved 26

4. Approach and Model Evaluation 27

4.1 Approach 27

4.1.1 Target of simulations 27

4.1.2 Extensibility 27

4.2 Model evaluation 28

4.2.1 Comparison with DOE-2 28

4.2.1.1 The test room 28

4.2.1.2 The structure of the walls 29

4.2.1.3 Results 30

4.2.2 Comparison with measured data 34
4.2.2.1 The test room 34
4.2.2.2 Wall composition 35
4.2.2.3 Loads 37
4.2.2.4 System 37
4.2.2.5 Boundary conditions 37
4.2.2.6 Results 38

5. Ceiling Performance 44

5.1 The test room geometry 44

5.2 The structure of the walls 44

5.3 Test room loads 46

5.4 System operation 47

5.5 Time periods for the runs 47

5.6 Results 48

6. Conclusions on performance analysis 57

6.1 RADCOOL provides useful results 57

6.2 Proposed future development of RADCOOL 57

6.2.1 Room air stratification 57
6.2.2 Air humidity, and condensation at cool surfaces 57
6.2.3 Thermal comfort and radiant temperature at the occupant location 57
6.2.4 Heating/cooling sources 58
6.2.5 Sizing 58

7. The Thermal Building Simulation Model RADCOOL 59

7.1 The structure of RADCOOL 59

7.1.1 The role of SPARK 59
7.1.1.1 Preliminary data processing 59
7.1.1.2 Run SPARK 60
7.1.1.3 The output data processing 61
7.1.2 An outline to the requirements for the SPARK part 61
7.1.3 A "quasi perfect" system for RADCOOL 61
7.1.3.1 Introduction 61
7.1.3.2 Units 63

7.2 The SPARK passive elements 64

7.2.1 Unidimensional heat transfer 64
7.2.1.1 The unidimensional heat conduction/storage equations 64

7.2.1.2 The RC approach to solve the heat conduction/storage equations for one solid layer in SPARK 66
7.2.2 The structure of the passive wall in SPARK 66
7.2.2.1 The equations for the temperature nodes in SPARK 68
7.2.2.2 Test to determine the accuracy of the RC wall model 69
7.2.3 Exterior surface radiant heat balance for a wall with thermal mass 72
7.2.3.1 The convective heat flux on the surface of a wall 72
7.2.3.2 The long wave (IR) heat flux exchange between a wall and its exterior surroundings 73
7.2.3.3 The solar radiation incident on the surface of a wall 74
7.2.4 Interior surface radiant heat balance for a wall with thermal mass 75
7.2.4.1 The convective heat flux on the interior surface of a wall 76
7.2.4.2 The IR radiative exchange between a wall and the other room surfaces 77
7.2.4.3 Solar and people/equipment radiation incident on the interior surface of a wall 79
7.2.5 The 4-layer passive underground floor with thermal mass 80
7.2.5.1 Comparison between the floor and the wall with thermal mass 80
7.2.5.2 Exterior surface radiant heat balance for a floor with thermal mass 80
7.2.6 The double-pane window with thermal mass 81
7.2.6.1 Comparison between a window pane and a wall 81
7.2.6.2 Heat conduction/storage for a double-pane window 81
7.2.6.3 The heat balance for the exterior pane of a double-pane window 83
7.2.6.4 The heat balance for the interior pane of a double-pane window 83
7.3 The core cooling ceiling 84
7.3.1 Two-dimensional heat transfer analysis 84
7.3.1.1 The heat conduction/storage equations in two-dimensional 84
7.3.1.2 The RC solution to the two-dimensional heat conduction/storage equations 85
7.3.1.3 The two-dimensional model of the wall in SPARK 86
7.3.1.4 Test to determine the accuracy of the RC model 88
7.3.2 The SPARK model of the core cooling ceiling 90
7.3.2.1 Forced heat convection transfer between water and the pipe walls 91
7.3.2.2 Heat conduction from the pipe to the water, when the water is recirculated 92
7.3.2.3 Heat conduction from the pipe walls to the water, when the water is not flowing 94
7.3.2.4 The two-dimensional model application in the case of a cooled ceiling 94
7.4 The cooling panel 97
7.4.1 The model of the cooling panel 97
7.4.1.1 Cooling panel heat transfer 97
7.4.1.2 Cooling panel heat balance 98
7.5 Radiant cooling system controls 99

7.5.1 Thermostat-based control 99
7.5.2 Timer-based control 100
7.5.3 Hybrid control 101
7.6 The room air 102
7.6.1 The air temperature 102
7.6.2 Discretization of the room air domain in SPARK 103
7.6.3 Room air heat balance 103
7.6.4 Plenum air heat balance 108
7.6.5 Room air moisture balance 109
7.7 Link objects 110
7.8 Preliminary data processing 110
7.8.1 Introduction 110
7.8.2 Weather-related data 111
7.8.2.1 Algorithms to calculate the direct and diffuse solar radiation on a surface 111
7.8.3 Shape factors 114
7.8.3.1 Surface-to-surface shape factors 115
7.8.3.2 Occupant-to-surface shape factors 117
7.9 Output data processing 117
8. Acknowledgments 118
9. References 119
Appendix A. The shape factor calculation in the case of rectangular surfaces 123
Appendix B. Guide to setting up a SPARK file for a test room 129
B.1 Introduction 129
B.2 First step: surfaces 129
B.2.1 Read in the .ps files 129
B.2.2 Connect the surface modules together 130
B.3 Second step: the room air 131
B.3.1 Read in the .ps file 131
B.3.2 Connect the room air module with the surface modules 132
B.4 Third step: the links between room components 132
B.4.1 The connection between the room air module and the room

surfaces 132
B.4.2 The total short wave radiation entering the room through transparent surfaces 134
B.4.3 The long wave radiation connection among the room surfaces 135
Appendix C. Cooling Power 138

Abstract

A significant amount of the electrical energy used to cool non-residential buildings equipped with All-Air Systems is drawn by the fans that transport the cool air through the thermal distribution system. Hydronic Cooling Systems have the potential to reduce the amount of air transported through the building by separating the tasks of ventilation and thermal conditioning. Due to the physical properties of water, Hydronic Cooling Systems can transport a given amount of thermal energy using less than 5% of the otherwise necessary fan energy. This improvement alone significantly reduces the energy consumption and peak power requirement of the air conditioning system.

Hydronic Cooling Systems are particularly suited to the dry climates that are typical of California. These systems have been used for more than 30 years in hospital rooms to provide a draft-free, thermally stable environment. However, the energy savings and peak-load characteristics of these systems have not yet been systematically analyzed. Moreover, adequate guidelines for their design and control systems do not exist. This has prevented their widespread application to other building types.

The evaluation of the theoretical performance of Hydronic Systems could most conveniently be made by computer models. Energy analysis programs such as DOE-2 do not yet have the capacity to simulate Hydronic Cooling Systems. The scope of this project is the development of a model that can accurately simulate the dynamic performance of Hydronic Radiant Cooling Systems. The model is able to calculate loads, heat extraction rates, room air temperature and room surface temperature distributions, and can be used to evaluate issues such as thermal comfort, controls, system sizing, system configuration and dynamic response. The model was created with the LBL Simulation Problem Analysis and Research Kernel (SPARK), which provides a methodology for describing and solving the dynamic, non-linear equations that correspond to complex physical systems. The potential for Hydronic Radiant Cooling Systems applications can be determined by running this model for a variety of construction types in different California climates.

1. Introduction

1.1 Disadvantages of All-Air Systems

Cooling of non-residential buildings equipped with *All-Air Systems* significantly contributes to the electrical energy consumption and to the peak power demand. Part of the energy used to cool buildings is consumed by the fans that transport cool air through the ducts. This energy heats the conditioned air, and therefore adds to the internal thermal cooling peak load. In a 1985 study, Usibelli et al. [1] found that, in the case of the typical office building in Los Angeles, the external loads account for only 42% of the thermal cooling peak (**see Figure 1**). At that time, 28% of the internal gains were produced by lighting, 13% by air transport, 12% by people, and 5% by equipment. The implementation of better windows, together with higher plug loads due to increased use of electronic office equipment, have probably caused these contributions to change in some extent since then.

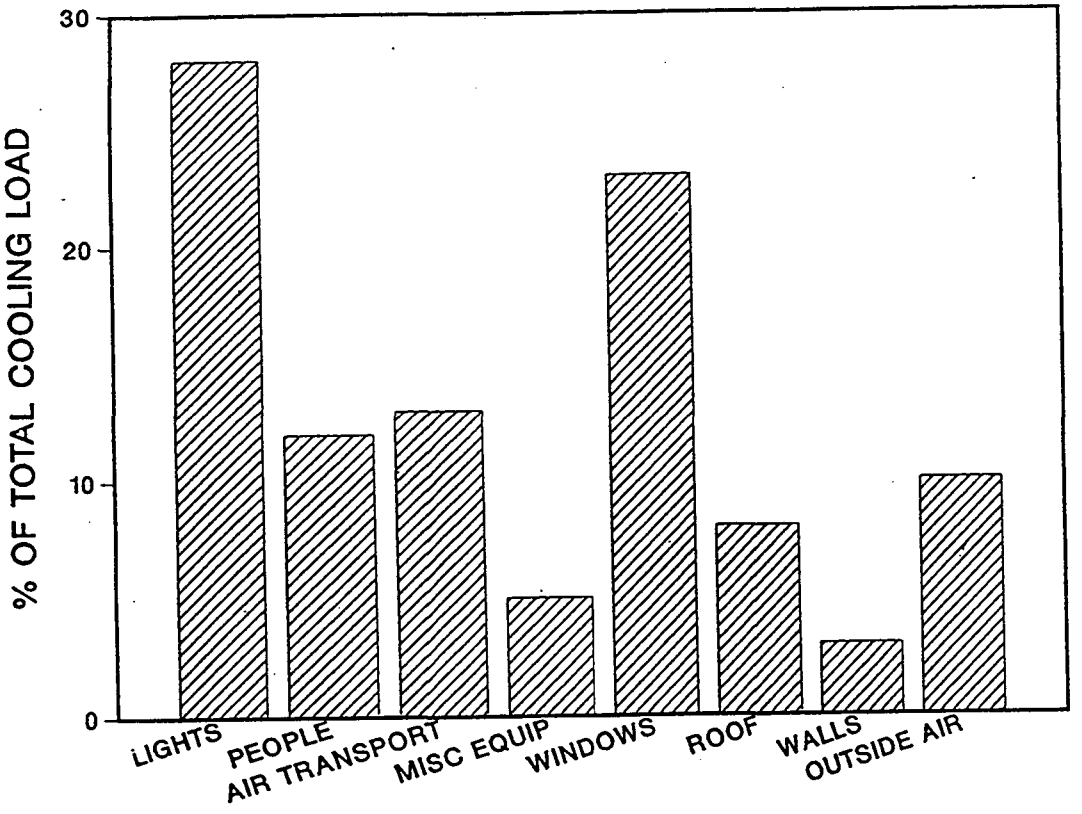

Figure 1. Peak cooling load components, typical office building, Los Angeles

SOURCE: Usibelli et al., *Commercial-Sector Conservation Technologies*, Lawrence Berkeley Laboratory Report LBL-18543, 1985

HVAC systems are designed to maintain indoor air quality and provide thermal space conditioning. Traditionally, HVAC systems are designed as *All-Air Systems*, which means that air is used to perform both tasks. Simulations with DOE-2 [2] for different California climates using the California Energy Commission (CEC) base case office building show that, at peak load, only 10% to 20% of the supply air is outside air [3]. Only this small fraction of the supply air is in fact necessary to ventilate the buildings in order to maintain a high level of indoor air quality. For conventional HVAC systems the difference in volume between supply air and outside air is made up by recirculated air. The recirculated air is necessary in these systems to keep the temperature difference between supply air and room air in the comfort range. The additional amount of supply air, however, often causes draft (air movement in an occupied enclosure causing discomfort), as well as indoor air quality problems due to the distribution of pollutants throughout the building.

1.2 The radiant cooling alternative

All-Air Systems achieve the task of cooling a building by convection only. An alternative is to provide the cooling through a combination of radiation and convection inside the building. This strategy uses cool surfaces in a conditioned space to cool the air and the space enclosures. The systems based on this strategy are often called *Radiative Cooling Systems*, although only approximately 60% of the heat transfer is due to radiation. If the cooling of the surfaces is produced using water as transport medium, the resulting systems are called *Hydronic Radiant Cooling Systems* (*HRC Systems*). By providing cooling to the space surfaces rather than directly to the air, *HRC Systems* allow the separation of the tasks of ventilation and thermal space conditioning. While the primary air distribution is used to fulfill the ventilation requirements for a high level of indoor air quality, the secondary water distribution system provides thermal conditioning to the building. *HRC Systems* significantly reduce the amount of air transported through buildings, as the ventilation is provided by outside air systems without the recirculating air fraction. Due to the physical properties of water, *HRC Systems* remove a given amount of thermal energy and use less than 5% of the otherwise necessary fan energy. The separation of tasks not only improves comfort conditions, but increases indoor air quality and improves the control and zoning of the system as well. *HRC Systems* combine temperature control of the room surfaces with the use of central air handling systems [4].

Due to the large surfaces available for heat exchange in *HRC Systems* (usually almost a whole ceiling), the temperature of the coolant is only slightly lower than the room temperature. This small temperature difference allows the use of either heat pumps with very high coefficient of performance (COP) values, or of alternative cooling sources (e.g., indirect evaporative cooling), to further reduce the electric power requirements. *HRC Systems* also reduce problems caused by duct leakage, as the ventilation air flow is significantly reduced, and the air is only conditioned to meet room temperature conditions, rather than cooled to meet the necessary supply air temperature conditions. Furthermore, space needs for ventilation systems and their duct work are reduced to about 20% of the original space requirements. Beside the reduction of space requirements for the shafts that house the vertical air distribution system, floor-to-floor height can be reduced, which offsets the initial cost of the additional system.

The thermal storage capacity of the coolant in *HRC Systems* helps to shift the peak cooling load to later hours. Because of the hydronic energy transport, this cooling system has the potential to interact with thermal energy storage systems (TES) and looped heat pump systems.

2. Background

2.1 Historical Development of Radiant Cooling

During the last decade, building inhabitants developed a critical attitude towards air conditioning systems. Terms like *complaint buildings* and *sick buildings* were born. Several publications dealing with occupant satisfaction in air-conditioned and naturally ventilated buildings came to the conclusion that the number of unsatisfied occupants in air-conditioned buildings is significantly higher than in naturally ventilated buildings [5 - 7]. Esdorn et al. [8] state that "the existence of air-conditioning systems is actually only noticed when it is not functioning properly."

Draft is a serious problem in many air-conditioned buildings. As the air from *All-Air* HVAC systems is normally turbulent in the occupied zone, even low air velocities (less than 0.1 m/s) might cause an unwanted local cooling of the human body [9]. In order to be able to remove cooling loads from a building, the cooled air either exceeds in volume the outdoor air needed for ventilation (recirculating air systems), or the temperature differences between the supply air and the room air have to be so large that the air supply might cause problems related to the uneven distribution in the occupied zone (cold air distribution systems). Because of comfort problems and the excessive use of transport energy for All-*Air Systems*, new ventilation strategies were developed [10] such as displacement ventilation.

The idea behind *displacement ventilation* is to overcome the problems of mixing ventilation systems. Air flows of low turbulent intensity supply clean air directly to the breathing zone and displace contaminants [11]. If the air is displaced upwards, cooling is also achieved, but this strategy will result in an increase of the vertical temperature gradient of the air. The natural driving forces of the vertical air transport are the heat sources in the space, as they create convective air currents (plumes). Displacement ventilation should not be mistaken for "plug flow" or "piston flow"; plume flow ventilation might be a better term. The resulting air flow pattern has greatly improved ventilation efficiency (for definition of ventilation efficiency, see Sutcliff [12]).

Upward displacement ventilation shows a characteristic temperature profile caused by the convective currents driven by the heat sources. As supply air enters the room at floor level, the temperature gradient forms a barrier that prevents low energy currents to reach high altitudes in the room. Due to comfort requirements, the temperature gradient between feet and head cannot exceed 3 °C, which limits the cooling capacity of displacement ventilation systems [11]. The fact that displacement ventilation systems use solely outside air further reduces their cooling capacity [13, 14].

The most efficient way to use displacement ventilation is to associate it with a cooling

source that does not require air transport inside the room. The logical choice is the coupling of displacement ventilation systems with hydronic radiant cooling, a strategy that allows the separation of the tasks of ventilating and cooling in the building. The theoretical air flow pattern in a room with a cooled ceiling is shown in **Figure 2.**

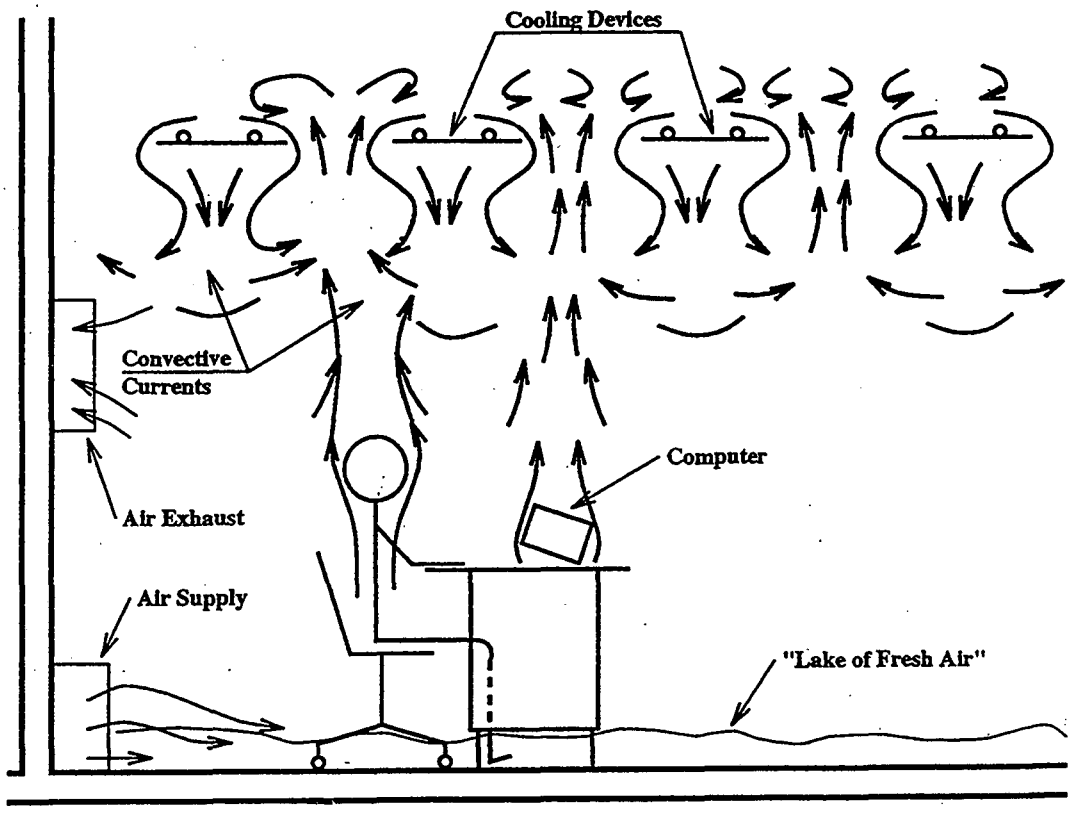

Figure 2. Air flow patterns in a room with a cooled ceiling

SOURCE: Skaret, E., *Displacement Ventilation*, In Proceedings "Roomvent '87", Stockholm, June 1987.

2.2 Thermal Comfort

In order to maintain normal functions, the human body needs to maintain the balance between heat gain and heat loss. Heat can be lost in different ways: radiation to surrounding surfaces, convection to the ambient air, evaporation, respiration and excretion. The most important loss is due to radiation, followed in order by convection and conduction. Respiration and excretion have less influence on the heat loss of a human body.

To explain the impact of radiation, Baker [15] gives the following example: "A person sitting out of doors under a clear sky on a summer evening may be chilly although the air temperature is in the high 70's (°F). Were he indoors at this same temperature, he probably would feel uncomfortably warm. The appreciable heat loss by radiation to the clear sky explains the different sensations of comfort between outdoors and indoors." This example

suggests that the surface temperatures surrounding a person inside an enclosure have to be considered.

Heat loss by convection only would require a high air velocity close to the human skin, and would eventually lead to draft and therefore, to uncomfortable conditions. The possibilities of increasing the heat loss by respiration or excretion are very limited.

Heat loss by radiation is caused by the difference between the body temperature and the mean radiant temperature, which depends on the temperatures of the surrounding surfaces. The mean radiant temperature is easy to define but quite complicated to calculate or measure in practice. Due to the non-uniform distances and angles of persons in relation to the walls, floor and ceiling of a space, each part of the space must be considered separately in the radiation exchange. If a given surface is found to not be isothermal, it has to be divided into smaller isothermal surfaces. Each surface can be assumed to have high emissivity. The radiation emitted and reflected from any surface is distributed as diffuse radiation, which is a good approximation for all normal non-metallic surfaces [16]. The enclosure surfaces often found in a normal room have rectangular shape and, therefore, the angle factor in the mean radiant temperature calculations is defined between a person and a vertical or horizontal plane. The body posture is also important. The mean radiant temperature in relation to a standing person is not necessarily the same as in relation to a seated one [16]. Likewise, the location and orientation of the person inside the room must also be known, because the mean radiant temperature often varies from point to point.

The first experiments of thermal and comfort sensations to radiation experienced by seated persons were conducted by McNall, Biddison [17], and Schlegel, McNall [18]. Fanger [16] defined mean radiant temperature as follows: "The mean radiant temperature in relation to a person in a given body posture and clothing placed at a given point in a room, is defined as that uniform temperature of black surroundings which will give the same radiant heat loss from the person as the actual case under study."

The combined effects of radiation and convection inside an enclosure can be evaluated by using a parameter called the "operative temperature". The operative temperature is calculated by averaging between the dry bulb temperature and the mean radiant temperature inside the enclosure. The definition of the operative temperature shows that this parameter does not reflect the presence of radiation asymmetry inside an enclosure. In the case when this effect is important, the use of operative temperature in evaluating thermal comfort might lead to erroneous results.

Air movement plays a special role among the comfort parameters. According to Esdorn et al. [8], air movement (draft) is the largest single cause for complaints. Beside the mean velocity, the fluctuation of the velocity has an important influence on the convective heat transfer from the human body. Mayer [19] relates comfort directly to the convective heat transfer coefficient, rather than to the average air velocity. According to Mayer [20], at an air temperature of 22 °C draft is felt if the convective heat transfer coefficient is above 12 W/m^2 K. This translates to an average air velocity of 1.35 m/s for laminar flows, 0.15 m/s for transition flows, and 0.10 m/s for turbulent flows. Lower air temperatures significantly reduce the acceptable air velocities. A different viewpoint on acceptable air velocities may be found in ASHRAE Standard 55-92, *Thermal Environmental Conditions for Human Occupancy* [21].

For extended discussion of recommended levels thermal comfort levels, see Chapter 8 of the 1993 ASHRAE Handbook of Fundamentals [22], Chapter 8, ASHRAE Standard 55-92 [21], and ISO Standard 7730, *Moderate Thermal Environments - Determination of PMV and PPD Indices and Specification of the Conditions for Thermal Comfort* [23].

2.3 Cooling Power

The cooling power of *HRC Systems* is limited due to the fact that in operating these systems the side-effects associated with the presence of cold surfaces in the space have to be prevented or minimized. A first effect to prevent is condensation. In theory, the surface temperatures of the cooling elements must not be lower than the dew point temperature of the air in the cooled zone. In practice however, condensation prevention reduces the effective cooling temperature difference (between the cold surface and the air) by a safety margin of approximately 2 °C. In the operation of the system the dew point can also be manipulated, by reducing the humidity content in the ventilation air. A second and more serious concern is the comfort effect of the asymmetrical distribution of the radiant temperature. Kollmar [24] shows that for offices, the lower limit for ceiling temperatures is approximately 15 °C.

To calculate the cooling power of an *HRC System*, the heat transfer between the room and the cold ceiling has to be evaluated. There are two components of the heat transfer: radiation and convection. While the radiation term is relatively easy to calculate, the convective heat transfer is a function of the air velocity at the ceiling level. This velocity is dependent on the room geometry, the location and power of the heat sources, and the location of the air inlet and exhaust.

Trogisch [25] compares heat transfer coefficients for cooled ceilings found in the literature with the description of convective heat transfer from a cold flat surface (downwards) as published in textbooks. Investigations dealing with cooled ceilings show overall heat transfer coefficients of 9 to 12 W/m^2 K. Given a heat transfer coefficient for radiation of about 5.5 W/m^2 K (for a temperature difference of 10 °C), the resulting convective heat transfer coefficient would be in the order of 3.5 to 6.5 W/m^2 K. These values for the convective heat transfer coefficient are, however, reached only if forced convection takes place (here forced means that phenomena other than the cooling at the ceiling are responsible for driving the air flow).

Radiant cooling elements extract heat from a room by cooling the air directly (convection) and indirectly, by cooling the other surfaces of the room envelope. If there is only a small difference between the average surface temperature of the room and the air temperature, the two effects can be estimated jointly [26]. Under this assumption, the specific cooling power (per unit area) of a cooled ceiling can be expressed by the following empirical equation (see Appendix C):

$$q_{tot} = 8.92\,(t_{air} - t_{surface})^{1.1}$$

q_{tot} is the sum of convective and radiant heat transfer [W/m^2]

A survey of cooled ceilings [27] shows cooling output ranging from 40 to 125 W/m^2. The data are, however, based on information from manufacturers and do not specify the

boundary conditions for the measurements. This problem brings up the necessity of standards for both the measurement conditions and techniques, and several attempts have already been made to set standards for testing radiant panels.

A test facility and a method of testing were developed at the Department of Veterans Affairs [28]. The method describes the testing procedure for thermal performance and pressure drop measurements in the test facility, as well as the accuracy of the instrumentation used.

ASHRAE's technical committee TC 6.5, *Radiant Space Heating and Cooling*, currently sponsors a committee on *Methods of Testing/Rating Hydronic Radiant Ceiling Panels* (SPC 138P). The purpose of SPC 138P is to establish a method of testing for rating the thermal performance of hydronic radiant cooling panels used for heating and/or cooling of indoor space [29].

In Germany, two competing test procedures have been recently published within five months. The Fachinstitut Gebaeude-Klima (FGK) presented its testing procedure in December 1992 [30]. The FGK industrial standard is based on a measurement in a box (2.4m x 1.2m x 1.5 m) with an internal operative temperature of 26 °C and water supply temperatures of 12, 14, and 16 °C.

The DIN-standard was presented in April 1993 [31]. It measures the performance of radiant panels in the presence of natural convection. The test is based on measurements performed in a closed test chamber (4m x 4m x 3m) with a conditioned metal envelope. The cooling load is simulated by 12 perforated tubes containing three 60W bulbs each. The measurements are performed under steady-state conditions, with different coolant mass flows.

While testing procedures and future standards can rate the performance of an *HRC System* with panels under given boundary conditions, the efficiency of the same system in a specific (but different) application is difficult to determine. The difficulty arises from the fact that the rated performance greatly depends on the testing procedure. For example, a procedure for measuring the efficiency of a cooled ceiling could use the temperatures of the ceiling and of the exhaust air in a test room as a measure for the convective heat transfer between the ceiling and the room air. If, in a hypothetical situation, a shortcut between the supply and the exhaust of the ventilation system in the test room provided high air velocities on the ceiling surface, a large fraction of the exhaust air would in fact be air that has been cooled by the ceiling without having interacted with the room loads at all. The difference between the temperatures of the ceiling surface and the exhaust air would in this case indicate lower convective heat transfer than in reality, the measurements would appear as having been performed under low air flows, and the ceiling would show high efficiency. The functioning of the same ceiling in a normal situation (without the forced convection) is very likely to give different results. These considerations show that a building designer should carefully consider all the details in a testing procedure before deciding to use a specific type of cooling ceiling panels.

2.4 Cooling Performance

Although several papers have been found that describe the cooling power of *HRC Sys-*

tems, only few papers are found that deal with the performance of these systems. Kuelpmann [32] reports on an experimental investigation in a temperature controlled test cell (see **Figure 3**). In this experiment, the air was supplied at floor level and exhausted approximately 0.2 m below the ceiling level. Internal loads were simulated by electrically heated mannequins standing next to a computer display, and by fluorescent lights. External loads were introduced by heating either one of the long side walls, or the floor. For displacement ventilation and no cooling with supply air, the room air temperatures measured at different heights did not differ very much (see **Figure 4**).

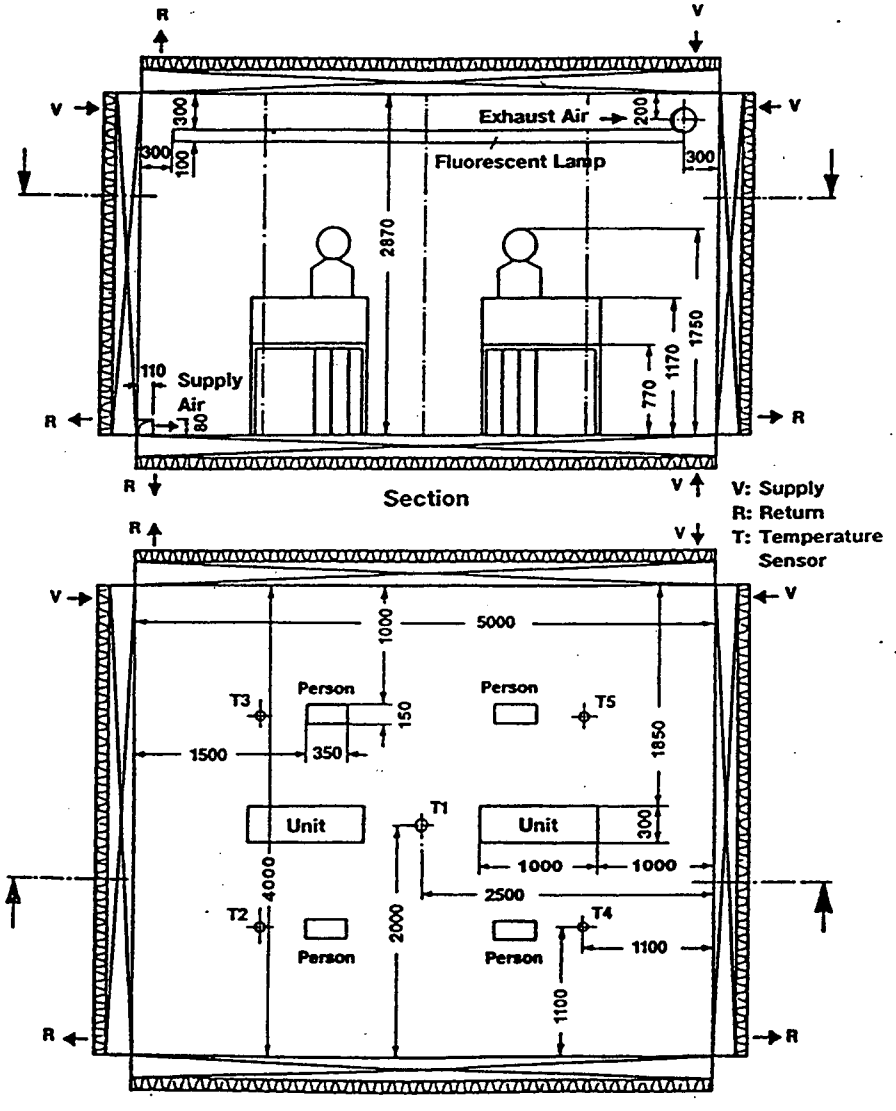

Figure 3. Test chamber used to test the cooling performance of hydronic cooling

SOURCE: Kuelpmann, R., *Thermal Comfort and Air Quality in Rooms with Cooled Ceilings - Results from Scientific Investigations*, Preprint to ASHRAE Transactions 1993, Vol. 99, Pt. 2, 1993

The extraction of 100 W/m^2 internal load by hydronic radiant cooling caused temperature

differences of approximately 2 °C between the supply and exhaust grilles. When increasing the temperature difference between the room air and the supply air, the profile became more pronounced. Especially in the lower part of the room, these temperature differences became close to, or exceeded the comfort limits.

In all cases examined, the differences between the room air temperature and the surface temperatures of the "internal walls" were relatively small (± 0.4 °C). Due to the radiation exchange with the cooled ceiling, the floor surface temperature was usually below the wall surface temperatures.

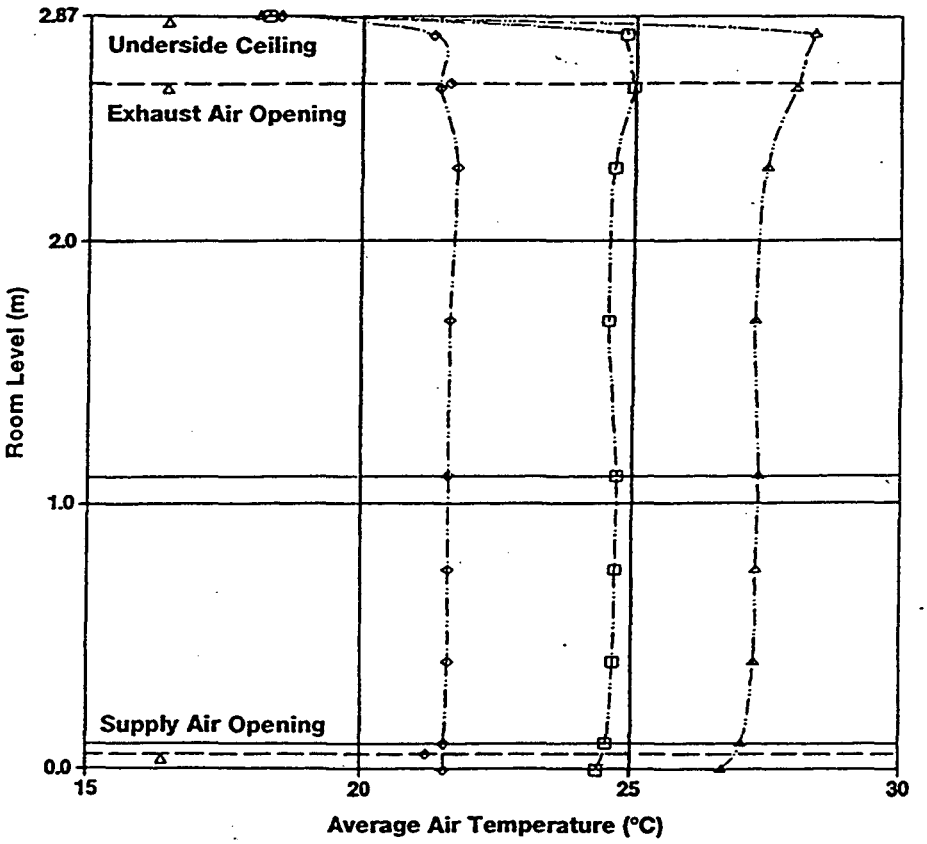

Symbol	Cooling Load (W/m²)	Room Temperature (°C)	Temp.-Diff. Walls-Air (K)	Performance Part (-) Ceiling ω_{De}	Ventilation ω_L
◊	35	21.4	0.2	0.96	0.04
□	67	24.4	-0.2	1.00	0.00
△	101	26.7	-0.3	1.00	0.00

Figure 4. Air temperature profile over the room height as a function of external loads; tabulated room temperature is measured at 1.1 m above the floor

SOURCE: Kuelpmann, R., *Thermal Comfort and Air Quality in Rooms with Cooled Ceilings - Results from Scientific Investigations*, Preprint to ASHRAE Transactions 1993, Vol. 99, Pt. 2, 1993.

Asymmetric or non-uniform thermal radiation may be caused in winter by cold windows, uninsulated walls or heated ceilings. In summer, cooled ceiling panels also produce asymmetric thermal radiation. Radiant asymmetry due to a cooled ceiling causes less discomfort than a warm ceiling. Based on Fanger's limit of 5% uncomfortable as a rule for determining the acceptability of a system, a radiant temperature asymmetry of 10 °C is acceptable in the presence of a cool wall, and of 14 °C in the presence of a cooled ceiling (see **Figure 5**) [33]. Measurements of radiant temperature asymmetry at 101 W/m^2 cooling power in the reported investigation resulted in 8 °C difference at 1.1m above the floor level, in the middle of the room (see Figure 4). This corresponds to less than 2% of occupants dissatisfied (see Figure 5).

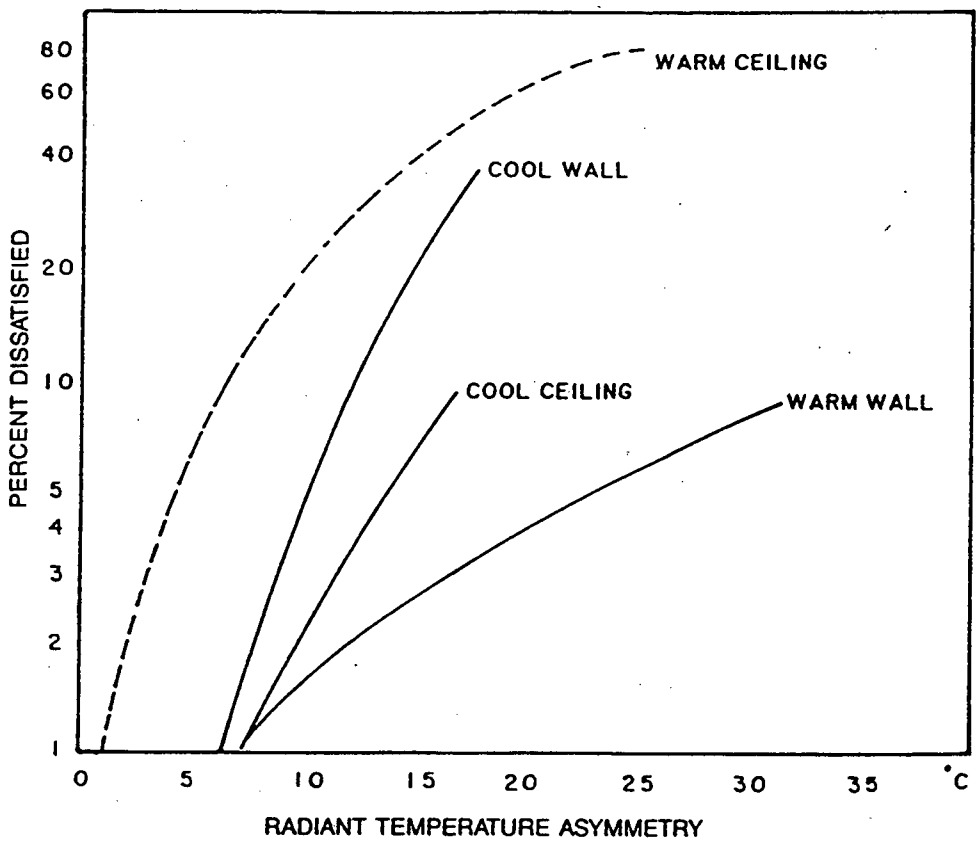

Figure 5. Measured percentage of people expressing discomfort due to asymmetric radiation

SOURCE: Fanger et al., *Comfort Limits for Asymmetric Thermal Radiation*, Energy and Buildings, 8 (1985), pp 225-236.

Air flow velocities were measured at 1m distance to the supply air grille, at 0.1m height above ground. At an air exchange rate of 3.2 ach and a supply air temperature of 19 °C,

exceptionally low values were measured for the air velocity (0.12 m/s) and the turbulence intensity (20%).

The performance of *Hydronic Radiant Cooling* was tested in two parliamentarian offices in Bonn, Germany [34]. Dry-bulb temperatures and relative humidity were measured for the outside air, the supply air and the room air. Temperature measurements were also made in the supply and return pipes of the hydronic system and at three points on the ceiling surface. For outside air temperatures of 30 °C, the air velocities measured in the occupied zone were below 0.10 m/s. This value shows that the risk of draft has been eliminated in the tested zones. Below the ceiling, surface velocities between 0.10 and 0.15 m/s were detected. These low velocities assure that the convective heat transfer is being kept in the desired range of less than 40%.

2.5 Energy Savings

The use of *HRC Systems* has the potential to be an energy conserving and peak-power reducing alternative to conventional air-conditioning, particularly suited to dry climates. A significant amount of the electrical energy used to cool buildings by *All-Air Systems* is consumed by the fans which are used to transport cool air through the ducts. Part of this electricity used to move the air is heating the conditioned air, and therefore, is part of the internal thermal cooling peak load. The electrical cooling peak load, if defined as the load from the fans and the chillers, has a breakdown of approximately 37% for running the fans, and 63% for using the chillers.

If the tasks of ventilation and thermal conditioning of buildings are separated, the amount of air transported through buildings can be significantly reduced. In this case the cooling is provided by radiation using water as the transport medium, and the ventilation by outside air systems without the recirculating air fraction. Although the supply air necessary for ventilation purposes is still distributed through ducts, the electrical energy for fans and pumps can be reduced to approximately 25% of the original value.

The elimination of recirculation air also increases the efficiency of air-handling luminaires, as the convective heat extracted from the light fixtures is not recirculated as it partly would be in an *All-Air System*, but vented directly to the exterior. 50% of the required thermal cooling energy produced by lighting can this way be removed. If an *HRC System* is compared to a *Constant Volume Air System*, an overall electrical cooling energy savings potential of more than 40% seems reasonable (see **Figure 6**).

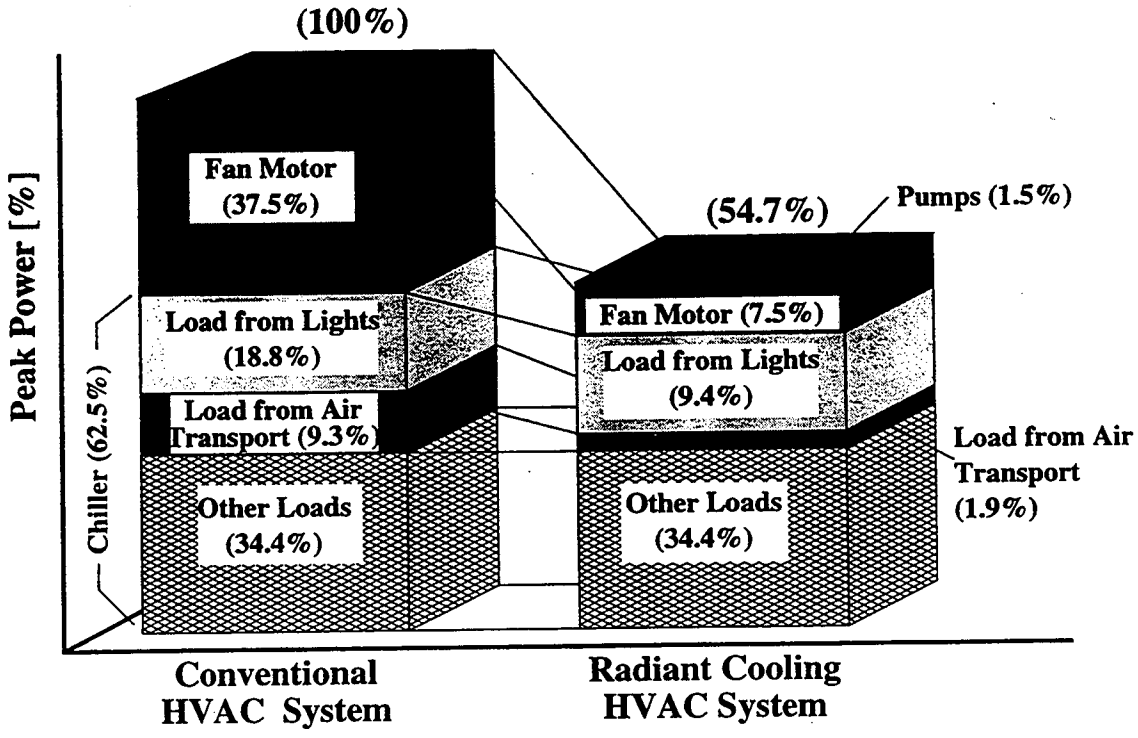

Figure 6. Comparison of electrical peak power load for an *All-Air System* and an *HRC System*, based on the peak-load data shown in Figure 1. Percentages for the *HRC System* are relative to the overall peak power of the *All-Air System*.

2.6 Peak-Power Requirement

In order to compare the electrical peak-power requirement for conventional systems (*All-Air Systems*) and advanced systems (*HRC Systems*), the power requirement for a simple example has been calculated. The example is based on an office with a floor area of 25 m^2, a two person occupancy and a total heat gain of 2000 W. The specific cooling load amounts to 80 W/m^2, which is in the range of *HRC Systems*. The room temperature is set to 26 °C. Additional assumptions and design considerations used for this example are shown in **Table 1**. Since in this example is based on a single zone building, the estimated savings are different than those calculated for a multi-zone building.

The *All-Air System* supplies cooling to the room as follows: a cooling coil dehumidifies the outside air according to the required room conditions. ASHRAE Standard 62 (ASHRAE 1989) requests a minimum air change rate of 36 m^3/h person, which means that for this example the minimum air change rate is 72 m^3/h. In order to remove the internal load, a recirculating air volume flow of 678 m^3/h is required. The assumed outside air condition of 32 °C leads to a mixing temperature of 25.6 °C.

After having mixed, the air enters a cooler. In order to adjust for the temperature increase due to the fan work, the air has to be cooled further than the 18 °C specified as supply air temperature. The temperature adjustment depends on the pressure drop, fan efficiency and volume flow. In our example, this air handling temperature rise has been assumed to be 1 °C.

TABLE 1. Assumptions used for the Comparison of Peak Power Requirements for an *All-Air System* and an *HRC System*

	Both Systems	
Room Conditions:		
Cooling Load [W/m^2]	80	
Room Air Temperature [°C]	26	
Relative Humidity [%]	50	
Humidity Ratio [g_{water}/kg_{dryair}]	10.6	
Number of People	2	
Outside Air Conditions:		
Air Temperature [°C]	32	
Relative Humidity [%]	40	
Humidity Ratio [g_{water}/kg_{dryair}]	12.1	
Enthalpy [kJ/kg]	63.0	
	All-Air System	HRC System
Design Consideration:		
Outside Air Flow [m^3/h]	72	72
Supply Air Flow [m^3/h]	750	72
Temperature Differences:		
Room Air - Supply Air [K]	8	3
Room Air - Ceiling [K]	0	8
Supply Water - Return Water [K]	--	2
Efficiencies:		
Fan: Hydraulic/Mechanical/Electrical [%]	60/80/98	60/80/98
Water Pump [%]	--	60
Pressure Drop:		
Supply Duct/Return Duct/Water pipe [Pa]	500/250/--	500/250/4000
COP	3	3

The electrical power for an *All-Air System* amounts in this example to

$$\sum Q_{el,\,All-AirSystem} = 1270W$$

In order to be able to compare the two systems, the boundary conditions have to be equal. This includes efficiencies of fans and motors, pressure losses for supply and exhaust ducts, and chiller COPs.

While the *All-Air System* removes the cooling load by means of supplying cold air, the *HRC System* removes the load mainly by means of water circulation. The tasks of the ventilation side of the system are thus to supply the room with the necessary air exchange rate for comfort reasons, and to control the dew-point in the room, to avoid humidity buildup. In order to provide a stable displacement ventilation, the supply air volume flow should be about 3 °C below the room air temperature. The required temperature of the supply air is thus 23 °C, which reduces the hydronic cooling load by around 3 W/m^2.

In order to control humidity, the cooling of the outside air below the supply air temperature might be necessary. A reheater can be installed which warms the air using waste heat from the compressor. The warming of the air could be done even more efficiently, if the air were channeled through building components before arriving to the room inlet. This would save the power to reheat and provide some conditioning at the same time. The electrical power of the *HRC System* amounts to

$$\sum Q_{el,\,HRCSystem} = 891W$$

Table 2 shows the electrical power calculated for an *All-Air System* and an *HRC System.*

The values in the table show that the power required by the *HRC System* is only about 71% of the total electrical power required by the *All-Air System.* The savings could be increased by venting the light fixtures in the building.

TABLE 2. Electrical Power Requirement to Remove Internal Loads from a Two-Person Office with a Floor Area of 25 m^2.

	All-Air System	HRC System
Supply Fan [W]	222	21
Air Cooler [W]	721	--
Pre-Cooler/Dehumidifier[W]	216	216
Exhaust Fan [W]	111	11
Water Pump [W]	--	20
Water Cooler [W]	--	641
Total	1270 W	909 W
	100%	71.5%

2.7 Economics

Although manufacturers of *HRC Systems* claim many installations of their systems, it is difficult to obtain information about the economics of the systems installed. There are only a few papers that deal with the economics of *HRC Systems.*

Feil [35] compares different ventilation/cooling systems for an office. In a first-cost comparison with a *VAV System*, the break-even point for *HRC Systems* is approximately at a specific cooling load of 55 W/m^2.

Hoenmann and Nuessle [36] estimate yearly energy consumption for an office building in Europe (see **Table 3**). The building has 5000 m^2 of floor area distributed over four floors. The specific cooling load is 50 W/m^2.

The relatively low savings potential for the overall energy consumption of the building (less than 8%), is due to the large energy consumption by heating and lighting. Unfortunately, the authors do not provide consumption data for cooling only. Furthermore, the outside-air-only *VAV System* utilized an economizer mode, while the same savings potential has not been matched in the *HRC System* by installing a water side economizer.

The space requirement for the two systems are shown in **Table 4**. The largest savings, 36%, appear in the equipment rooms, followed by 28% for the distribution shafts. For systems with false ceilings, the reduction in height per floor is in the order of to 15 to 20 cm. *HRC Systems* which are integrated into the ceiling produce even higher savings.

TABLE 3. Yearly Energy Consumption in kWh/m^2 for an Office Building in Europe

	VAV System	HRC System
Heating	43	43
DHW	4	4
Lighting	34	34
Miscellaneous	10	10
Ventilation	12	8
Fans/Pumps	31	24
Cooling	7	8
Sum	141	131

SOURCE: Hoenmann et al., *Kuehldecken verbessern Raumklima*, in: Kuehldecke und Raumlueftung, Fachinstitut Gebaeude-Klima e.V., Bietigheim-Bissingen, F.R.G., 1991.

TABLE 4. Space Requirements for Systems in Office Buildings

	VAV System	HRC System
Shafts [m^2]	25	18
Equipment Rooms [m^2]	165	107
Plenum Height [m]	0.4	0.1

SOURCE: Hoenmann et al., *Kuehldecken verbessern Raumklima*, in: Kuehldecke und Raumlueftung, Fachinstitut Gebaeude-Klima e.V., Bietigheim-Bissingen, F.R.G., 1991.

For first cost calculations, Hoenmann et al. [36] show a break-even point for their aluminium panel system at 50 W/m^2 at an air exchange rate of 3 ach (see **Figure 7**).For a typical hot-climate California office, the specific cooling load is 100 W/m^2.

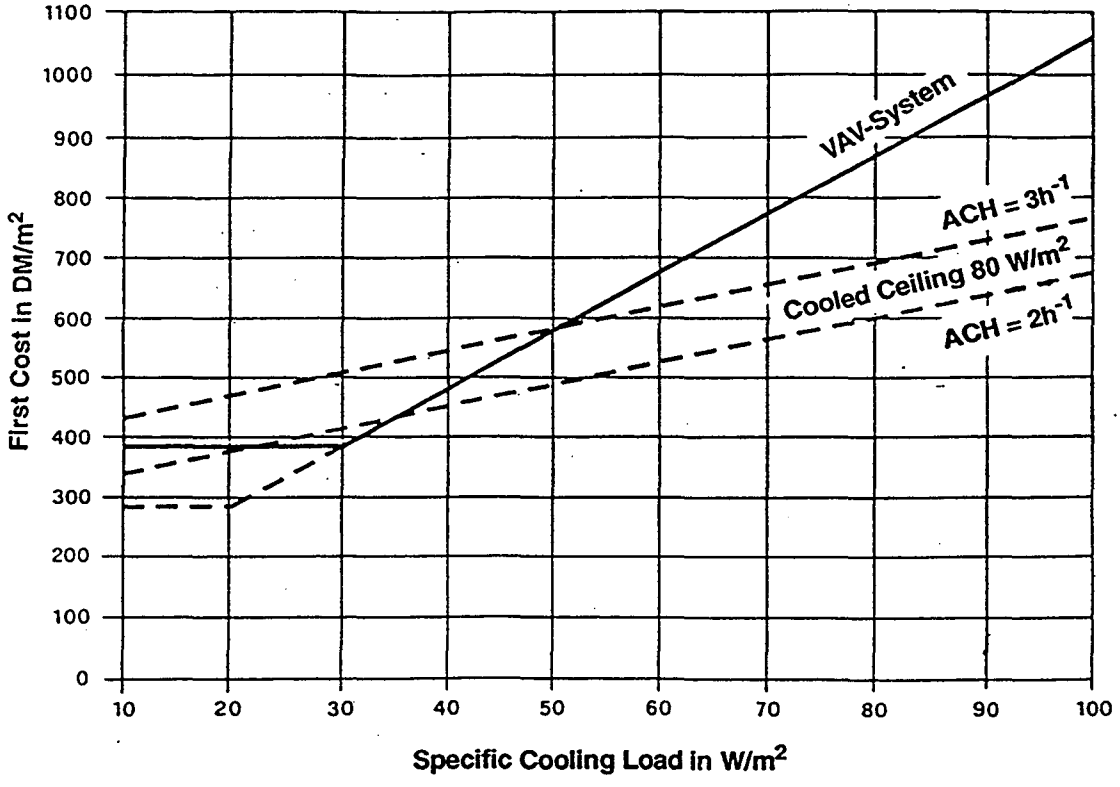

Figure 7. Comparison between first cost for *VAV Systems* and *HRC Systems*, as a function of the specific cooling load

SOURCE: Hoenmann et al., *Kuehldecken verbessern Raumklima*, in: Kuehldecke und Raumlueftung, Fachinstitut Gebaeude-Klima e.V., Bietigheim-Bissingen, F.R.G., 1991.

2.8 System types

Most *HRC Systems* belong to one of four different system designs: cooling panels, cooling registers, (ceiling) slab cooling and floor cooling. The dynamic performance of the system is most critical for systems with high thermal mass. A research project funded by the Swiss agency for energy efficiency (NEFF) [37] has provided performance data for a slab cooling project.

2.8.1 The panel system

The most often used system is the panel system. This system is built from aluminum panels with metal tubes connected to the rear of the panel (see **Figure 8**).The panel ceiling is usually suspended under a ceiling slab.

The connection between the panel and the tube is critical. Poor connections provide only limited heat exchange between the tube and the panel, which results in increased temperature differences between the panel surface and the cooling fluid. Panels built in a "sandwich system" include the water flow paths between two aluminum panels (like the evaporator in a refrigerator). This arrangement reduces the heat transfer problem and increases the directly cooled panel surface.

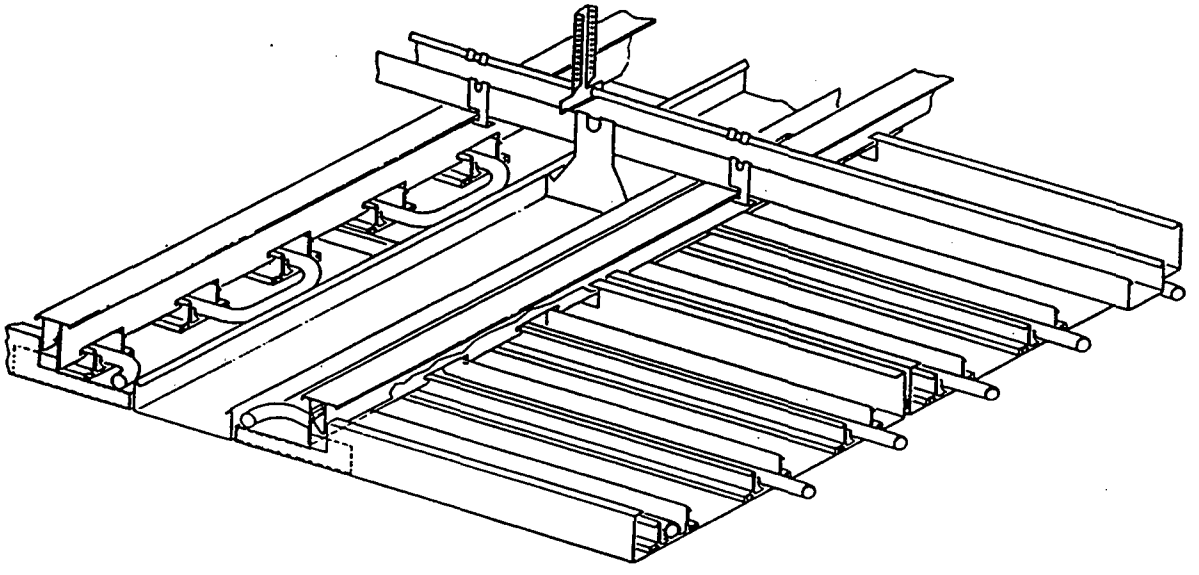

Figure 8. Construction of a cooling panel system

SOURCE: Hoenmann et al., *Kuehldecken verbessern Raumklima*, in: Kuehldecke und Raumlueftung, Fachinstitut Gebaeude-Klima e.V., Bietigheim-Bissingen, F.R.G., 1991.

In the case of panels suspended below a concrete slab, approximately 93% of the cooling power is available to cool the room. The remaining 7% cools the floor of the room above (see **Figure 9**). **Figure 10** shows a typical installation of suspended ceiling panels. A closed panel arrangement with insulated panel backsides uncouples the thermal storage of the slab in this arrangement. This arrangement improves the response time for start-up conditions, but lacks the ability of smoothing cooling load peaks.

The temperature profiles for the different ceiling panel systems have been published by Graeff [38].

Ceiling panels are marketed by:

Flakt (Sweden): Flaekt Inc., Products Division
Winston-Salem, NC

Airtex, Corp. Chicago. IL

Gebr. Trox GmbH
Neukirchen-Vluyn, FRG

Turbon-Tunzini Klimatechnik
Bergisch Gladbach, FRG

Hesco Pilgersteg AG
Rueti/Zuerich, Switzerland

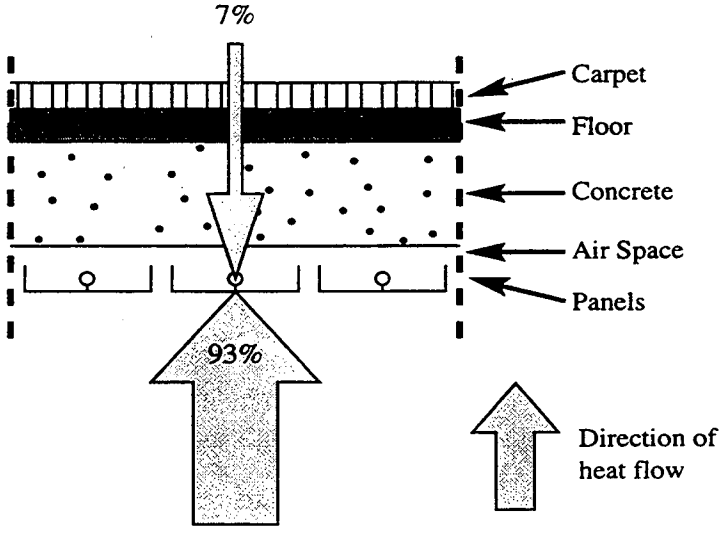

Figure 9. Heat transfer for panel system (cooling mode)

2.8.2 The cooling grid system

Cooling grids made of small plastic tubes placed close to each other can be imbedded in plaster or gypsum board, or mounted on ceiling panels (e.g., acoustic ceiling elements) (see **Figure 11**). This second system provides an even surface temperature distribution. Due to the flexibility of the plastic tubes this system might be the best choice for retrofit applications. It was developed in Germany and has been on the market for several years [39].

When the tubes are imbedded in plaster, the heat transfer from above is higher than in the case of cooling panels (see **Figure 12**). The heat transfer to the concrete couples the cooling grid to the structural thermal storage of the slab. Plastic tubes mounted on suspended cooling panels show thermal performance comparable to the panel systems described above. Tubes imbedded in a gypsum board can be directly attached to a wooden ceiling structure without a concrete slab. Insulation must be applied to reduce cooling of the floor above. **Figure 13** [39] shows cooling grids attached to a concrete ceiling before being covered with plaster.

Plastic cooling registers are marketed by:
D. Herbst, Ka.Ro InfoService
Berlin, FRG

Kraftanlagen Heidelberg AG

Heidelberg, FRG

Heinrich Nickel GmbH
Betzdorf, FRG

Figure 10. Cooling ceiling in an office environment (system REDEC)

SOURCE: Courtesy of REDEC AG

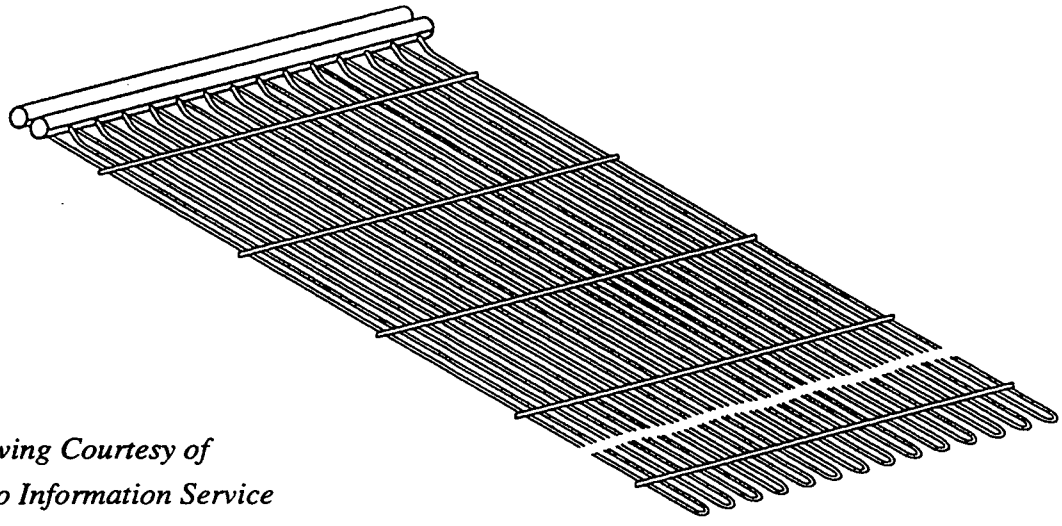

Drawing Courtesy of
KaRo Information Service

Figure 11. Construction of a cooling grid

SOURCE: Anon, *The KA.RO Air Conditioning System from Herbst*, Product Information Herbst Technik, Berlin, F.R.G., 1991.

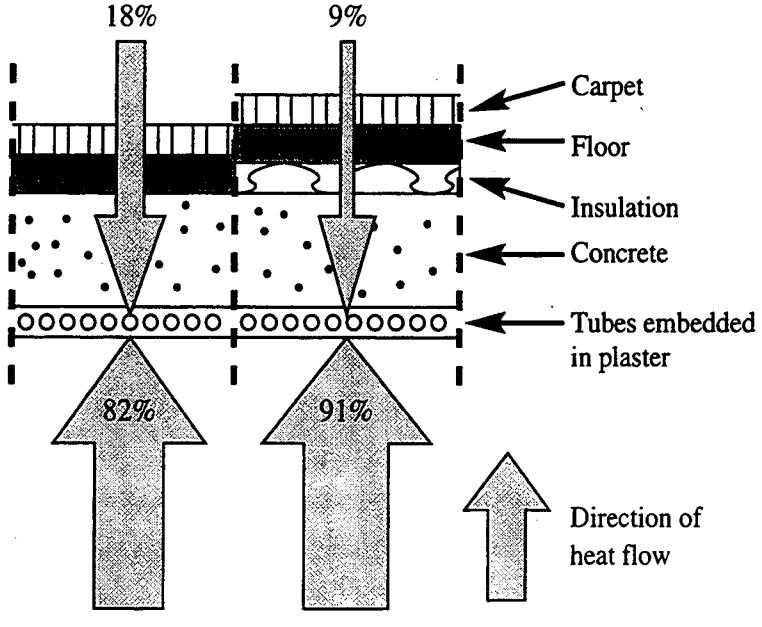

Figure 12. Heat transfer for ceiling with cooling grid

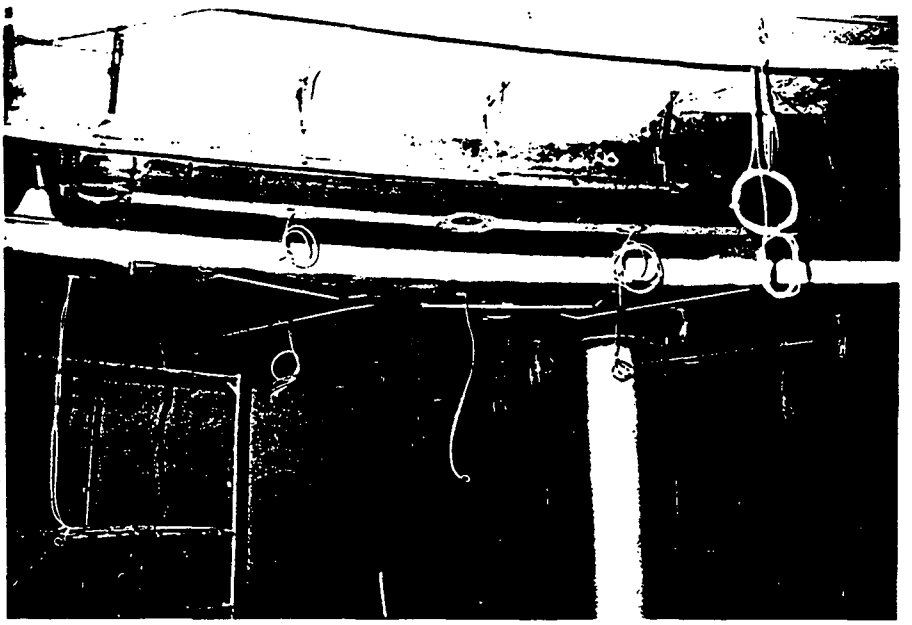

Figure 13. Cooling grid attached to concrete ceiling before being covered with plaster

SOURCE: Anon, *The KA.RO Air Conditioning System from Herbst*, Product Information Herbst Technik, Berlin, F.R.G., 1991.

2.8.3 The core cooling system

A third system is based on the idea of a floor heating system. The tubes are imbedded in the core of a concrete ceiling. The thermal storage capacity of the ceiling allows for peak load shifting, which provides the opportunity to use this system in association with alternative cooling sources. Due to the thermal storage involved, the control of this system is limited. This leads to the requirement of relatively high surface temperatures to avoid uncomfortable conditions in the case of reduced cooling loads. The cooling power of the system is therefore limited [40].

This system is particularly suited for alternative cooling sources, especially the heat exchange with cold night air. The faster warming of rooms with a particular high thermal load can be avoided by running the circulation pump for short times during the day to achieve a balance with rooms with a lower thermal load.

Due to the location of the cooling tubes in this system, a higher portion of the cooling is applied to the floor of the space above the slab. Approximately 83% of the removed heat originates in the room below, while 17% originate in the room above (see **Figure 14**).

2.8.4 The raised floor cooling system

A fourth system, developed in Germany, is also commercially available in California. It provides cooling to a raised floor. The floor provides space for the tubes and the supply plenum. Air is supplied below the windows, reducing the radiative effect of cold window surfaces in winter and hot window surfaces in summer [41].

The floor cooling system is marketed by:
nf eht-Siegmund, Inc.
Tustin, CA

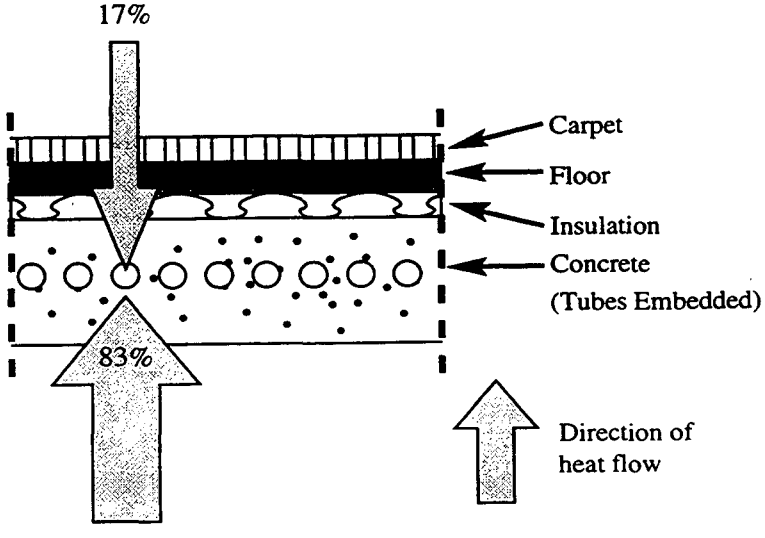

Figure 14. Heat transfer for slab cooling

2.9 Control Issues

As mentioned before, the cooling power of radiative heat exchange is limited by the dew-point of the room air. In order to avoid condensation the cooling surface is kept above the dew-point for all operation conditions. If the dew-point is reduced by dehumidifying the supply air, higher thermal loads can be removed by means of radiation. This means that the surface temperature of the cooled area can be reduced to increase the operative temperature difference. Precautions should however be taken in order to keep the inside air within the specified comfort limits.

Beside the option of reducing the dew-point in order to avoid damage due to condensation, there is the possibility of switching off the supply of cold water as soon as the relative humidity reaches "dangerous" levels. An alternative to this is a type of control consists of window contacts that cut off the water supply when windows are opened. In this way, the ventilation system avoids operating outside design conditions.

Temperature controls for different *HRC Systems* have very different response times. All of the systems working with thermal mass are relatively slow in response to load changes. If operation allows the room temperature to swing, the cooling loads can be matched by these systems; they are the most energy efficient systems available. Systems with water supply close to the cooling surface and with little thermal mass (panel systems) have a response time comparable to *All-Air Systems.*

Although controlling the dew-point by dehumidifying the outside air requires lower cooler temperatures in the air handling system than in the case when outside air is used together with recirculation air for this task, the process is usually more energy efficient because of the smaller amount of air which has to be cooled before the dew-point is reached.

2.10 Summary

Although hydronic radiant cooling is used in the US, a significant market penetration has never been reached. Hydronic radiant cooling was more or less also abandoned in Europe, after some applications in the late thirties and in the fifties. User complaints about *All-Air Systems* have nevertheless changed the designers' attitude towards these systems, and have led to new system designs with better control. Together with efficient ventilation systems and humidity control, *HRC Systems* provide several advantages when compared to conventional HVAC systems.

The reviewed literature shows that *HRC Systems* provide draft-free cooling, reduce space requirements, increase indoor air quality, reduce the energy consumption for thermal distribution and for space conditioning, and might even have lower first-cost, if specific cooling loads are above 55 W/m^2.

Table 5 summarizes the features of *HRC Systems* and their effects.

TABLE 5. Summary of *HRC Systems*

Features	Effect
Separate ventilation and thermal conditioning	Reduce air movement Improve comfort
Transport cooling energy by means of water	Reduce transport energy Reduce peak-power requirement
Eliminate recirculation air	Improve indoor air quality
Reduce convection	Improve comfort
Reduce size of thermal distribution system	Improve space usage Reduce building cost
Use large cooling surfaces	Cool at high temperature level
Increased risk of condensation	Need good humidity control
Can utilize alternative cooling sources	Reduce energy consumption Reduce peak-power requirement
Limited cooling output	Need accurate sizing

Unfortunately, literature has not been found which describes the dynamic thermal behavior of the system and the building. Dynamics might be an important issue in further studies, because the comfort temperature in a space is not only dependent on the air temperature, but also on the (dynamic) distribution of the surface temperatures in the space. Since currently available thermal building simulation programs do not provide the data necessary for evaluating the performance of radiant systems, the development of dynamic models is needed to better understand comfort issues.

3. Problems to be solved

Hydronic Radiant Cooling Systems have become an alternative to conventional *All-Air Systems* in Europe. Although research results have been found which support the data used by manufacturers in Europe, there is not sufficient data available for proving that these systems could perform well in US climates. An analysis based on typical US climates is necessary for a full assessment of the possible applications of hydronic radiant cooling. Hand calculations based on characteristic humidity levels provide results showing that hydronic radiant cooling could work even for climates other than the dry California or Arizona climates.

Due to the limited cooling power available from *HRC Systems*, the building design has to be done carefully, with focus on the reduction of the building cooling peak power requirement. There is obvious potential for the systems to perform well in different California climates, but a study outlining the building design measures associated with the implementation of the systems should nevertheless be performed.

Several *HRC Systems* have already been installed in California. There is some anecdotal evidence that some of these systems do not perform to the satisfaction of the occupants: they either seem to consume more energy than predicted, or to have problems providing thermal comfort. These buildings should be studied to determine the status of the systems, and to unveil the causes of the performance problems.

Performance test-methods should be developed to compare different products under standard conditions, and field tests should be performed showing the influence of climate, building design and room layout on hydronic radiant cooling performance.

As mentioned earlier, because they function at low temperature differences between the room air and the coolant, hydronic radiant cooling strategies are obvious candidates to be associated with cooling sources other than compressors. Alternative cooling sources should therefore be investigated, and their energy savings potential, peak-power reduction and interaction with the *HRC Systems* should be determined.

Current energy analysis programs such as DOE-2 cannot model *HRC Systems*. As a result, there was no way to predict the expected performance of these systems until now, which inhibited their use. The computer model RADCOOL, which was developed in the present project, will allow users to calculate heat extraction rates and room surface temperature distributions for radiant cooling systems. By means of parametric runs, RADCOOL can assist the designing of radiant cooling systems. RADCOOL can also be used to determine the performance of radiant cooling systems in different climates.

RADCOOL was not intended to be a stand-alone program for general use. Rather, it is a research-oriented test bed for investigating the primary performance issues related to radiant cooling. It is anticipated that RADCOOL will later be integrated into DOE-2 and other whole building energy analysis programs.

4. Approach and Model Evaluation

4.1 Approach

Chapter 2 has shown that radiant cooling has the potential to be an energy efficient alternative to all-air cooling systems (see also [42 - 44]). Radiant cooling systems have the potential to achieve high savings, especially if used with alternative cooling sources and elements with large thermal mass. Unfortunately there is not enough design data available for these cooling systems, and the strong influence of the transient response of this cooling system causes difficulties in defining simple design rules. A Lawrence Berkeley Laboratory survey sent to about 300 researchers and practitioners in building science showed general interest for a design tool for radiant cooling and heating systems. A building simulation program appears to be a useful tool for the understanding and predicting the thermal behavior of buildings equipped with a radiant cooling system.

Existing building simulation programs like DOE-2 are often not very flexible in incorporating new technologies [45]. In handling the simulation of cooling systems in general, there is a need for highly modular programs which are easily extendable and easy to use. The program RADCOOL has been designed to accurately simulate the dynamic performance of hydronic radiant cooling systems. The ultimate goal for RADCOOL is to operate as a DOE-2 SYSTEMS module, with other DOE-2 routines modeling the weather and HVAC components that now constitute input to RADCOOL.

4.1.1 Target of simulations

The RADCOOL model, which is described in detail in Chapter 7, is designed to calculate loads, heat extraction rates, room air temperature and room surface temperature distributions. It can be used to evaluate issues such as dynamic response and controls, and it can be extended to evaluate thermal comfort, system sizing, system configuration, and energy use. The simulation program is created with the LBL Simulation Problem Analysis and Research Kernel (SPARK) [46], which provides a methodology for describing and solving the dynamic, non-linear equations that correspond to complex physical systems.

4.1.2 Extensibility

The design of the program allows adding new modules in a straightforward way. This is important when new assumptions need testing.

4.2 Model evaluation

4.2.1 Comparison with DOE-2

To determine RADCOOL's ability to model heat transfer, a SPARK "passive" test room was created that:

- is of rectangular shape
- may have several exterior surfaces with several windows
- can have different wall structures (wall layer sequences)
- can be ventilated
- can have several cooling systems (including non-radiant), and cooling sources.

The same test room was modeled with DOE-2, and the results of the two models were compared.

4.2.1.1 The test room

The test room is 4m x 5m x 3 m, and all its walls are exterior. The floor is in direct contact with the ground.The west wall has a window. The room and window geometry are shown in Figure 15. The same room was modeled in DOE-2.

In order to compare the results of the RADCOOL simulation with the results of a DOE-2 calculation, a test room with the same dimensions was modeled in DOE-2, in the same climate, and with the same wall structure. By simulating the heat transfer in the test room using the same set of assumptions, the comparison of the two sets of results became legitimate.

The Red Bluff, California, Typical Meteorological Year (TMY) weather file was used. A TMY file is created by recording solar radiation and surface meteorological data on an hourly basis over the period from January 1953 and December 1975, and selecting specific calendar months from this period as the most representative or typical. A TMY weather file is therefore a representative weather file for a given location.

To match the DOE-2 model, a "pre-heating" period was simulated: the weather corresponding to a chosen day was repeated several times in order to provide the conditions for the building structure to adjust for the thermal storage effects. In our case, the selected test day was June 1, and the pre-heating period was set to 7 days.

No internal loads, or mechanical systems, were modeled inside the test room. The comparison of the two models was aimed at showing the similarities, or discrepancies, in their respective heat transfer calculations.

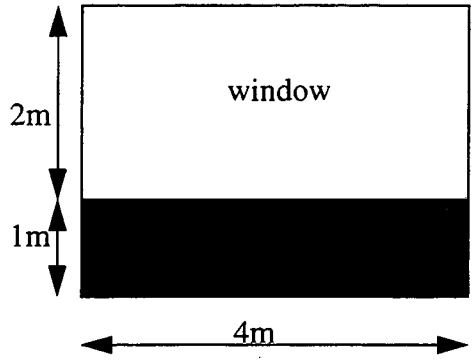

Elevation - the west-facing wall

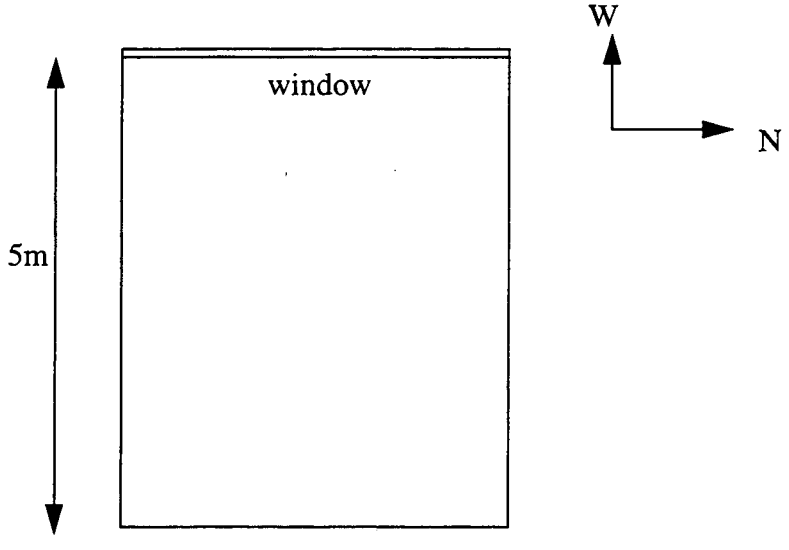

The test room - plan

Figure 15. Test room description for performance evaluation in California

4.2.1.2 The structure of the walls

Three different wall structures were modeled (Figure 16). For simplicity, each structure was applied to all six passive walls.

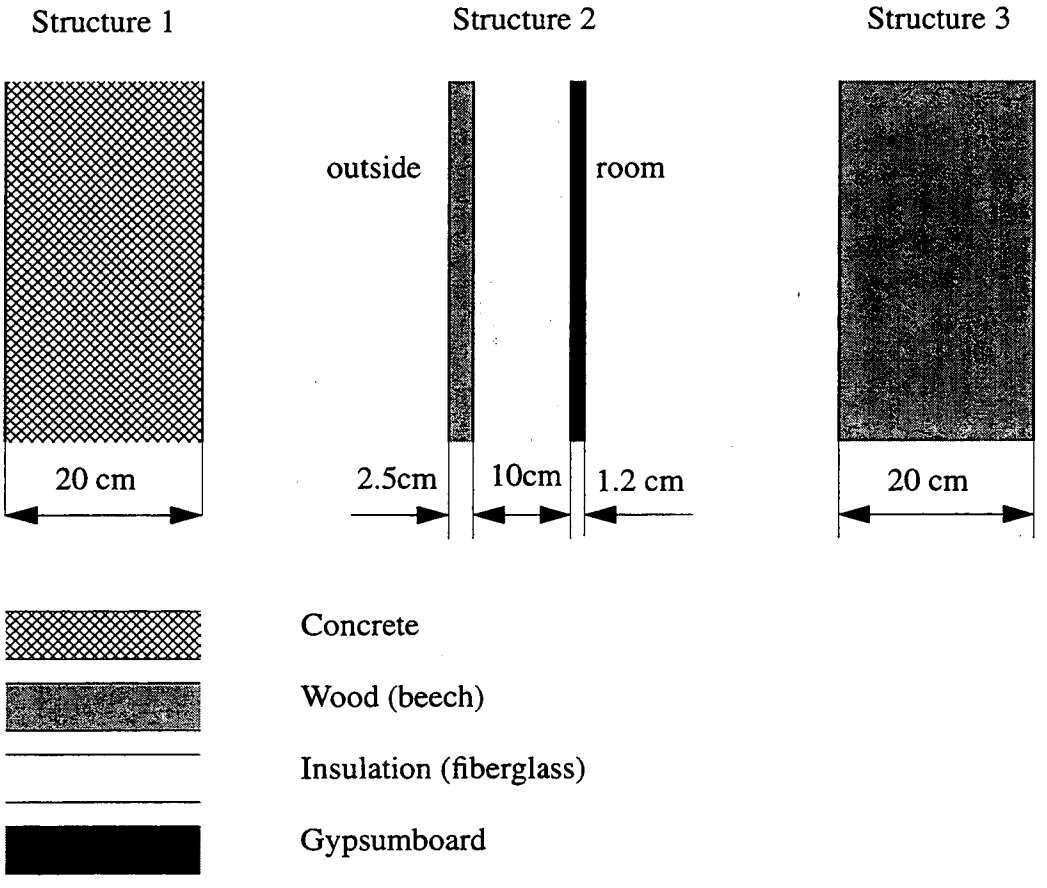

Figure 16. The material structure of the walls in the test room

The material properties of the layers and of the window glass are the following:

	Density [kg/m^3]	**Specific heat [kJ/kg K]**	**Conductivity [W/mK]**
Concrete	2400	1.04	1.80
Wood	800	2.20	0.20
Gypsumboard	1000	0.80	0.40
Fiberglass	90	0.60	0.036
Glass	2700	0.84	0.78

4.2.1.3 Results

The parameter chosen in the comparison of the two models was the indoor air temperature. Figures 17 - 19 compare the RADCOOL and DOE-2 calculations of the test rooms indoor air temperature of the test room, for varying outside air temperature.

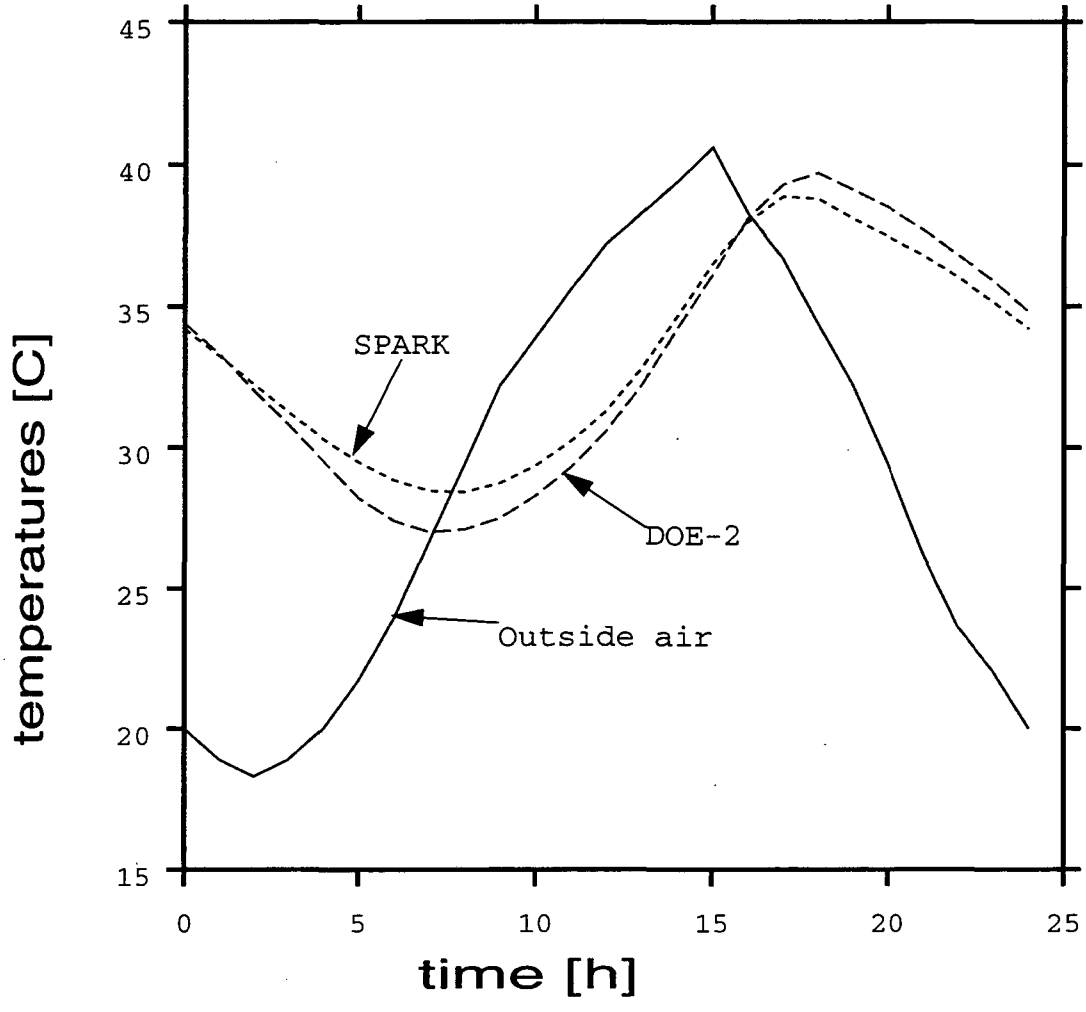

Figure 17. Indoor air temperature: structure 1 (concrete)

The first structure has high thermal mass. The concrete conducts to its core and stores the heat incident on its surface. As a result, the diurnal swing of the test room indoor air temperature is damped and delayed relative to the outside air temperature.

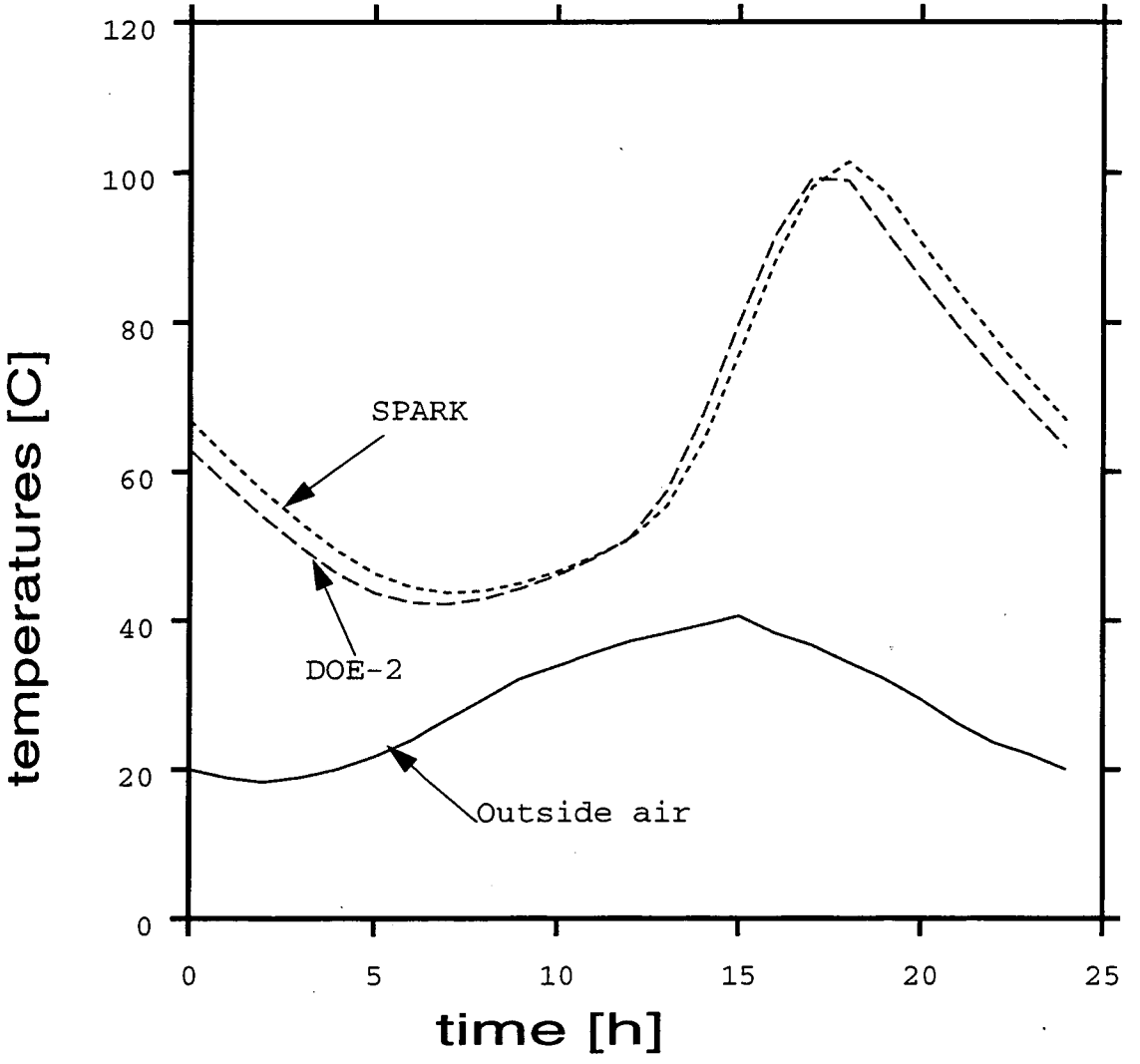

Figure 18. Indoor air temperature: structure 2 (wood - insulation - gypsumboard)

The second structure represents a custom exterior wall. Insulation is sandwiched between the wooden exterior and the gypsumboard interior layers. This structure is designed to reduce the heat conducted through the building envelope. As a result, the test room becomes very hot during the day, since insulation retards conduction back out of the room of the solar heat gain through the window.

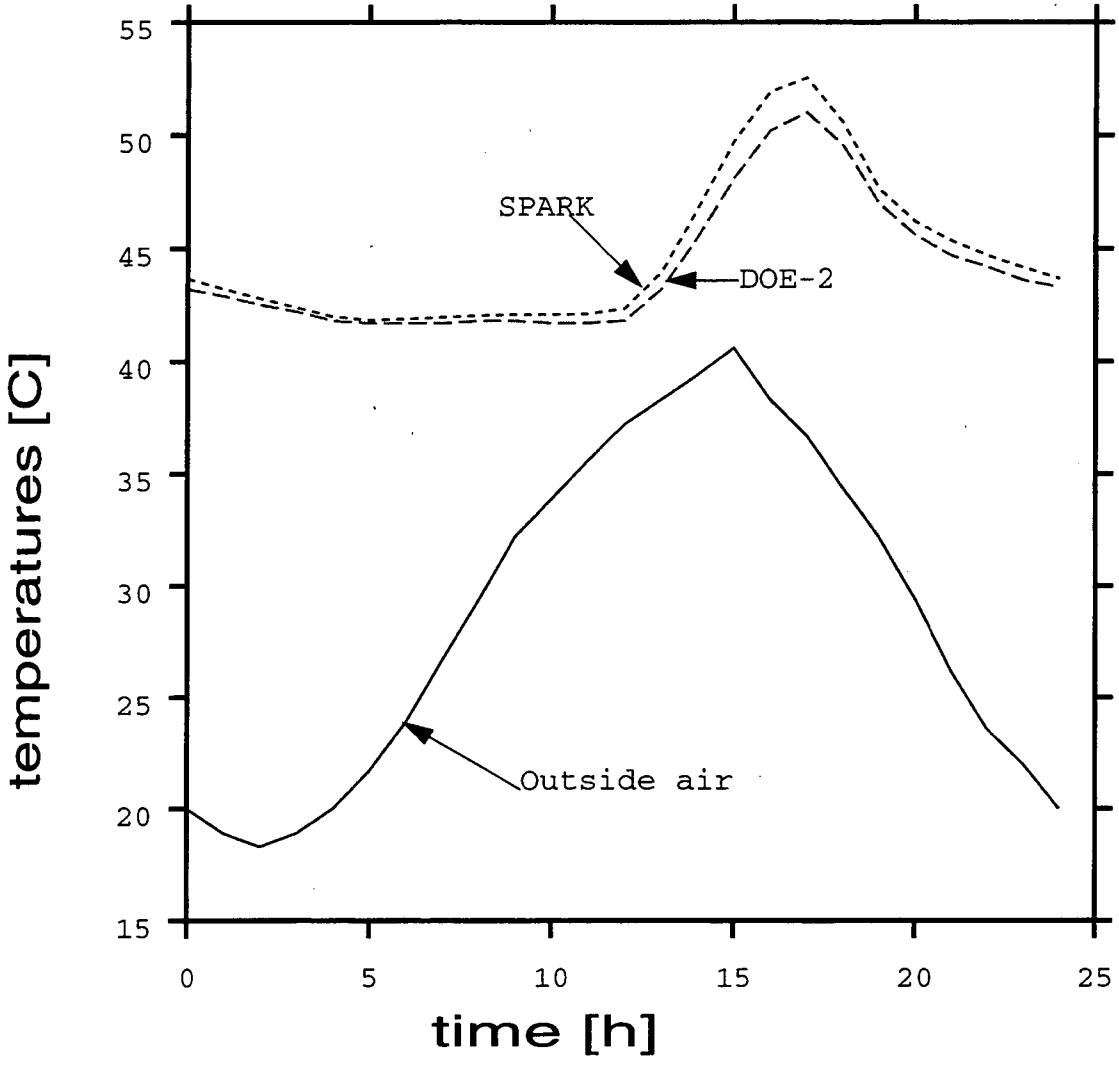

Figure 19. Indoor air temperature: structure 3 (wood)

The third structure is an "all-wood" room. It behaves like the concrete structure, but there is less heat storage in the walls since less heat is conducted into the walls due to the lower conductivity of wood. as compared to concrete. The diurnal swing of the inside air temperature is damped, but the temperatures are higher than in the case of the concrete structure.

For all structures, RADCOOL and DOE-2 agree within 2° C.

4.2.2 Comparison with measured data

RADCOOL was compared with measurements on a building in Horgen, Switzerland (near Zürich) with a core cooling system. On-site weather data was available.

4.2.2.1 The test room

Room: 2.9 m x 4.3 m x 2.85 m (see Figure 20)
- orientation: SE (65° east of south)
- position: top floor (height = 12.8 m above the ground), facade office (not a corner office)

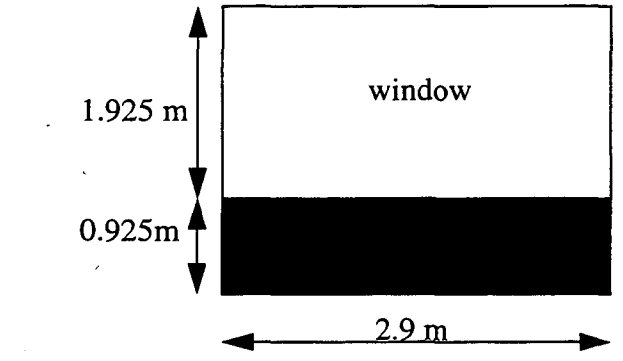

Elevation - the SE-facing wall

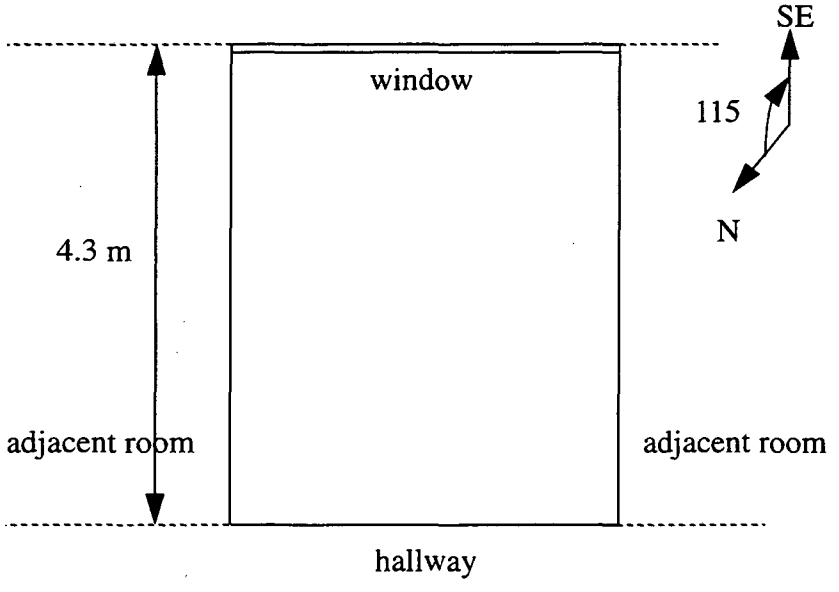

The test room - plan

Figure 20. The test room orientation and layout

4.2.2.2 Wall composition

Facade (exterior wall): 2.9 m x 2.85 m

- lower piece: 2.9 m x 0.925 m; 9.7 cm insulation (mineral wool) sandwiched between a 3 mm aluminum plate (outside) and a 2 mm steel plate (inside); overall U=0.34 W/m^{2}K
- window: 2.9 m x 1.925 m, double pane; overall U = 1.75 W/m^{2}K; transmissivity = 60%, absorptivity considered 5% for each pane (10% total), in both direct and diffuse radiation
- shades: exterior, automatic blinds, with threshold for closing at 120 W/m^{2}incident solar radiation; transmissivity when closed: 15%

Interior walls:

- an 8 cm layer of sheetrock sandwiched between 2- 4 mm layers of plaster (Figure 21)

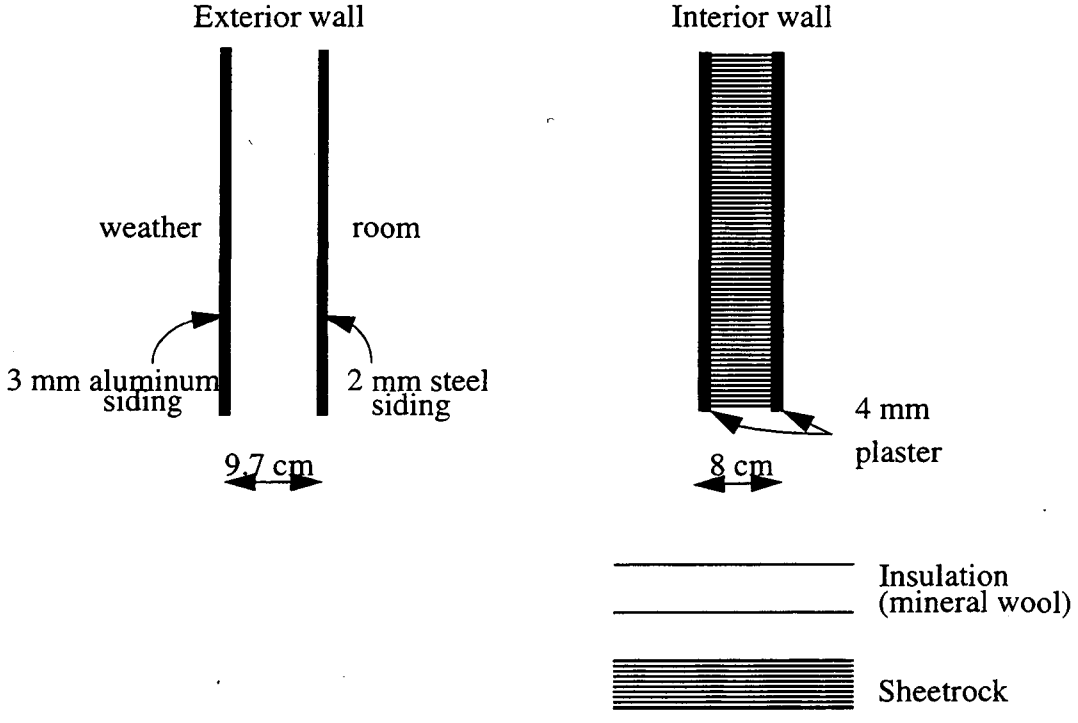

Figure 21. Wall composition in the test room.

Ceiling (also roof): 2.9 m x 4.3 m

- 47 cm concrete with pipes, 1 mm vapor barrier, 10 cm roofmate insulation, 1 mm tar paper, 4 cm gravel, 12 cm concrete tiles; overall U=0.32 W/m^{2}K

Floor: 2.9 m x 4.3 m

- raised floor over concrete slab
- 25 cm concrete, 5.5 cm still air layer, 4 cm plywood (or chipboard) and 8 mm carpet; overall U=2.5 W/m^{2}K

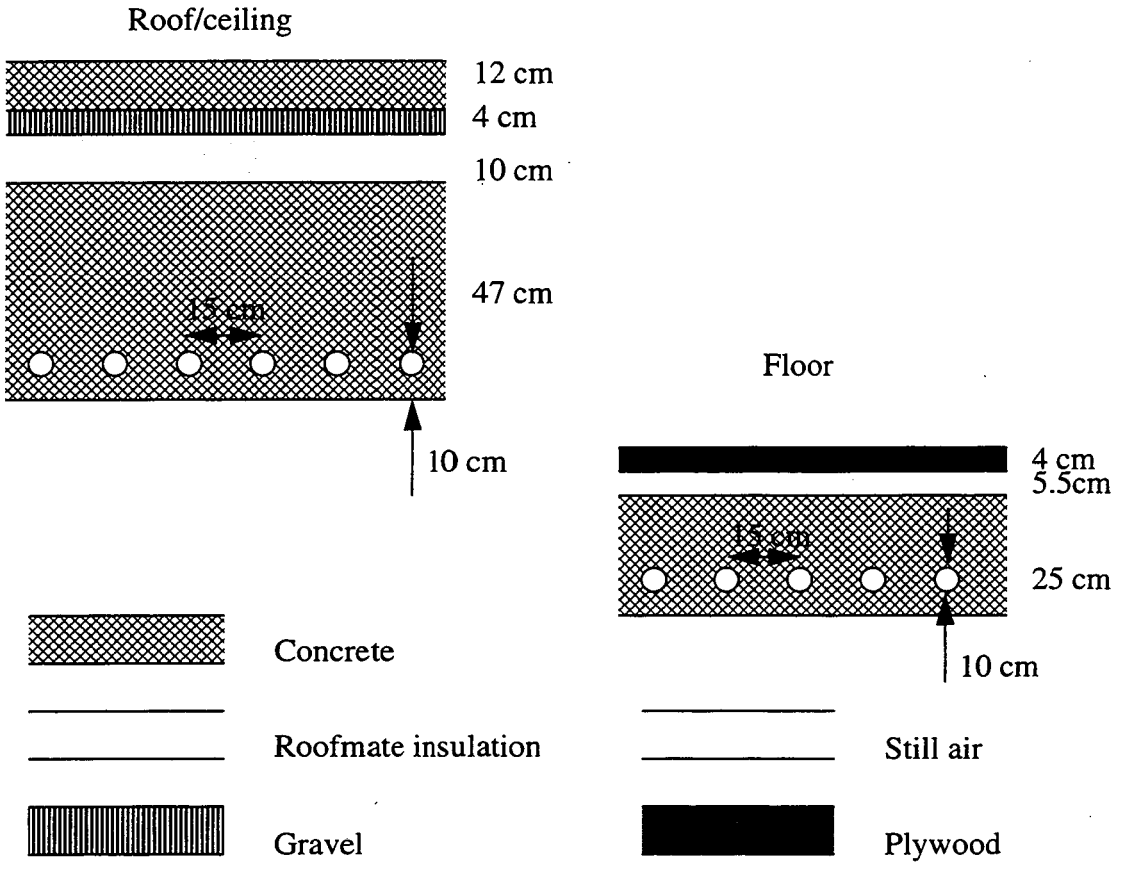

Figure 22. Roof and floor composition in the test room.

The described materials have the following properties:

	ρ [kg/m3]	c_t [KJ/kg-K]	λ [W/mK]
Mineral wool	85	0.83	0.034
Gypsumboard	1000	0.80	0.40
Sheetrock	1000	1.10	0.40
Concrete	2400	1.04	1.80
Roofmate insul.	33	1.40	0.032
Gravel	1650	0.90	0.70
Still air	1.2	1.00	0.59
Plywood	800	2.50	0.15
Polyethylene			0.35

4.2.2.3 Loads

1. The following **occupancy pattern** was simulated during the measurement period: 35 W/m^2 (a total of 436 W), from 8 am to 12 pm and 1 pm to 5 pm, Monday through Friday.

2. **Solar**: intensities from the weather recorded at a station located about 20 km away (in Waedenswil, 47.25° N and 8. 7° E); there are no tall buildings on the site, so the building does not get shading from any obstacles.

3. **Infiltration**: 0.2 ACH (7.1 m^3/h = 0.002 m^3/s at 2 m/s wind speed).

4.2.2.4 System:

1. **Cooled ceiling**: 100 l/h per register; there are 1.5 registers on the cooled ceiling, which gives 150 l/h (0.042 kg/s) total; water is supplied at a known (variable) temperature.
- pipes: polyethylene, 16 mm exterior and 12 mm interior diameters, 15 cm on center; 10 cm deep inside the concrete.

2. **Ventilation**: 1.1 ACH over the day (39 m^3/h = 0.011 m^3/s) when people are in, (8 am to 5 pm, Mon - Fri) and 0.55 ACH (19.5 m^3/h = 0.005 m^3/s) at night; air is supplied at a known (variable) temperature.

4.2.2.5 Boundary conditions:

1. There are measurements of the air temperature in only one adjacent room. We used this air temperature for the other adjacent room as well. We used the measured hallway temperature as a boundary condition for the "back" wall.

2. There are measurements of the air temperature inside the room, but not in the room below. We considered the air temperature of the room below to be the same as the air temperature of the test room.

3. There are measurements of the air temperature 10 cm above the floor, and the report that came with the data says that the floor surface temperature is about equal to that air temperature. We took the average air temperature as the air temperature near the floor as well.

4. There are measurements of the inlet water temperature in the ceiling of the test room, but not in the cooled floor (ceiling of the room below). We took the water temperature in the cooled floor to be the same as the water temperature in the ceiling.

5. There are measurements of the outside air temperature near the building, and at the weather station 20 km away from the building. We used the temperatures measured near the building. We took the solar radiation measurements from the weather station.

6. The shade operation was "measured", but the last two days do not agree with the inside air profile. We used a calculated shade operation (based on the 120 W/m^2 threshold) for the first 5 days, and simulated the shades shut during the weekend.

7. In the program, 57% of the solar radiation entering the space is directed on the floor, 38% equally distributed among the vertical surfaces, and 5% is reflected back out through the window. These values were determined in a preliminary DOE-2 calculation.

8. In the program, 100 W (50% radiative and 50% convective) of the internal load were considered as generated by occupants and 336 W (30% convective and 70% radiative) by equipment and lights; this gives a total of 151 W (35%) convective, and 285 W (65%) radiative internal loads.

9. In the program, the absorptivity of the window panes is considered constant, and equal to 5% for both direct and diffuse radiation.

4.2.2.6 Results

The following figures show a comparison of simulation results and measurements in the test room.

Figure 23: air temperature in the test room

Figure 24: cooled ceiling surface temperature

Figure 25: return water temperature

Figure 26: simulation=floor surface temperature, measurements=air temperature at 10 cm above the floor

Figure 27: window inside surface temperature.

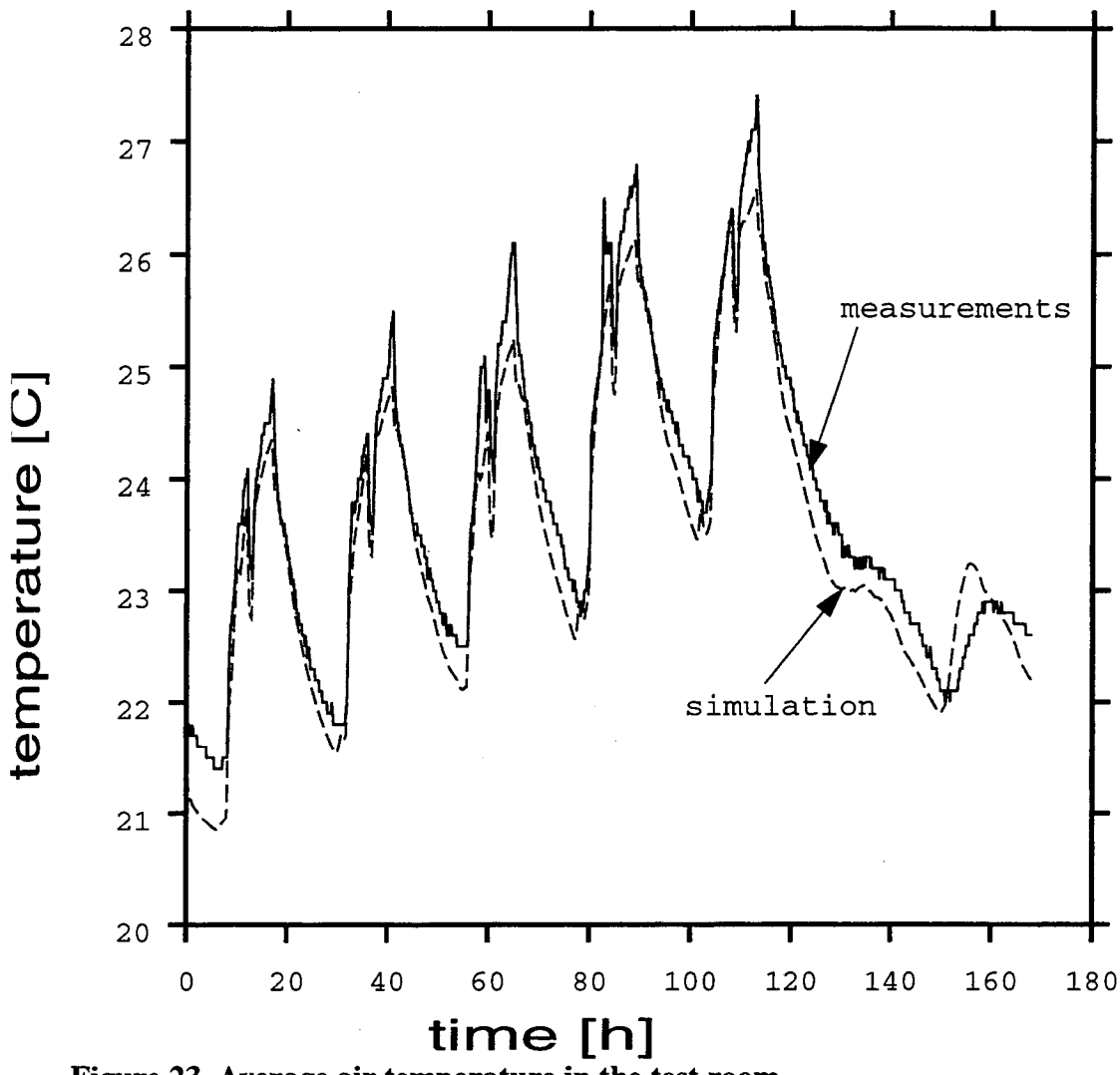

Figure 23. Average air temperature in the test room.

The simulation results for the room air temperature show good agreement with the air temperature measured at 1.1 m above the floor. The last day shows the highest discrepancy, with the simulated time of the peak temperature occurring about 4 hours earlier than the time of the measured peak. This might be due to a discrepancy between the simulated and actual schedule of the blinds.

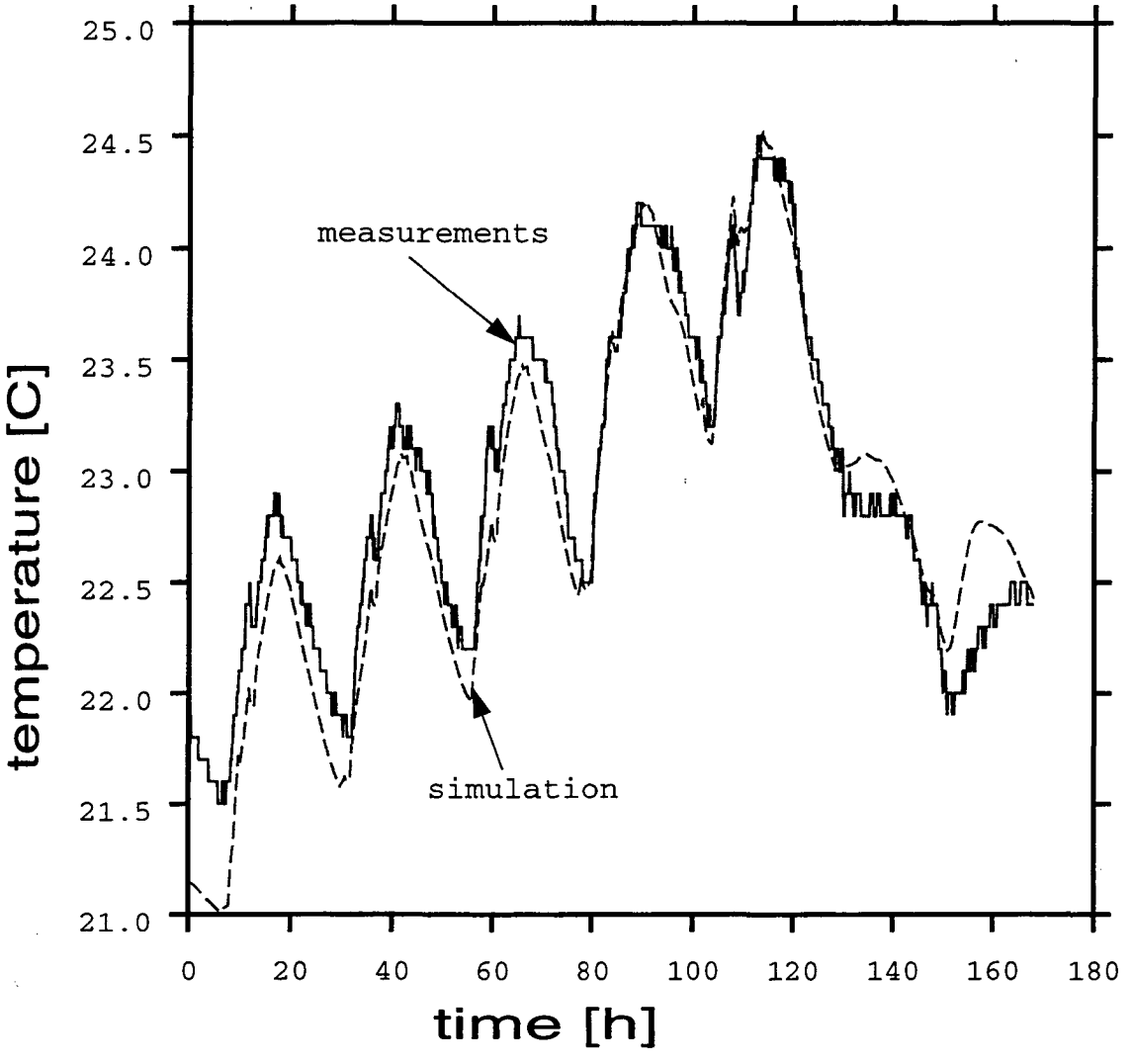

Figure 24. Cooled ceiling surface temperature in the test room.

The simulation results for the cooled ceiling surface agree well with the measurements. Again, the last two days show the highest discrepancy, probably due to a difference between the modeled and actual operation of the blinds.

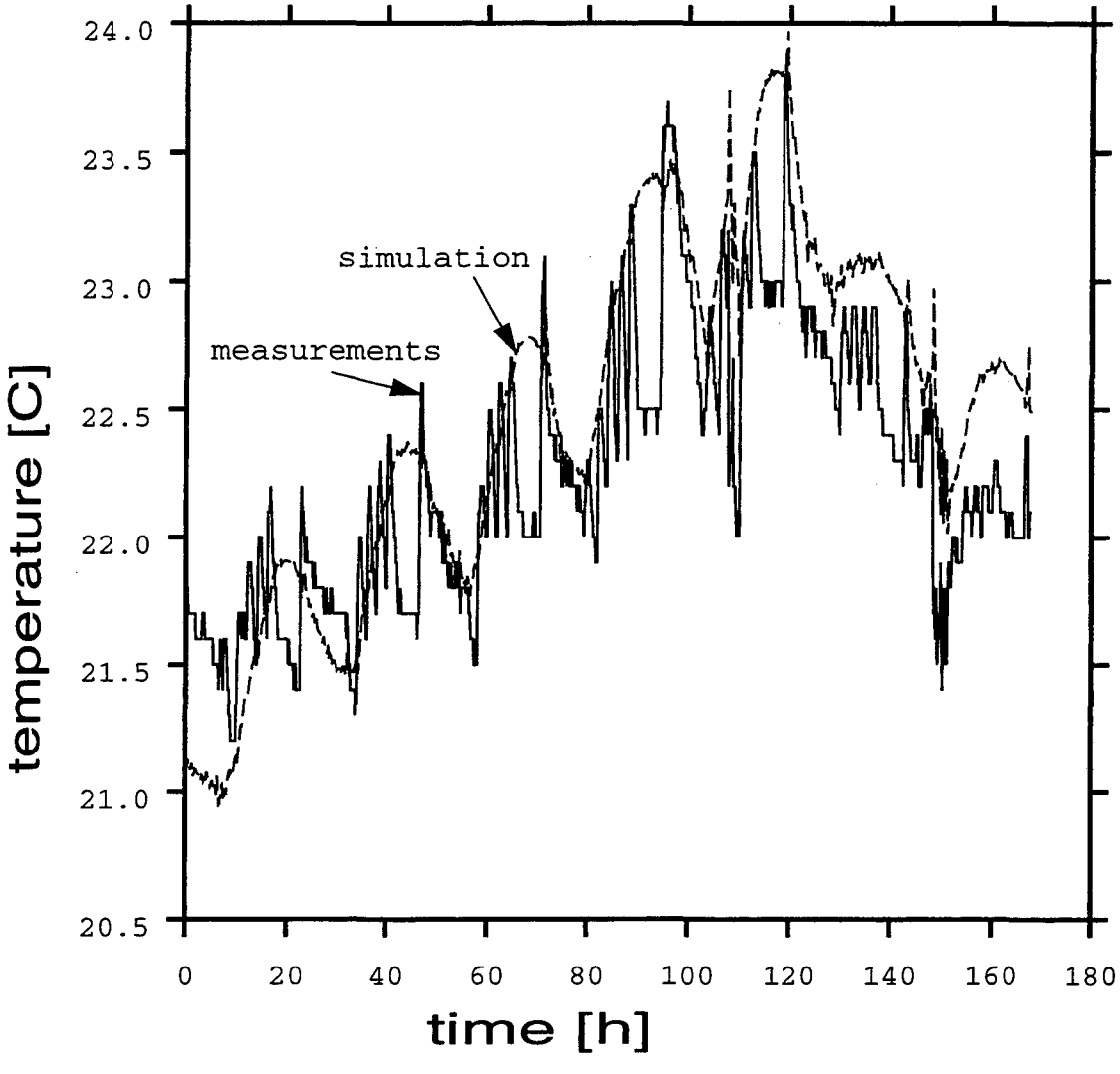

Figure 25. Return water temperature in the cooled ceiling of the test room.

The simulation results for the return water temperature differ from the measured values due to the control strategy employed in the building: when the inlet and return water temperatures differ by less that 1 °C, the system pump is stopped. The simulation assumes that the water runs all the time, so it does not model the pump off-times.

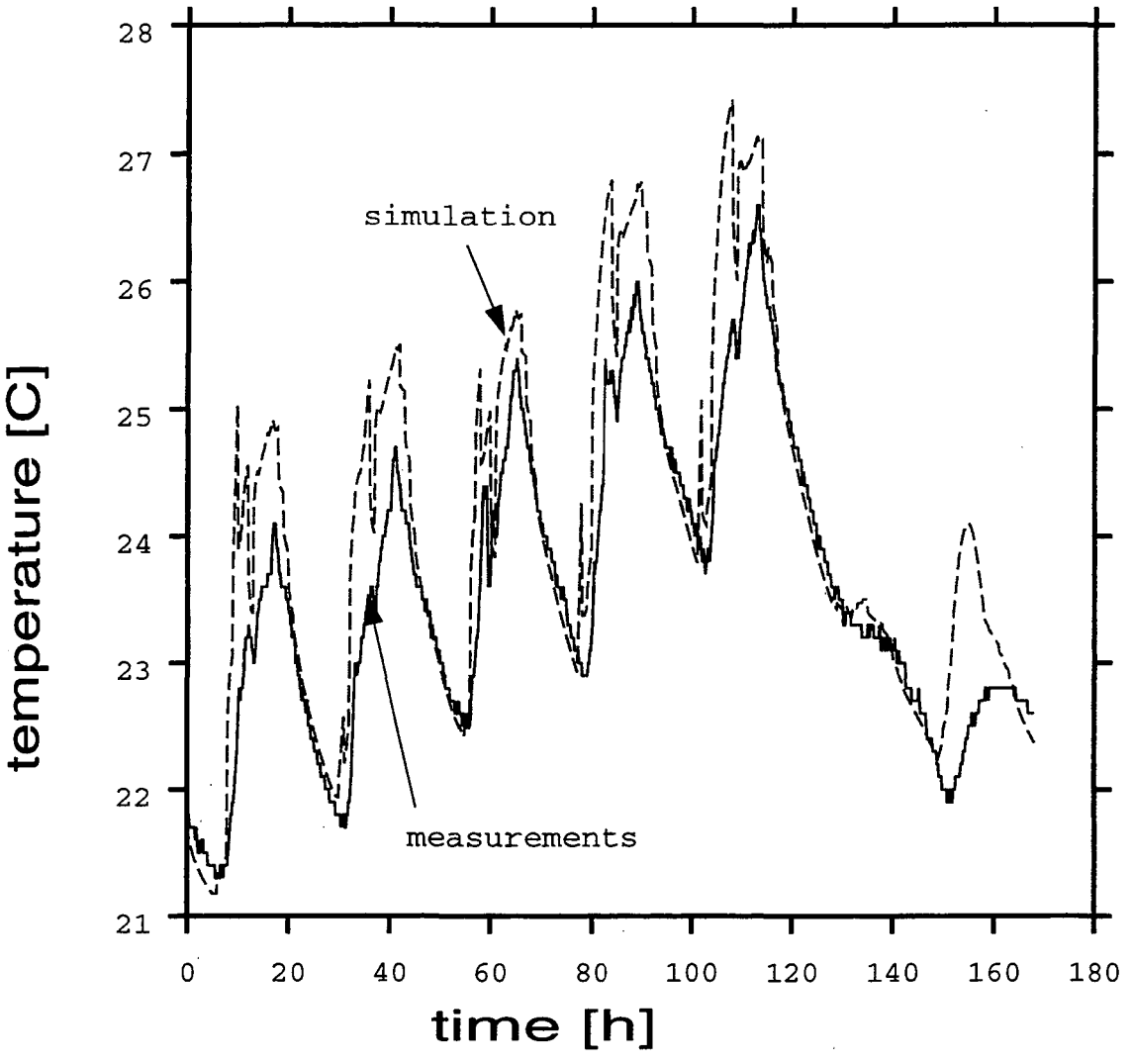

Figure 26. Floor surface temperature in the test room.

The report received with the measurements [37] states that the floor surface temperature is very close to the air temperature measured 10 cm above the floor. We see a discrepancy, which is largest during the day, between the modeled floor surface temperature and the air temperature at 10 cm above the floor. The discrepancy is a result of the fact that in the program 57% of the short wave radiation entering the room is absorbed by the floor. The floor thus gets this amount of solar radiation even at those times when most of the solar radiation is absorbed by the walls. Moreover, in the measurements, the sensor located at 1.1 m above the floor was shielded from solar radiation.

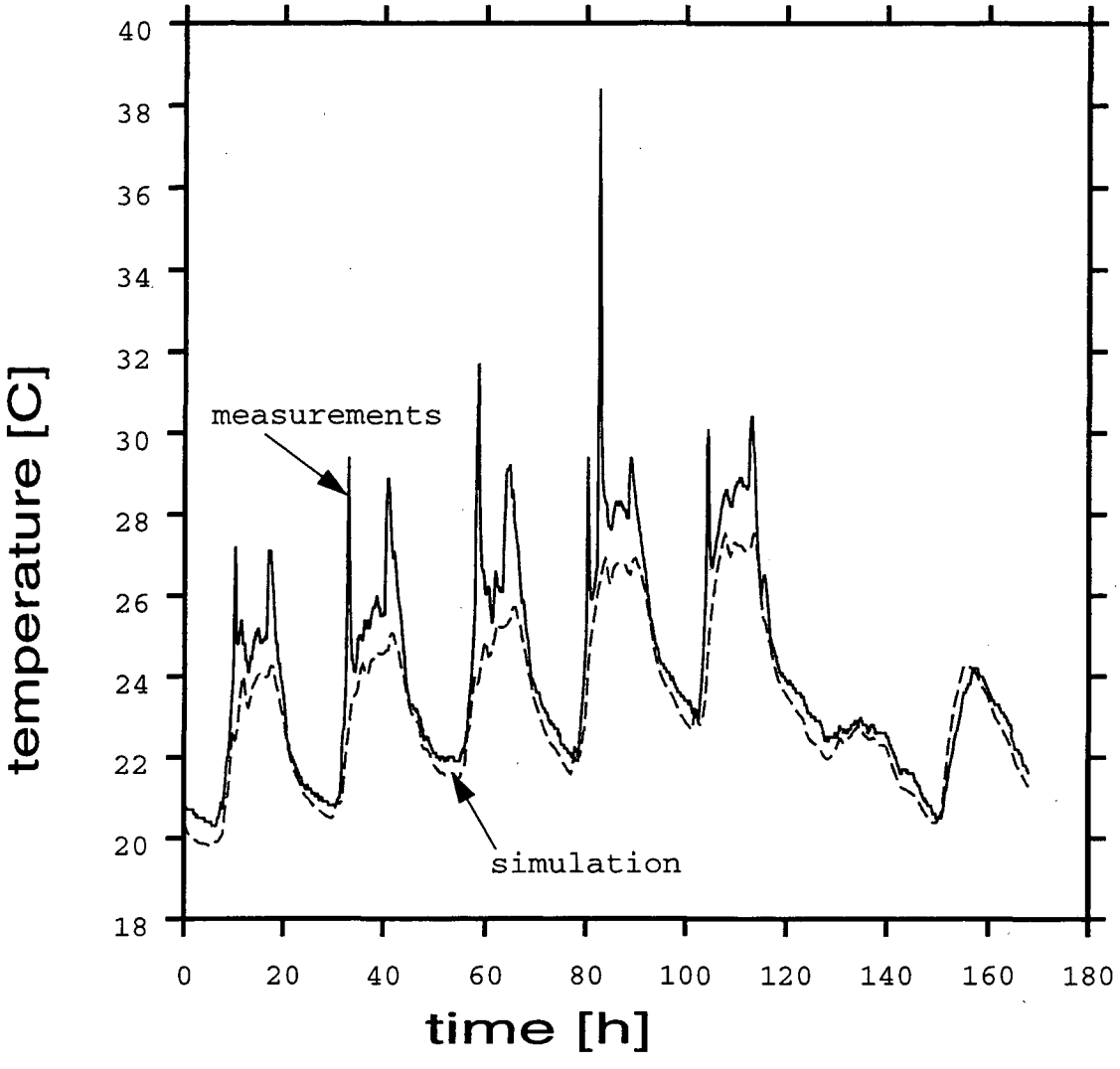

Figure 27. Window surface temperature in the test room.

The simulated and measured inside surface temperature of the window are generally in good agreement. The models differ for the morning and afternoon temperature spikes for the first five days, seen in the measurements but not in the simulation. We believe that these spikes occur at times when the blinds are open (so the glass absorbs direct solar radiation and heats up), but the modeled control assumes they are closed.

5. Ceiling Performance

To evaluate the performance of radiant cooling in California climates, RADCOOL was used to model the heat transfer mechanisms in a hypothetical test room. The San Jose and Red Bluff climates were selected to represent different California climates, and the behavior of the test room equipped with a radiant cooling system was studied.

5.1 The test room geometry

The test room is rectangular, 4m wide, 5m deep and 3 m high. Only the west-facing wall is exterior. The other walls, and the ceiling and floor, represent separation structures between the test room and adjacent rooms. Except for the room behind the "back" wall, all the adjacent rooms are considered to have the same interior conditions as the test room. The back wall is considered as the separation between the test room and a hallway kept at constant temperature. The geometry of the test room and the west-facing wall are shown in Figure 15.

5.2 The structure of the walls

In the set of tests aimed at testing the performance of radiant cooling, the approach was to model a wall structure representative of California office buildings. Figure 16 shows the cross-sections of the exterior and interior walls, of the core cooling ceiling, and of the cooling panel. The material properties of the layers, panel and of the window glass are the following:

	Density [kg/m^3]	**Specific heat [kJ/kg K]**	**Conductivity [W/mK]**
Plywood	800	2.50	0.15
Fiberglass	90	0.60	0.036
Gypsumboard	1000	1.10	0.40
Stagnant air	1.3	1.00	0.57
Aluminum panel	2700	0.89	200
Glass	2700	0.84	0.78

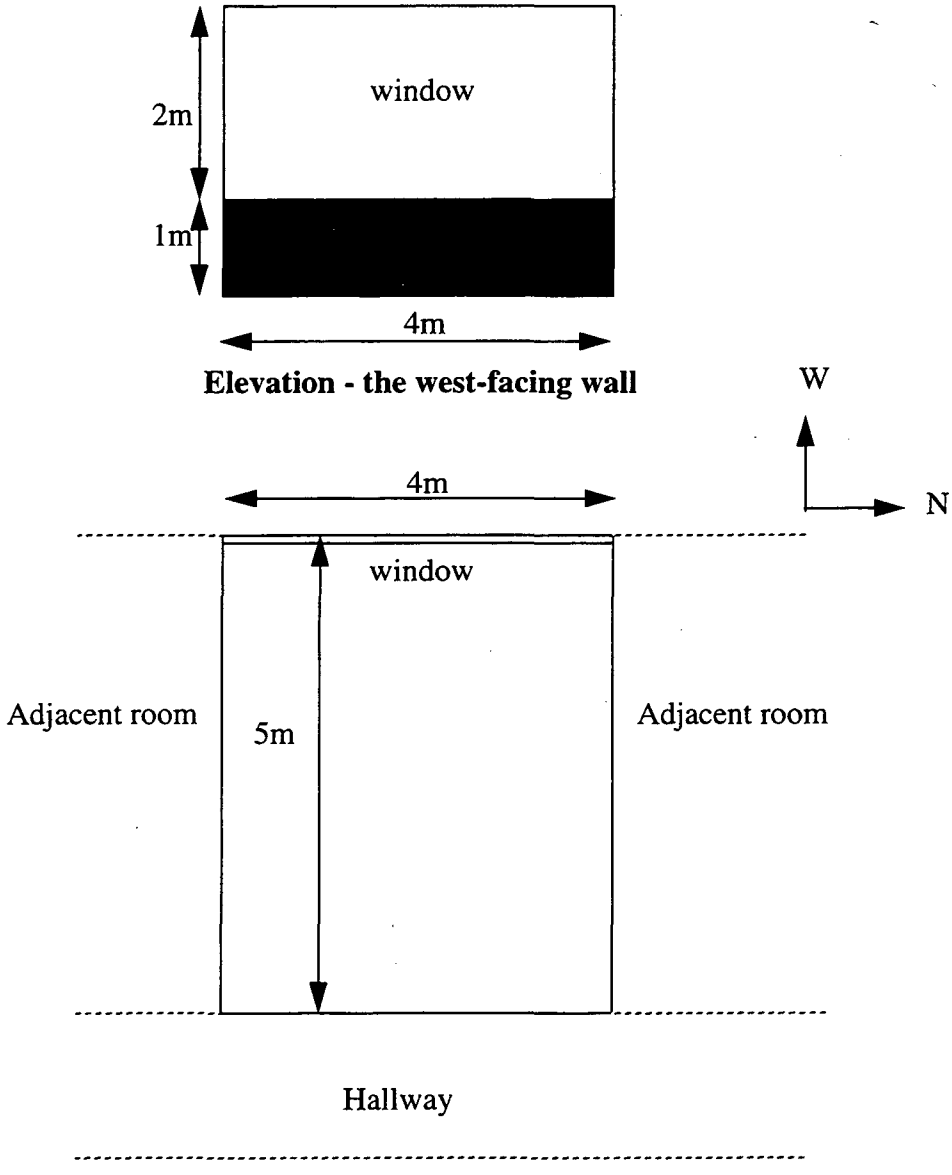

Figure 28. Test room description for performance evaluation in California

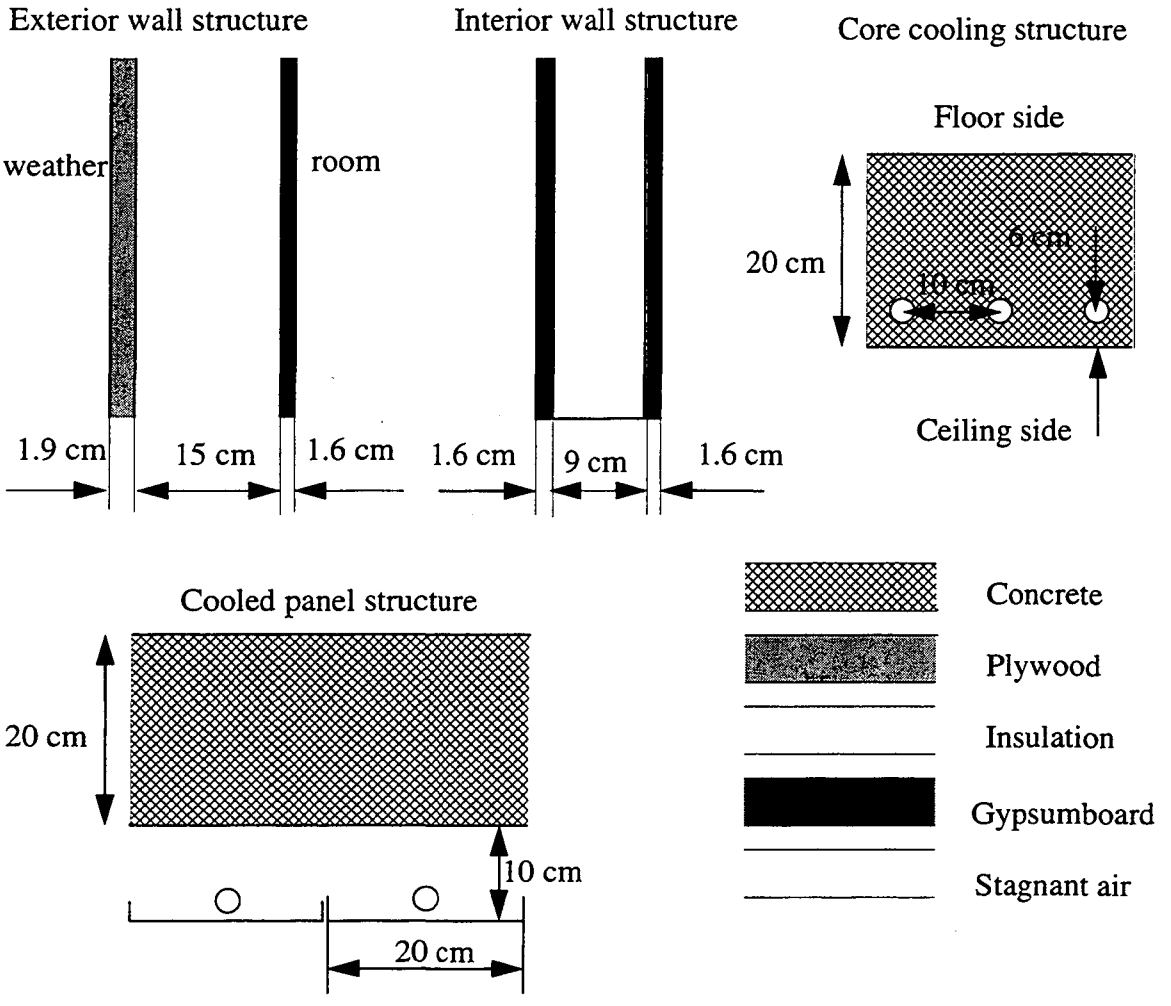

Figure 29. The material structure of the walls

5.3 Test room loads

In order to create the environment specific to an office in California, internal loads from occupants and equipment were added to the window solar loads. The internal loads are described below.

	Load	**Schedule**
Occupants	2 people, 100W each	9 a.m. to 5 p.m.
Equipment and lights	900 W total	9 a.m. to 5 p.m.

5.4 System operation

The cooling in the test room is provided by circulating water through pipes imbedded in the core cooled ceiling, or attached to a suspended cooling panel. In both core cooling and panel cooling the system operation has "mixing control". This control functions as follows. The temperature of the air is compared to the system setpoint temperature. When the room air exceeds the system setpoint the water starts flowing through the pipes. The system setpoint is also the lower limit of a pre-determined mixing band, so at the moment when the water flow has just been turned on, the inlet water is all recirculated water. As the air temperature rises, cold water is mixed with the recirculated water. When the room air reaches the upper limit of the mixing band, the inlet water is all cool water. The mixing fraction (fraction of the cool water flow to the total water flow) is proportional to the air temperature "level" inside the mixing band.

The test room ventilation is provided by supplying outside air.

The system characteristics were chosen as follows. The water flow was calculated so that the water only warms up 2 °C when it removes a load of 100 W/m^2 of ceiling. The inlet water temperature was chosen lower for the core cooling than for the cooled panel strategy because the large thermal mass of the ceiling produces a damping of the cool water flow effect.

	Flow	**Inlet temperature**	**Setpoint**	**Mixing band**
Core cooling	0.24 kg/s	15 °C	21 °C	21 to 22 °C
Cooled panel	0.24 kg/s	17 °C	21 °C	21 to 22 °C
Ventilation	20 l/s	19 °C	-	-

5.5 Time periods for the runs

The time period for the runs was chosen so that the results represent the test room behavior at peak cooling load. DOE-2 calculations were made to determine the time of the peak cooling load in the San Jose and Red Bluff climates. The results show that:

- in San Jose, the day with the highest cooling load is June 14, and

- in Red Bluff, the day with the highest cooling load is July 15.

The run period was consequently set as follows:

- for San Jose, the programs ran with a 3-day pre-heating period using June 12 weather, then with the weather corresponding to June 12-13-14; the results are shown only for the last 3 days;

- for Red Bluff, the programs ran with a 3-day pre-heating period using July 13 weather, then with the weather corresponding to July 13-14-15; the results are shown only for the last 3 days.

5.6 Results

Results are shown for core cooling in Figures 30 - 33 and for panel cooling in Figures 34 - 37. Two graphs presented for each case. The first shows the indoor air temperature of the test room, the operative temperature, and the outside air temperature (the operative temperature is the average of the "equivalent mean radiant temperature" and the room air temperature; the "equivalent mean radiant temperature" is the area-weighted average of the walls, ceiling, floor, and window temperatures).

The second graph shows the room loads and the heat removed by the water. The room loads are those due to window solar gain and internal gains from people and equipment. Not included are the exterior wall conduction gains.

The heat removed by the water is calculated as

$$Q_{into-water} = \dot{m} c_t (t_{return} - t_{inlet})$$

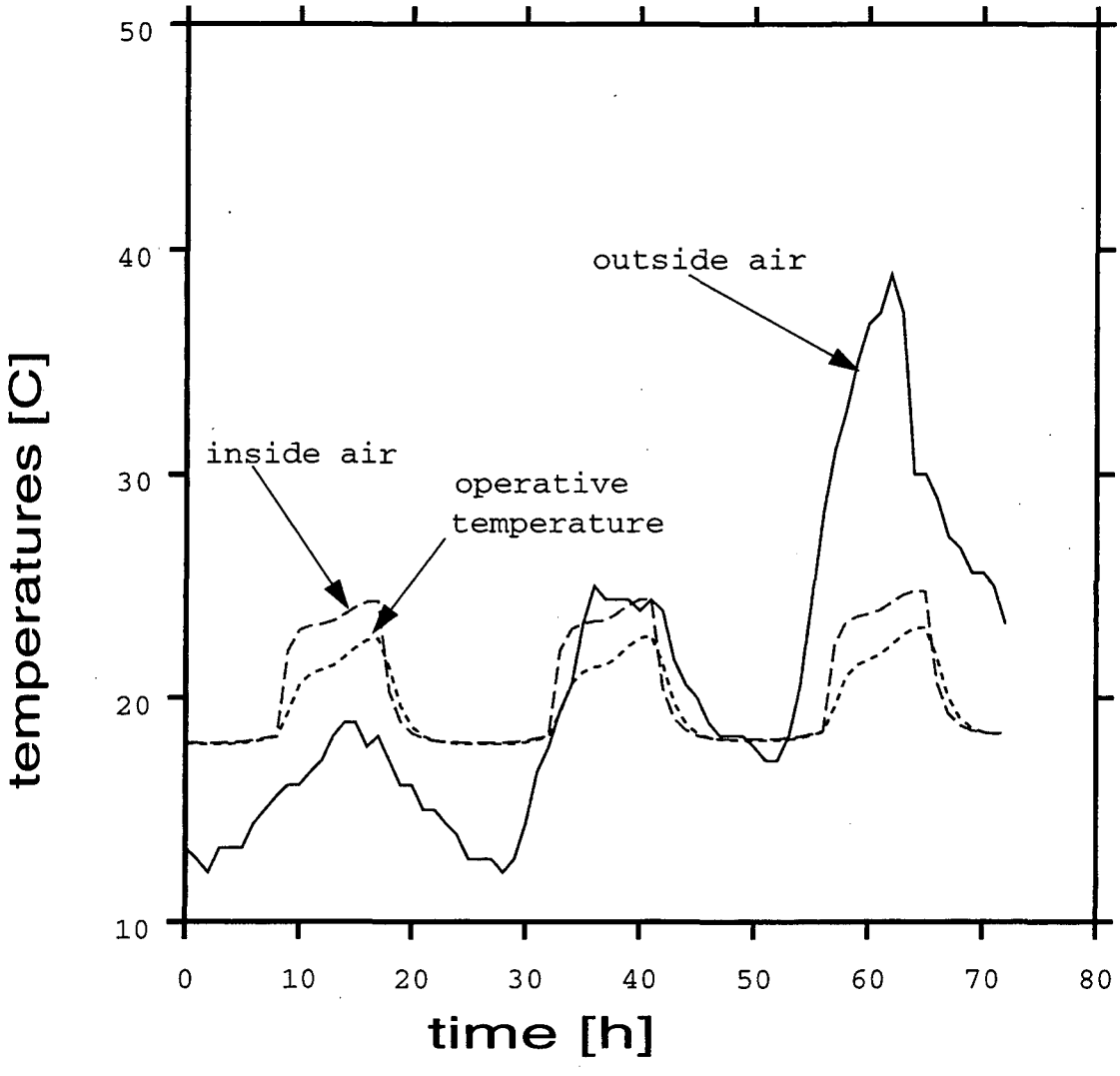

Figure 30. Core cooling in San Jose for June 12-14 weather.

The test room conditioned by core cooling in San Jose is maintained within a comfortable temperature range: 18 °C to 24 °C. The system allows the same inside temperature swing even during the last day, when the outside air temperature has a swing of 22 °C.

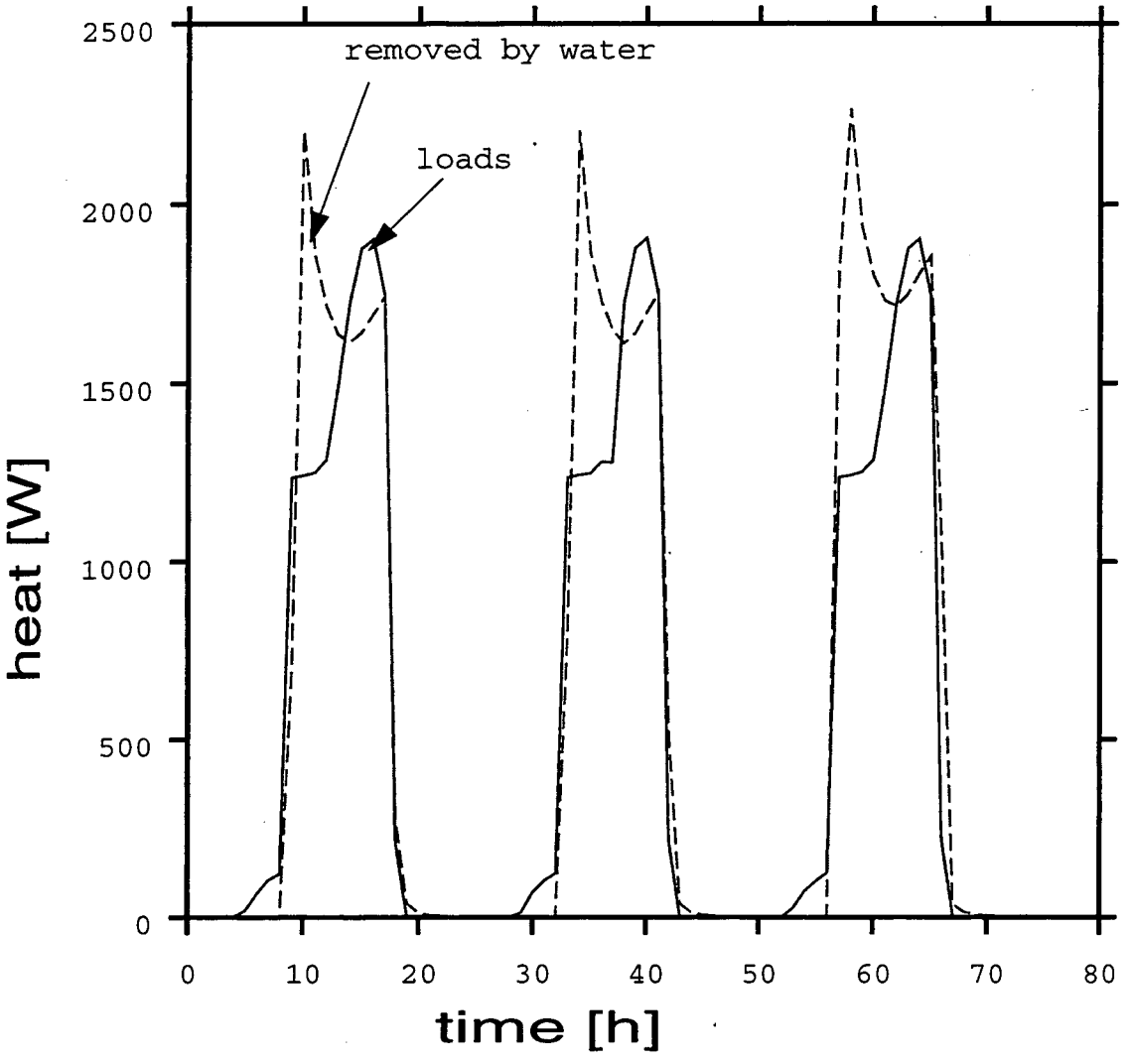

Figure 31. Core cooling in San Jose: comparison between loads and heat removed by the water.

In the case of core cooling, a high initial load (due to occupant arrival and equipment start-up) results in an initial spike of the heat incident on the ceiling surface. The inside air temperature is lower than the system setpoint when this initial load appears, so the water is not flowing through the pipes at this moment. The concrete layer between the ceiling surface and the water pipes stores some of this incident load. As a result, when the water starts flowing through the pipes, the heat removed by the water is higher than the initial room load. Overall, the system has the potential of removing most of the ceiling load in the San Jose climate.

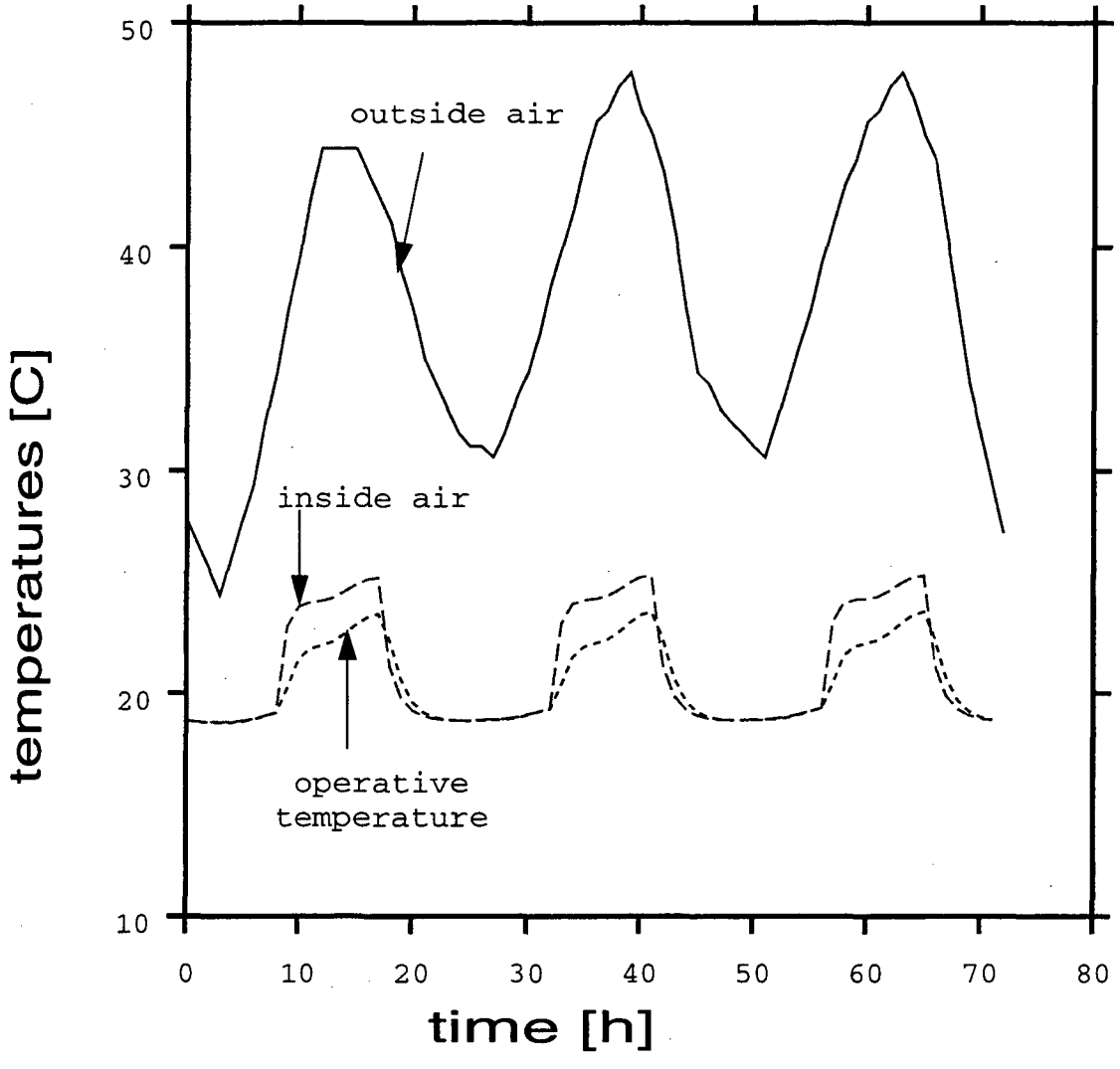

Figure 32. Core cooling in Red Bluff for July 13-15 weather.

In Red Bluff, the outside air temperature shows consistent daily swings of 15 °C to 20 °C. The cooling system can still maintain the inside air temperature within a comfortable range, 19 °C to 25 °C. The operative temperature never exceeds 24 °C.

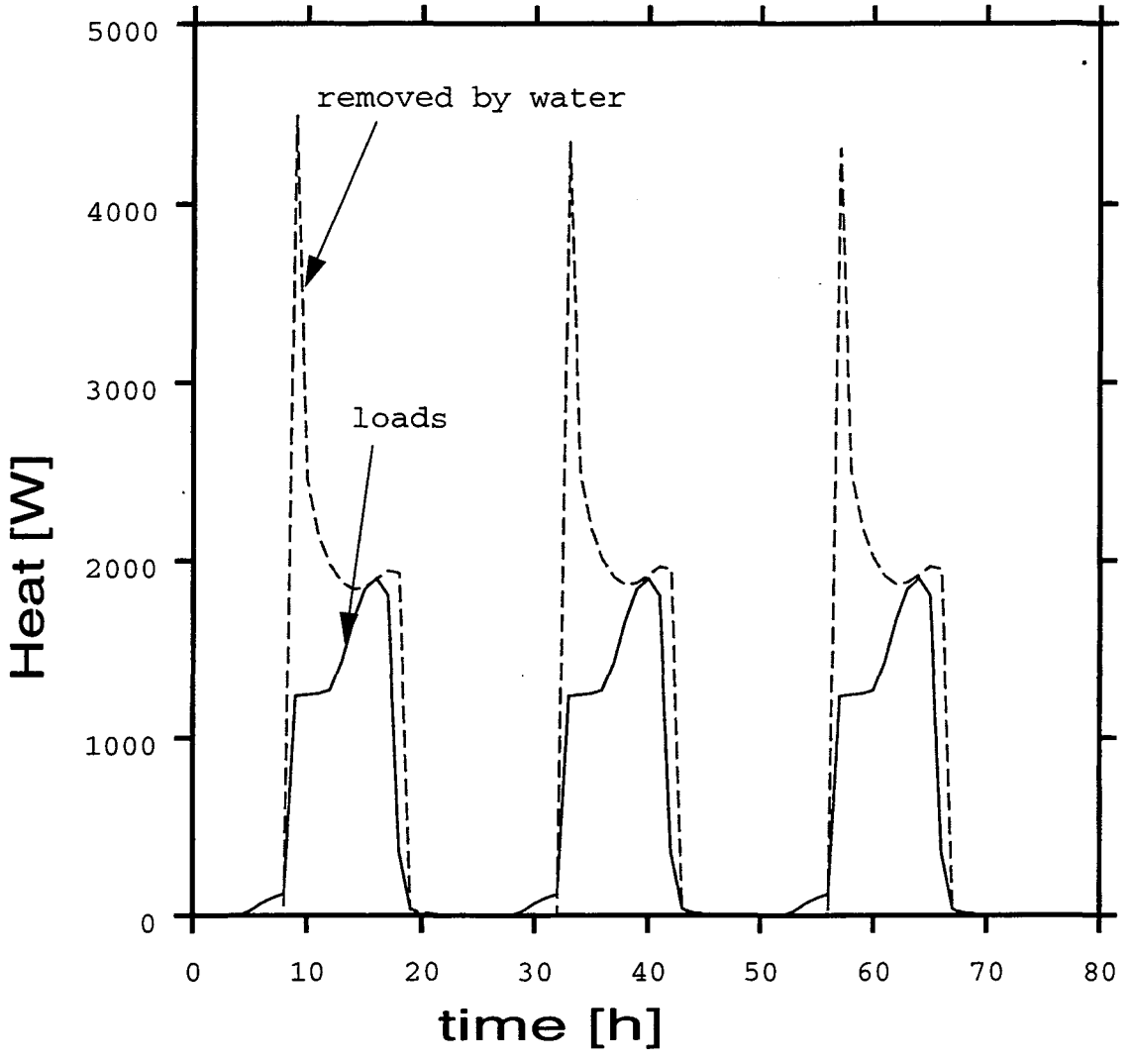

Figure 33. Core cooling in Red Bluff: comparison between loads and heat removed by the water.

Due to the hot weather in Red Bluff, heat conduction through the exterior walls adds significantly to the solar and internal loads. Consequently, the spike of the heat removed by the water at start-up is much higher than in San Jose. Moreover, the heat removed by the water in the afternoon exceeds the sum of the solar and internal loads. The inside air temperature in Red Bluff is higher than in San Jose. Overall, the water cooling system can maintain the test room temperature at a comfortable level.

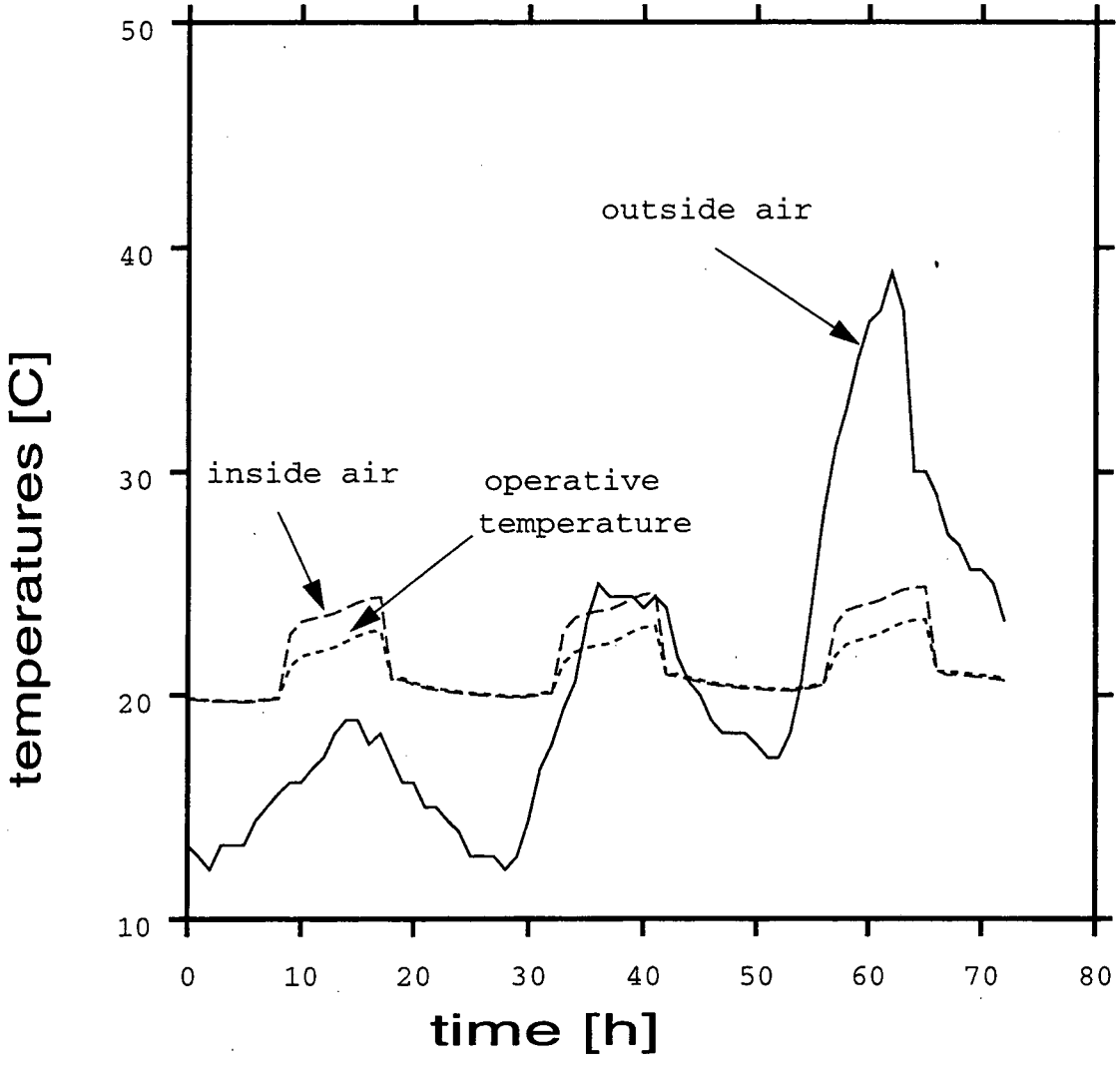

Figure 34. Panel cooling in San Jose for June 12-14 weather.

The aluminum panel cooled with 17 °C water can maintain the test room air temperature in San Jose within the range of 20 °C to 25 °C. The operative temperature does not exceed 23 °C.

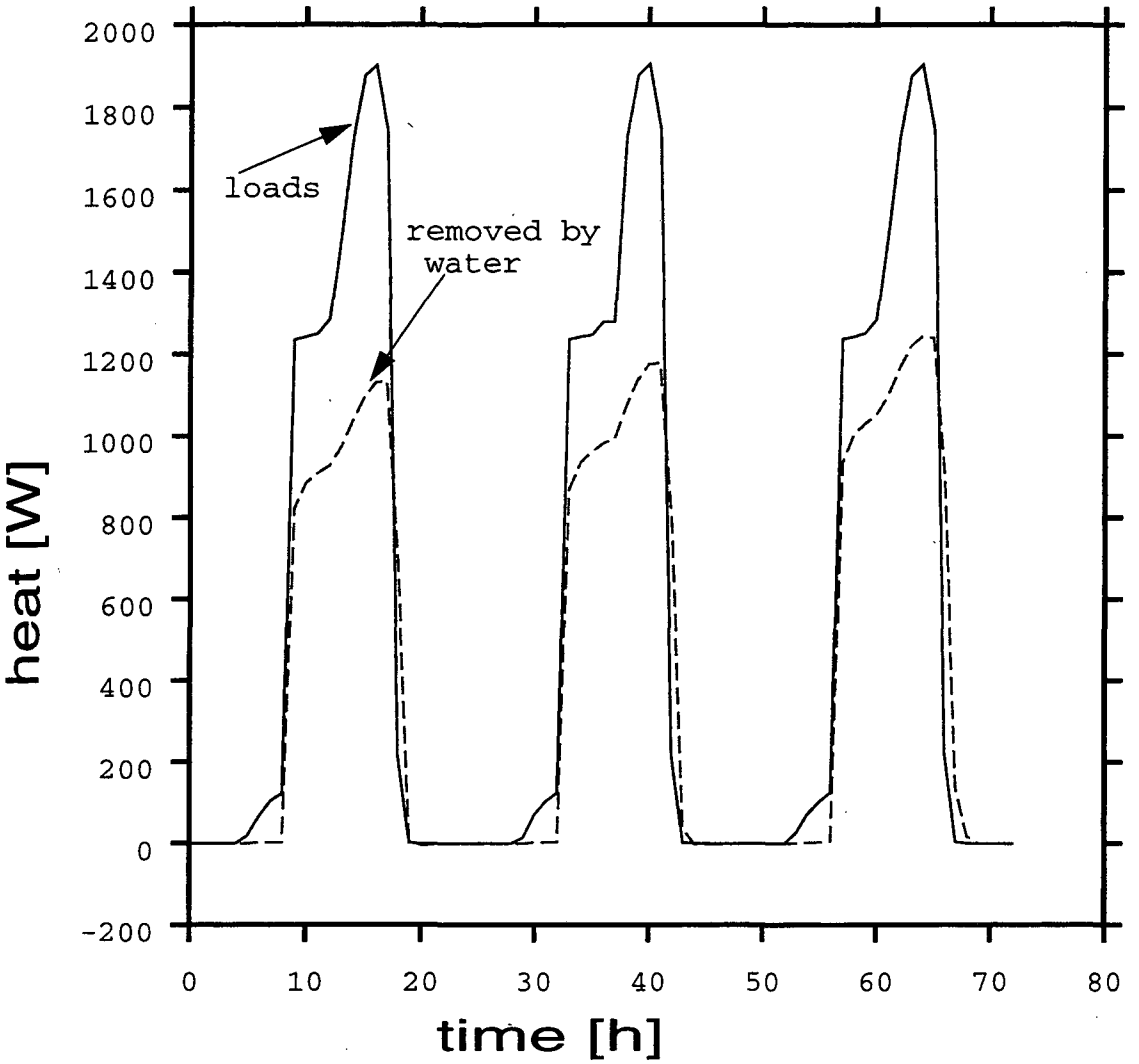

Figure 35. Cooling panel system in San Jose: comparison between loads and heat removed by water.

The suspended cooling panel provides close contact between the cooled water and the room heat. Consequently, a fraction of the room heat is quickly removed by the water, another small fraction is removed by ventilation, while the rest contributes to the inside air temperature increase shown in Figure 34.

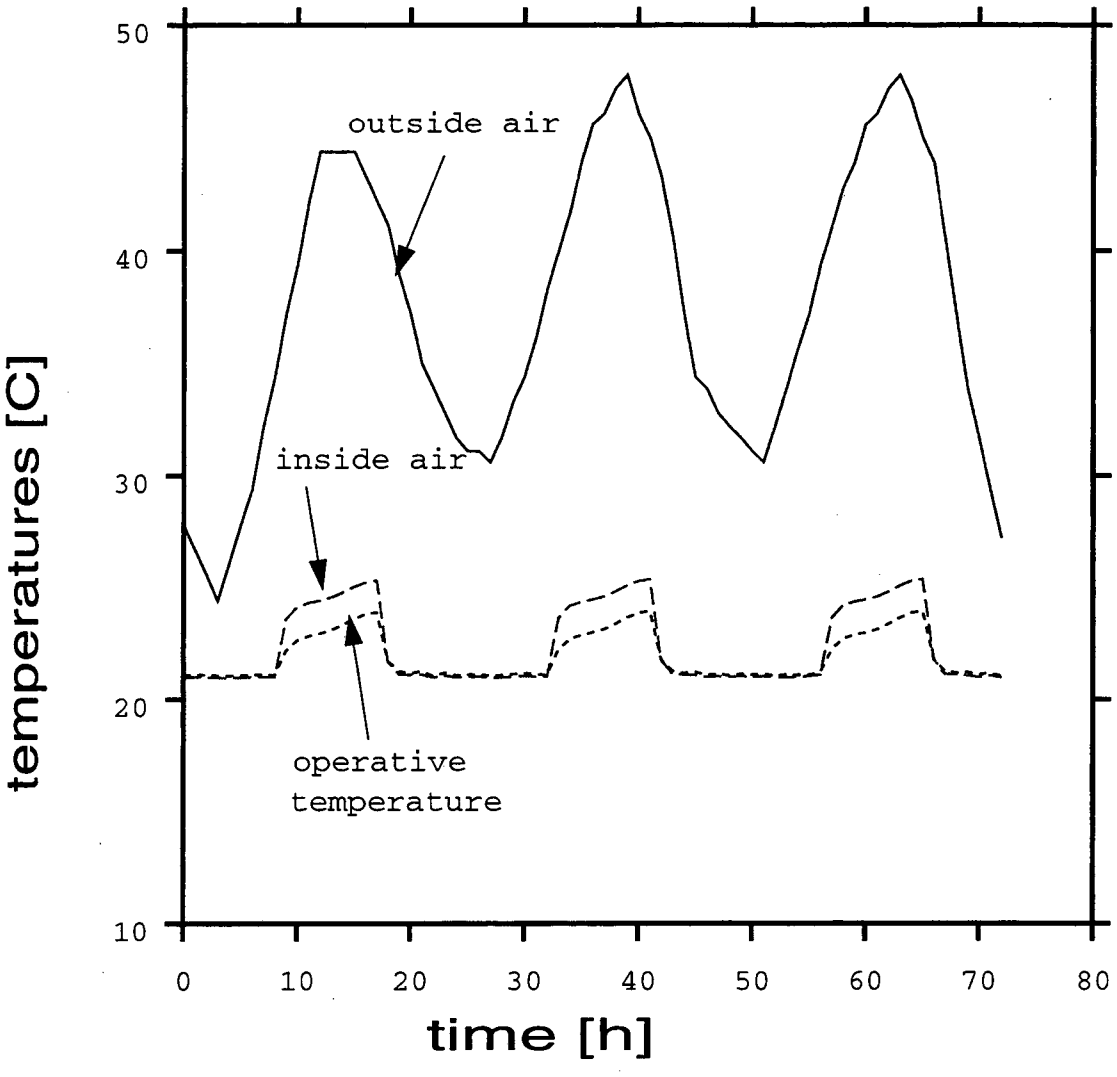

Figure 36. Panel cooling in Red Bluff July 13 - 15 weather.

The higher loads imposed by the more extreme climate in Red Bluff cause higher inside air temperature than in San Jose. However, the inside air is still kept within the comfortable range of 21 °C to 26 °C.

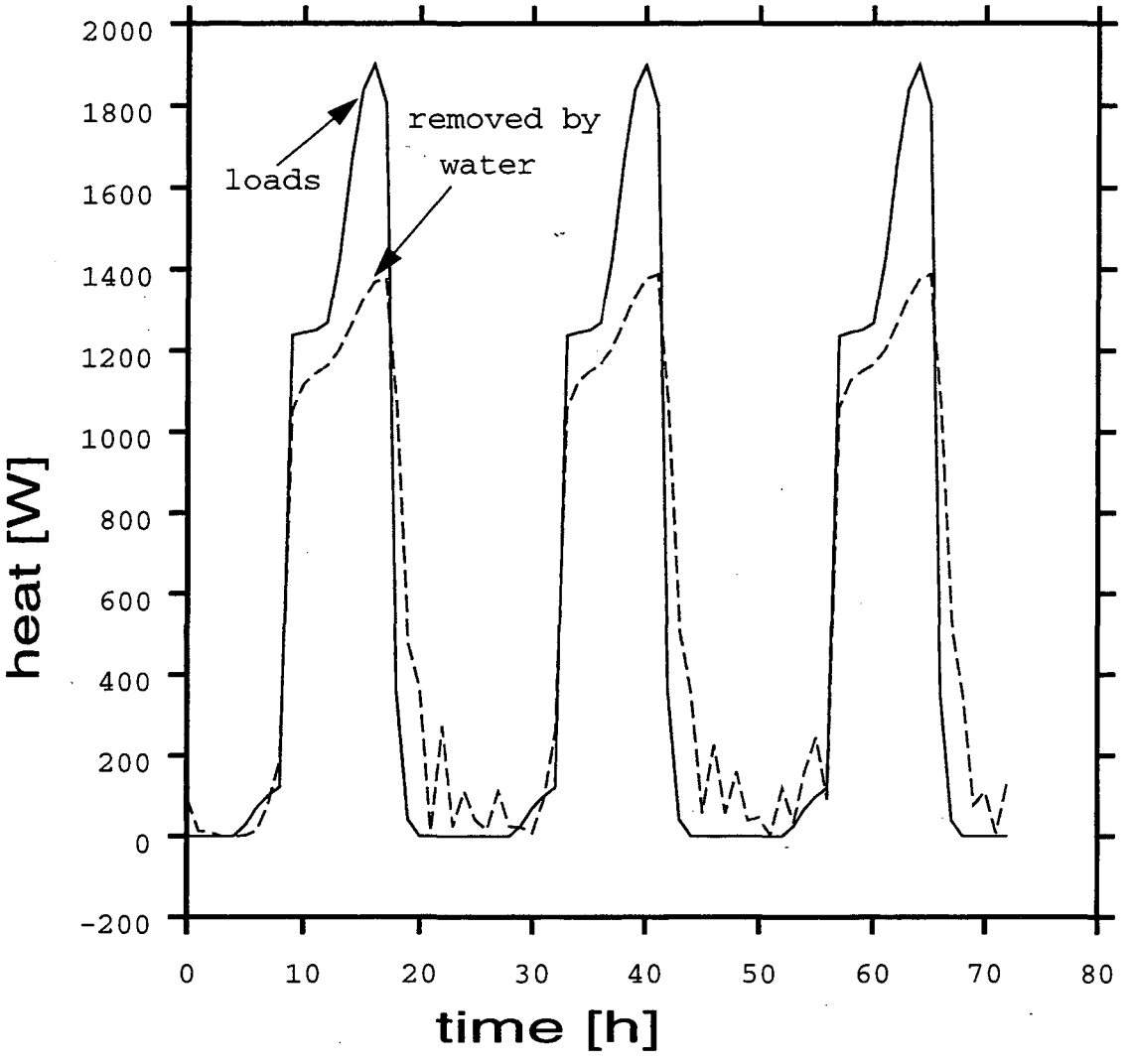

Figure 37. Cooling panel system in Red Bluff: comparison between loads and heat removed by the water.

The panel structure provides good contact between the cooled water and the higher weather-induced loads. The result is that the water removes a large fraction of the ceiling heat, including the extra load due to heat conduction through the exterior wall. As in San Jose, another fraction of the loads is removed by ventilation, while the remaining heat produces an increase of the inside air temperature. The jaggedness of the heat removed by water is due to the fact that the inside air temperature at night is close to the system set-point (21 °C), resulting in a repeated on/off switching of the water flow.

6. Conclusions on performance analysis

6.1 RADCOOL provides useful results

The results in Chapter 5 show that both core cooling and panel cooling have the potential to maintain comfortable conditions inside the test room, even in hot climates. The fact that the cooling is performed with water at temperatures as low as 15 °C, however, shows that dehumidification of the ventilation air is required to provide room air dewpoint control. This is particularly important for a system with imbedded tubes, as condensation might form inside the slab and cause structural damage even when the surface temperature is well above the dewpoint.

Further analyses with RADCOOL can determine the range of weather conditions and room configurations that can be handled with radiant cooling.

6.2 Proposed future development of RADCOOL

In this section we propose enhancements to RADCOOL that would increase its usefulness.

6.2.1 Room air stratification

Air stratification plays an important role for radiant cooling systems. In the case of a cooling ceiling, the cooling load that the system needs to remove increases with stratification. Conversely, if the air in the vicinity of the ceiling is cooled too much, it will move downwards and hinder efficient functioning of a displacement system. There is a secondary effect of air displacement: contaminated air that usually rises and is removed through the exhaust registers is instead recycled.

Air stratification can be introduced in the RADCOOL program using correlations from computational fluid dynamics calculations.

6.2.2 Air humidity, and condensation at cool surfaces

There is a risk of condensation if the surface temperatures in a radiatively cooled room are close to the dew point temperature of the ambient air. Condensation may cause damage to the building materials and to the objects in the space. Furthermore, the air humidity is a comfort factor and moderate relative humidities should be maintained.

A moisture adsorption model for the wall surfaces can be developed [47], to determine the relations between the thermal and humidity effects in a space.

6.2.3 Thermal comfort and radiant temperature at the occupant location

A SPARK module for calculating the heat exchange between the occupants of a room and the room envelope would be a useful addition to RADCOOL, to determine the variables that affect thermal comfort.

A similar model for the heat transfer between the equipment in a space and the room envelope would also be useful.

6.2.4 Heating/cooling sources

The present development of RADCOOL allows for ventilation to take place in the test room but does not model the cooling, heating, or dehumidification of the ventilation air.

A SPARK HVAC library that is under development [48] could serve as a source of modules for modeling primary heating and cooling systems in RADCOOL.

6.2.5 Sizing

Currently the sizing of water flow and temperature to meet the peak cooling load is done manually in RADCOOL. This process could be automated by developing a front end module that calls RADCOOL iteratively with different water flows and temperatures.

7. The Thermal Building Simulation Model RADCOOL

7.1 The structure of RADCOOL

7.1.1 The role of SPARK

As mentioned in section 4.1.1, SPARK was chosen as the environment for RADCOOL due to its ability to describe and solve dynamic equations. SPARK is an environment that was developed to treat problems as networks. A major advantage of this is that fairly complex problems may be defined in an intuitive way. For simple problems, however, using SPARK might be rather cumbersome. SPARK is appropriate if there are many correlations between different variables, i.e. the problem is describable as a large network of simultaneous equations).

Logical statements are difficult to use in SPARK. The reason is that logical statements are by nature bound to a sequential approach to a problem, while the network approach solves a problem for all variables simultaneously. Use of logical statements in SPARK can also lead to long computation times and require large amounts of disk space.

For example, consider a case in which a variable needs to be calculated but only one of ten different cases in which the variable is defined is the "right" case. A sequential approach starts by defining the case to take and then calculates the variable; a network approach calculates the variable in all ten cases and then decides which one to take.

For these reasons, simple tasks and case distinctions are done in RADCOOL outside the SPARK environment. The program flow shown in Figure 38 was chosen for RADCOOL to reduce the number of acyclic calculations and to avoid most of the logical statements.

7.1.1.1 Preliminary data processing

In the data processing section of RADCOOL the complete description of the simulation problem is created. This includes the room geometry, building materials, internal load schedules, weather data, run period, time steps, and other numerical data. Among these are the calculation of shape factors, convection film coefficients, and weather-related variables. All of these calculations are sequential and do not involve cyclic variables, i.e. those requiring an iterative solution.

Another task in this section is creating the files needed for running SPARK. It is worth mentioning that, based on the SPARK library, the problem specification (`.ps`) file, and both the fixed and dynamic input files are created in this process. Since the SPARK interactive user interface is still under development, Appendix B provides the user with the information needed to perform this task.

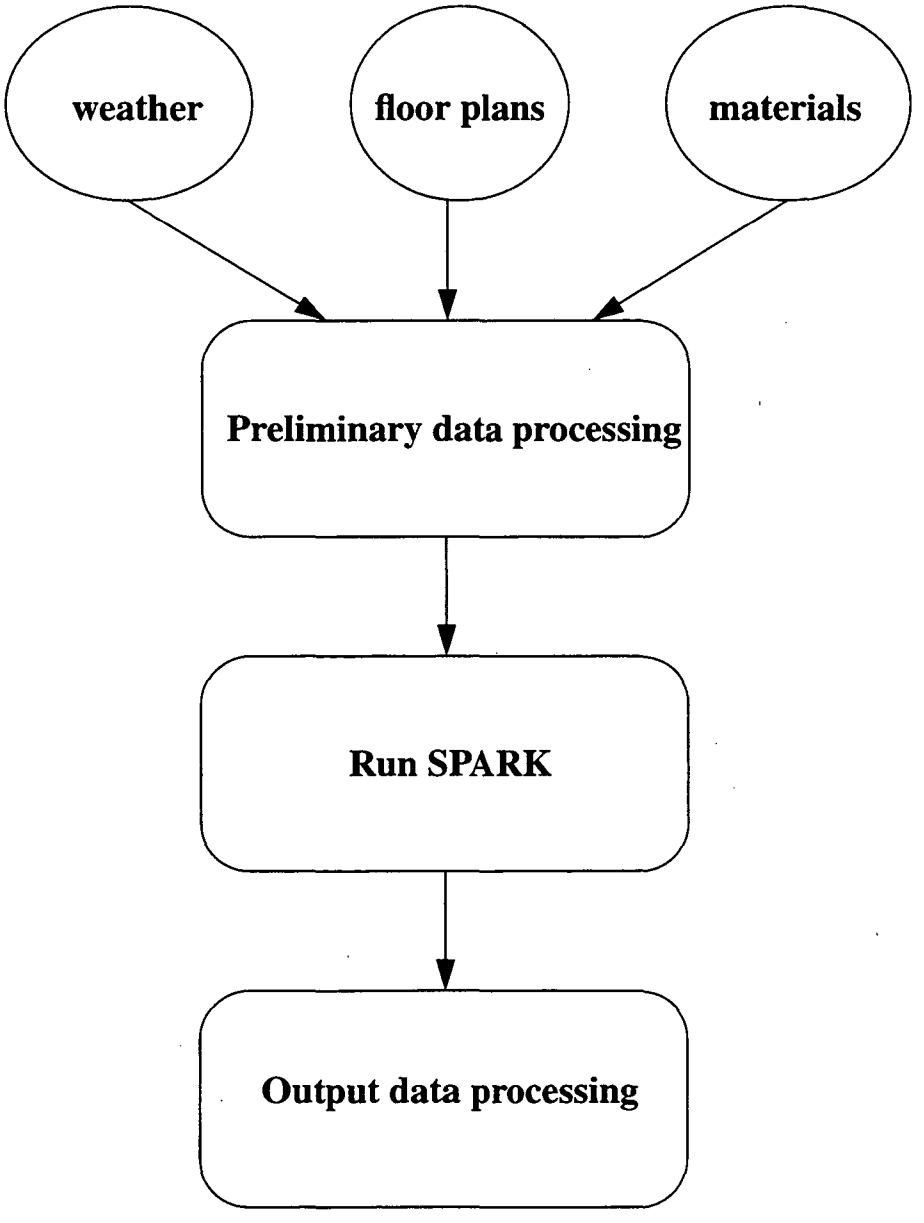

Figure 38. Program Flow for RADCOOL

7.1.1.2 Run SPARK

After the preliminary data processing has created all the necessary SPARK code and input files, RADCOOL runs SPARK.

7.1.1.3 Output data processing

In the output data processing section, the user displays the results of the SPARK simulation as tables and graphs.

7.1.2 An outline to the requirements for the SPARK part

The task derived from sections 4.1.1 and 7.1 is to generate a `.ps` file that correctly describes the building to be modeled. Three requirements have to be met for this task to be successful:

(1) The program has to be able to model several different components: passive wall, cooled wall, window, etc. To this end, a "SPARK library" containing modules (programs) that simulate these components has been created.

(2) The user should be able to connect these components at will, which means that there cannot be a "predetermined" building structure. Therefore, RADCOOL was provided with a highly modular structure. The modules were designed so that they can be connected in any order and in any quantity.

(3) To meet the extensibility requirement of section 4.1.2 it should be possible to add new features and components ought to be possible to be added to the "library" at any time.

A system meeting these requirements would be a "perfect" system. There is no proof that such a system can be designed. However, if rules are defined for the existing components and restrictions are imposed to new components that can be added to the system, a "quasi perfect" system that meets all three requirements is possible. The usability of the system would strongly depend on the rules and restrictions that were applied.

A draft version of a quasi perfect system was developed and a `.ps` file for a test room was created. A step-by-step description of creating a `.ps` file in RADCOOL is described in Appendix B.

7.1.3 A "quasi perfect" system for RADCOOL

7.1.3.1 Introduction

In RADCOOL the problem of modeling the thermal behavior of a building is broken down into different classes of components. A class of components is defined by its specific properties, by the links to the other classes, and by the internal links between its subclasses. The input required for a class reflects the character of the class, and can differ from class to class. There are seven different classes in the current version of RADCOOL:

1. Passive 4-layer wall with thermal mass
2. Passive 4-layer underground floor with thermal mass
3. Double-pane window with thermal mass

4.Active core-cooling ceiling with 5x5 grid

5. Active cooling panel

6. Heat and moisture balance for room and plenum air

7. Linking objects between components

Each class has sub-classes that depend on the character and role of the parent class. The sub-classes are:

1. For the passive 4-layer wall:

a. heat conduction/storage for each of the four layers of the wall.

b. exterior surface radiant heat balance, including solar calculations and IR radiation exchange with the surroundings.

c. interior surface radiant heat balance, including short wave radiation calculations.

2. For the passive 4-layer floor:

a. heat conduction/storage for each of the 4 layers of the floor.

b. exterior heat balance of the floor (ground contact).

c.interior surface radiant heat balance, including short wave radiation calculations.

3. For the double-pane window:

a.heat conduction/storage for each of the two panes.

b. exterior surface radiant heat balance (for first pane), including calculations of the incident and transmitted solar radiation, and IR radiation exchange with the surroundings.

c. interior surface radiant heat balance (for second pane), including IR and short wave radiation calculations.

4. For the active core-cooling ceiling:

a. heat conduction/storage for each of the grid cells, and into the water pipes.

b. heat conduction/storage in the two water regimes (flowing/stagnant).

c. control strategies.

d. exterior surface radiant heat balance.

e. interior surface radiant heat balance.

5. For the active panel:

a. heat balance on top and bottom surfaces and heat transfer to water pipes.

b. heat conduction/storage in the two water regimes (flowing/stagnant).

c. control strategies.

d. heat conduction/storage, surface balance for the slab above plenum.

6. For the heat and moisture balance on room and plenum air:

a. room air heat balance.

b. plenum air heat balance.

c. air moisture balance.

7. For the linking objects:

a. connection between the room air module and the room surfaces.

b. connection between the plenum air module and the plenum surfaces, where applicable.

c. interior total short wave radiation calculations.

d. interior long wave radiation calculations.

The sub-classes are linked together as each class is created.

In order to construct a building from components, elements of different classes have to be linked together. Since this is done manually in the current version of RADCOOL, a single-valued syntax is crucial. In what follows the syntax is the same as that of the program, causing a somewhat clumsy appearance of the text and the equations. For better orientation of future RADCOOL users, readability was given preference over aesthetics.

7.1.3.2 Units

All variables described in the text have SI units: kilogram [kg], meter [m], second [s] and Kelvin [K], and units derived from these four. Variables which start with a q or I have units of [W/m^2]; variables that start with Q have units of [W]. The temperatures are denoted by t, unless in a differential equation involving time, where they are denoted by T.

7.2 The SPARK passive elements

7.2.1 Unidimensional heat transfer

A good approximation for building components such as passive walls and windows is to consider that their surfaces (and each imaginary internal plane parallel to the surfaces) are isothermal. This approach neglects surface temperature gradients and edge effects. The simplicity of unidimensional heat transfer offsets, the inaccuracies in the model.

7.2.1.1 The unidimensional heat conduction/storage equations

Consider an infinitely high and wide wall, with homogenous and isotropic material properties, and one-dimensional heat flow perpendicular to the surface of this wall. The temperature at each point over the thickness of the wall can be defined as a space- and time-dependent function, $T = T(x, t)$, where x is the space variable, and t the time variable.

Consider a volume element, ΔV, with heat flow of $q(x, t)$ incident at one surface and $q(x + \Delta x, t)$ at the opposite surface, as shown in Figure 39. The Fourier equation gives the conduction heat flux as:

$$q(x, t) = -k\frac{\partial}{\partial x}T(x, t) \tag{1}$$

where

k is the thermal conductivity of the material [W/m K].

Define $\bar{T}(x, t, \Delta t)$ as

$$\bar{T}(x, t, \Delta t) = \frac{1}{\Delta t}\int_{t}^{t+\Delta t} T(x, \tau)\, d\tau \tag{2}$$

$T_M(x, \Delta x, t)$ as

$$T_M(x, \Delta x, t) = \frac{1}{\Delta x}\int_{x}^{x+\Delta x} T(\xi, t)\, d\xi \tag{3}$$

and $\bar{q}(x, t, \Delta t)$ as

$$\bar{q}(x, t, \Delta t) = -k\frac{\partial T(x, t, \Delta t)}{\partial t} \tag{4}$$

Then the heat balance for this volume element over the time period Δt is:

$$\begin{aligned} &S\Delta t\,(\bar{q}(x + \Delta x, t, \Delta t) - \bar{q}(x, t, \Delta t)) \\ &+\Delta V \rho c_t\,(T_M(x, \Delta x, t + \Delta t) - T_M(x, \Delta x, t)) = 0 \end{aligned} \tag{5}$$

where:

S is the surface area of the volume element normal to the direction of heat flow [m^2]

ρ is the density of the material [kg/m^3], and

c_t is the specific heat of the material [J/kg K].

Considering (4), and the relation between the volume and the thickness of the volume element

$$\Delta V = S\Delta x \tag{6}$$

the heat balance equation becomes

$$k\left(\frac{(\frac{\partial \bar{T}}{\partial x})_{x+\Delta x} - (\frac{\partial \bar{T}}{\partial x})_{x}}{\Delta x}\right) = c_t \rho \frac{T_M(x, t+\Delta t) - T_M(x, t)}{\Delta t} \tag{7}$$

In the limit $\Delta x \rightarrow 0$ and $\Delta t \rightarrow 0$, we get the heat diffusion equation

$$\frac{\partial T}{\partial t} = \alpha \frac{\partial^2 T}{\partial x^2} \tag{8}$$

where α is the thermal diffusivity [m^2/s]:

$$\alpha = \frac{k}{\rho c_t} \tag{9}$$

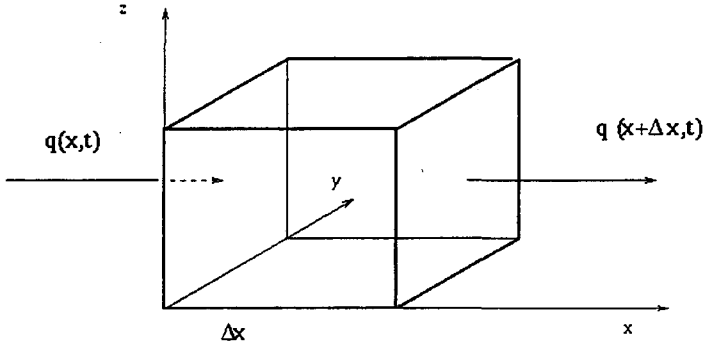

Figure 39. Volume element for conduction heat flow

7.2.1.2 The RC approach to solve the heat conduction/storage equations for a single solid layer in SPARK

Consider the wall from Section 7.2.1.1. Equations (1) and (8) are the differential equations for heat conduction through the wall. In this section we simplify the two equations and bring them into a form that SPARK can easily solve. To this end, the space dependence of the temperature needs to be expressed in finite difference form.

The analogy of the Fourier equation and the heat diffusion equation with Ohm's law and the electrical diffusion equation is obvious. By virtue of this analogy, we can define

a "lumped thermal resistance" R_t given by

$$q = \frac{\Delta T}{R_t} \tag{10}$$

and a "lumped thermal capacitance" C_t given by

$$q = C_t \frac{\partial T}{\partial t}. \tag{11}$$

The idea of the RC approach is to express equations (1) and (8) by means of (10) and (11), so that we obtain a finite expression for the right-hand side of equation (8). Comparing (10) and a finite expression of (1), the thermal resistance of a layer of thickness Δx can be defined as

$$R_t = \frac{\Delta x}{k} \tag{12}$$

Now comparing (8), (11) and (12), the thermal capacity of a layer of thickness Δx can be defined as

$$C_t = \rho c_t \Delta x \tag{13}$$

Using (9) we get from (12), (13)

$$\alpha = \frac{(\Delta x)^2}{R_t C_t} \tag{14}$$

Equations (10) - (13) give the "lumped RC" model of a homogenous, isotropic wall layer. This model is, however, a crude approximation of the real case, in which each infinitesimal layer dx of the wall can have its own resistance and capacity. To use the RC approach more accurately, a wall has to be modeled as composed of a number of layers, each having a resistance and capacity expressed by (12) and (13), respectively. The larger the number of layers simulated, the thinner each layer becomes (Δx decreases), and the more the model approaches the real case.

7.2.2 The structure of the passive wall in SPARK

Based on the general scope of RADCOOL, the SPARK module corresponding to the heat conduction/storage sub-component of a wall should be able to handle 4 layers of different

materials. An RC model of each layer was therefore needed. The overall wall module was then designed to solve the system formed by the RC equations for each layer.

Several test programs were written in SPARK to determine the number of sub-layers that need to be defined to give good agreement with analytical solutions. The results show that a combination of 3 resistances and 2 capacities (Figure 40) differs only in the order of a few percents from a combination of 4 resistances and 3 capacities (Figure 41), but that the computation time increases significantly for the second case as compared to the first. It was therefore considered appropriate that each layer have a maximum of 3 resistances and 2 capacities.

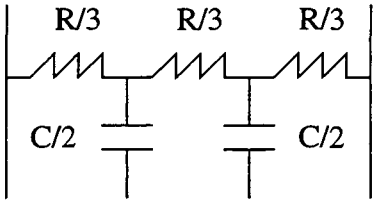

Figure 40. A 3R, 2C model of the wall layer

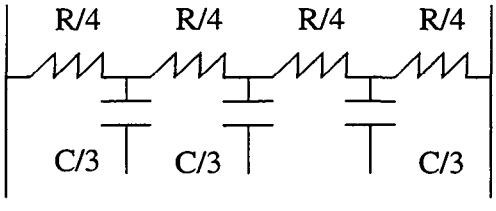

Figure 41. A 4R, 3C model of the wall layer

Another important consideration in selecting the final "equivalent circuit" for the wall was that, of the 4 layers of the wall, only the two in the middle are not exposed other radiation sources, whereas the surface layers are exposed to convection, long wave (IR) radiation, and solar radiation (for exterior layer). It was therefore considered appropriate that for each of the two middle layers a 2R, 1C circuit be modeled, while for each of the two surface layers, a 3R, 2C circuit be modeled. The resulting RC circuit is shown in Figure 42.

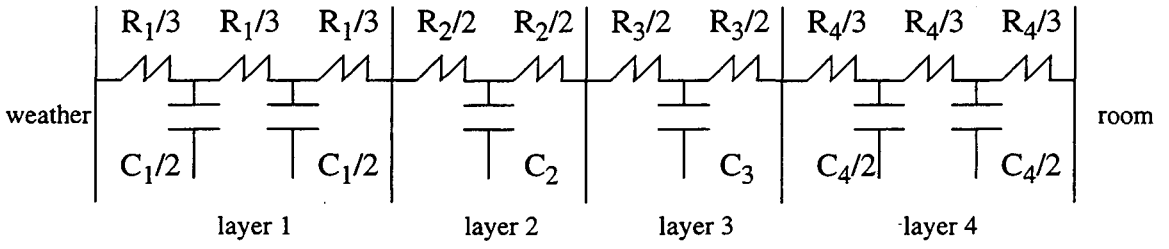

Figure 42. The RC model of the 4-layer wall

7.2.2.1 The equations for the temperature nodes in SPARK

The SPARK module that simulates heat conduction/storage in a 4-layer passive wall solves the system of equations for the heat balance at each temperature node. The temperature nodes can be identified from Figure 42: each surface layer contains 2 temperature nodes, each interior layer contains 1 temperature node, each interface contains 1 temperature node, and each surface contains 1 temperature node.

Consider interior node i. Denote by i-1 and i+1 the nodes located immediately to the left and right of node i. Denote by R_{i-1} and R_{i+1} the resistances of the sub-layers (i-1, i) and (i, i+1), and by C_i the capacity corresponding to node i. The heat balance equation for node i is:

$$\frac{T_{i-1}-T_i}{R_{i-1}} = C_i\frac{dT_i}{dt} + \frac{T_i-T_{i+1}}{R_{i+1}} \tag{15}$$

Consider interface node i. Denote by i-1 and i+1 the nodes located immediately to the left and right of node i. Denote by R_{i-1} and R_{i+1} the resistances of the sub-layers (i-1, i) and (i, i+1). The heat flux balance equation for interface node i is

$$\frac{T_{i-1}-T_i}{R_{i-1}} = \frac{T_i-T_{i+1}}{R_{i+1}} \tag{16}$$

Consider surface node i. Denote by i+1 the node locate immediately inside the wall. Denote by R_{i+1} the resistances of the sub-layers (i, i+1), and by q_i the exterior heat flux incident on the wall. The heat flux balance equation for the surface node i is

$$q_i = \frac{T_i-T_{i+1}}{R_{i+1}} \tag{17}$$

The system of equations for a 4-layer wall with the equivalent circuit shown in Figure 42 is composed of

- 6 differential equations of type (15), corresponding to the interior nodes
- 2 linear equations of type (16), corresponding to the interface nodes, and
- 2 linear equations of type (17), corresponding to the surface nodes.

7.2.2.2 Test to determine the accuracy of the RC wall model

In order to determine the accuracy of the RC wall model the results from the SPARK model of a given problem were compared to the analytical solution of the same problem.

The problem

Consider the problem of one-dimensional heat in a homogenous and isotropic wall with $0< x <l$, with zero initial temperature, and with the planes $x = 0$ and $x = l$ kept at temperatures zero and $\sin(\omega t+\varepsilon)$, respectively [49].

The analytical solution

The temperature of a node at x is [49]:

$$T(x,t) = A\sin(\omega t+\varepsilon+\phi) + 2\pi\alpha\sum_{n=1}^{\infty}\frac{n(-1)^n(\alpha n^2\pi^2\sin\varepsilon-\omega l^2\cos\varepsilon)}{\alpha^2 n^4\pi^4+\omega^2 l^4}\sin\frac{n\pi x}{l}e^{-\frac{\alpha n^2\pi^2 t}{l}} \tag{18}$$

where

$$A = \left|\frac{\sinh\mathbf{k}x(1+i)}{\sinh\mathbf{k}l(1+i)}\right| = \left\{\frac{\cosh 2\mathbf{k}x-\cos 2\mathbf{k}x}{\cosh 2\mathbf{k}l-\cos 2\mathbf{k}l}\right\}^{\frac{1}{2}} \tag{19}$$

$$\phi = \arg\left\{\frac{\sinh\mathbf{k}x(1+i)}{\sinh\mathbf{k}l(1+i)}\right\} \tag{20}$$

and

$$\mathbf{k} = \left(\frac{\omega}{2\alpha}\right)^{\frac{1}{2}} \tag{21}$$

The input data

To compare SPARK and analytical solutions, a 20 cm concrete wall was modeled and the temperature at half the thickness of the wall (x=10 cm) was calculated. The thermal diffu-

sivity was $\alpha = 7.2 \times 10^{-7}$ m^2/s. The sine temperature function at the x = l surface was chosen to have a period of 24 hours ($\omega = 7.3\ 10^{-5}$ s^{-1}) and no time lag ($\varepsilon = 0$).

To determine the analytical solution a FORTRAN program was written in which 100,000 terms in (18) were summed to calculate the temperature at each time step.

The SPARK program was designed so that all 4 layers of the wall had the same thickness (5 cm) and thermal properties: density $\rho = 2400$ kg/m^3, heat capacity $c_t = 1040$ J/kg K, and conductivity k = 1.8 W/m K (which gives $\alpha = 7.2\ 10^{-7}$ m^2/s).

Results

Figure 43 compares SPARK and analytical solutions for the temperature at the node x = 10 cm of the wall. The sinusoidal temperature at the x = 20 cm plane of the wall is also shown. We see good agreement between SPARK and analytical solutions.

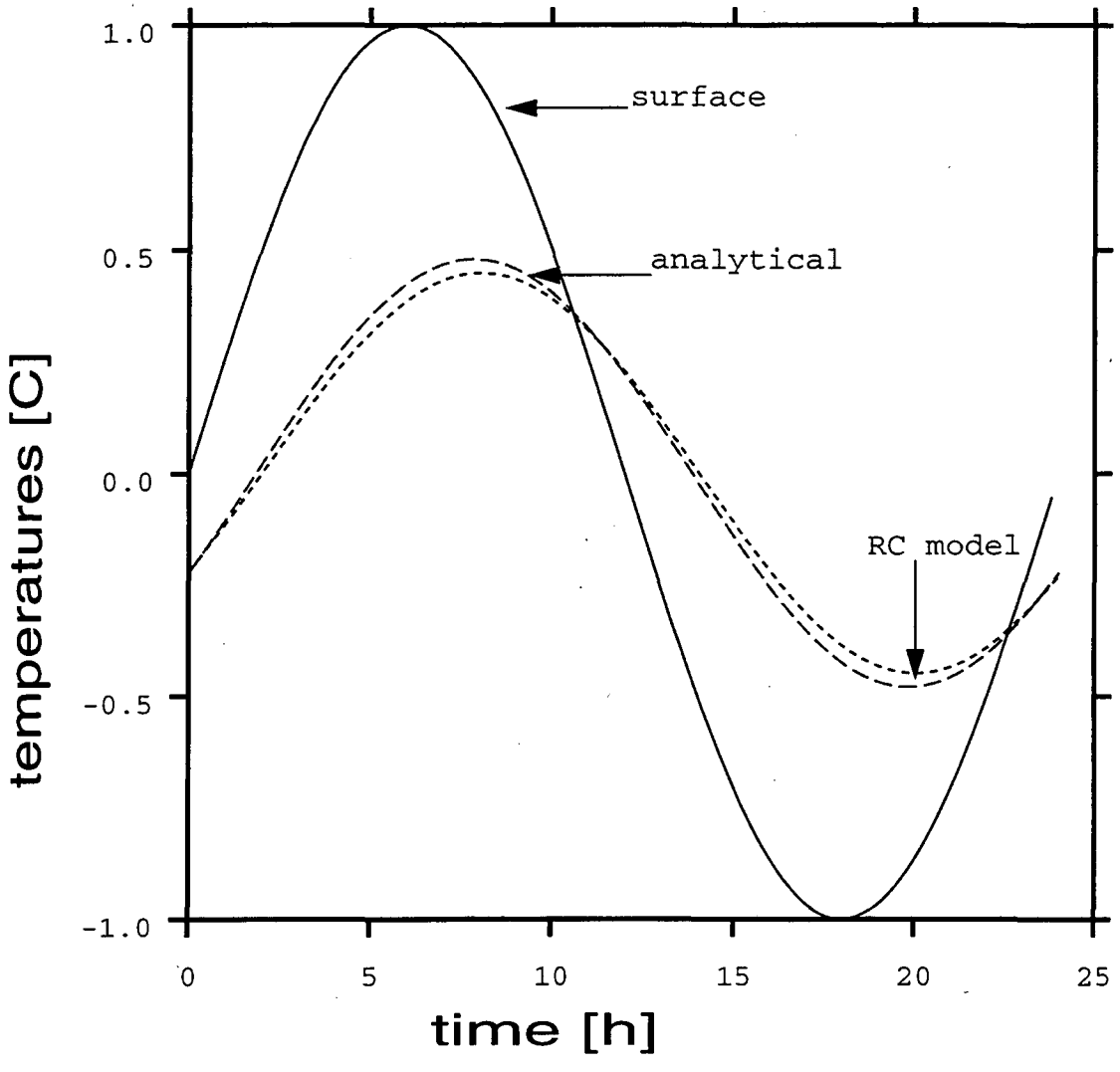

Figure 43. Comparison of SPARK model and analytical solution for the temperature at the mid plane of a homogeneous wall with a sinusoidal surface temperature variation

7.2.3 Exterior surface radiant heat balance for a wall with thermal mass

In this section the radiant heat balance is defined for the exterior (weather-exposed) surface temperature node of a wall (see Figure 42). The heat fluxes that enter the heat balance equation are shown in Figure 44.

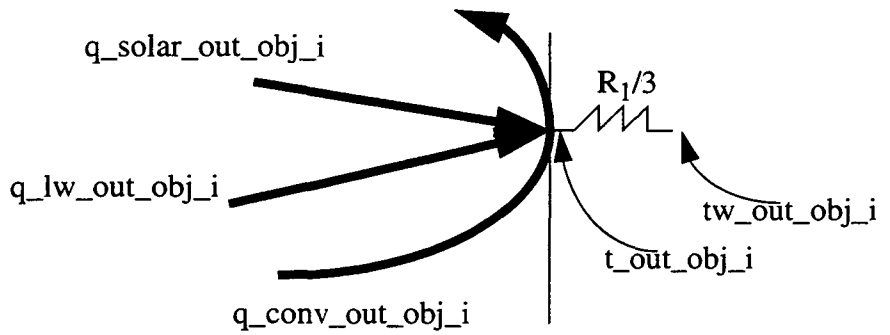

Figure 44. The heat flux balance at the exterior surface node

Heat fluxes the surface node point are considered positive. All variable names in this object have the suffix `out_obj_i` to emphasize the reference to the outside surface of wall i. The heat balance is given by:

$$q_{conv-out-obj-i} + q_{lw-out-obj-i} + q_{solar-out-obj-i} = \frac{t_{out-obj-i} - t_{w-out-obj-i}}{\frac{R_1}{3}} \quad (22)$$

where

$q_{conv\_out\_obj\_i}$ is the convective heat flux at the exterior surface of wall i [W/m^2]

$q_{lw\_out\_obj\_i}$ is the long wave (IR) heat flux from the surroundings of wall i [W/m^2]

$q_{solar\_out\_obj\_i}$ is the solar radiation incident on surface of wall i [W/m^2]

The right-hand side of equation (22) is the conduction flux through the first exterior sublayer of wall i (refer to Figure 42 and equation (17)).

7.2.3.1 The convective heat flux on the surface of a wall

The convective heat flux incident on a surface is defined as the product of the temperature difference between the air and the surface, and the convective film coefficient:

$$q_{conv} = h_{conv}(t_{air} - t_{surface}) \quad (23)$$

The air temperature and the convective film coefficient usually vary over the wall surface. Also, the convective film coefficient of an exterior wall depends on the air temperature

and on the wind speed and direction. Consequently, this coefficient is not constant for a surface.

In RADCOOL, the air temperature in equation (23) is considered equal to the outside air temperature. For the convective film coefficient, hourly values were obtained from a DOE-2 calculation (based on [50]).

7.2.3.2 The long wave (IR) heat flux exchange between a wall and its exterior surroundings

The long wave radiation exchange between the exterior surface of a wall and the building surroundings (the ground, sky and atmosphere) is represented in Figure 45 [51].

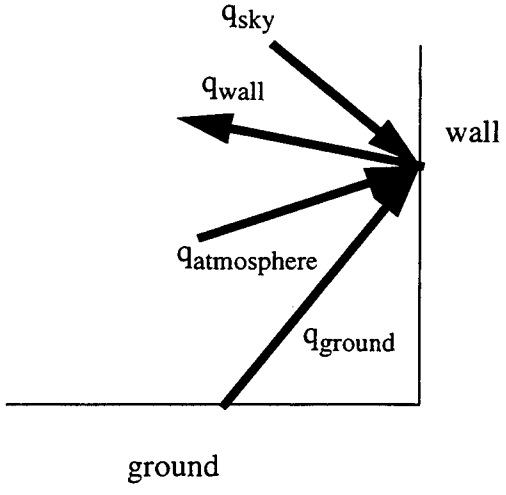

Figure 45. The long wave radiation exchange at the exterior surface of a wall

q_{sky} is the long wave radiation from the sky that is absorbed by the wall surface:

$$q_{sky} = \varepsilon_{wall}\sigma\varepsilon_{sky}T_{air}^4 F_{sky}\cos\left(\frac{\Phi_{wall}}{2}\right) \qquad (24)$$

where

T_{air} is the ambient air drybulb absolute temperature [K]

ε_{wall} is the wall surface emissivity (~0.9)

ε_{sky} is the effective sky emissivity; it depends on the outside air dewpoint absolute temperature T_d and cloud cover fraction N according to

$$\varepsilon_{sky} = (0.787 + 0.76ln(\frac{T_d}{273}))\ (1 + 0.224N - 0.0035N^2 + 0.00028N^3) \qquad (25)$$

where

σ is the Stefan-Boltzmann constant (5.67 10^{-8} W/m^{2}K^4)

F_{sky} is the fraction of the hemisphere seen by the wall surface that is subtended by the sky (sky form factor); it depends on the tilt of the wall, Φw (Φw = 90 for a vertical wall, Φw = 180 for a floor and Φw = 0 for a horizontal roof) according to

$$F_{sky} = \frac{1 + \cos\Phi_{wall}}{2} \tag{26}$$

$q_{atmosphere}$ is the long wave radiation from the atmosphere that is absorbed by the wall surface:

$$q_{air} = \varepsilon_{wall}\sigma T_{air}^4 F_{sky}\left(1 - \cos\left(\frac{\Phi_{wall}}{2}\right)\right) \tag{27}$$

q_{ground} is the long wave radiation from the ground absorbed by the wall surface:

$$q_{ground} = \varepsilon_{wall}\sigma\varepsilon_{ground}T_{air}^4 F_{ground} \tag{28}$$

ε_{ground} is the ground emissivity (~0.9)

F_{ground} is the fraction of the hemisphere seen by surface as subtended by the ground (ground form factor; $F_{sky} + F_{ground} = 1$):

$$F_{ground} = \frac{1 - \cos\Phi_{wall}}{2} \tag{29}$$

q_{wall} is the long wave radiation emitted by the wall surface:

$$q_{wall} = \varepsilon_{wall}\sigma T_{wall}^4 \tag{30}$$

ε_{wall}: the wall surface emissivity

T_{wall}: the wall surface absolute temperature [K]

The long wave radiation gain on the exterior surface of the wall can be expressed as:

$$q_{lw} = q_{sky} + q_{atmosphere} + q_{ground} - q_{wall} \tag{31}$$

7.2.3.3 The solar radiation incident on the surface of a wall

The solar radiation incident on the exterior surface of a wall has a direct and a diffuse component. The wall absorbs a fraction of each, according to the direct and diffuse absorption coefficients of the wall. The total solar radiation absorbed by the wall is therefore the sum of the absorbed direct and absorbed diffuse solar radiation:

$$q_{solar-out-i} = I_{dir-abs-out-i} + I_{diff-abs-out-i} \tag{32}$$

where

$$I_{dir-abs-out-i} = abs_{dir-oout-i} I_{dir-out-i} \quad (33)$$

$$I_{diff-abs-out-i} = abs_{diff-out-i} I_{diff-out-i} \quad (34)$$

where

$I_{dir\_abs\_out\_i}$ is the portion of the direct solar radiation incident on the exterior surface of wall i that is absorbed by the surface [W/m^2]

$abs_{dir\_out\_i}$ is the direct absorption coefficient of wall i

$I_{dir\_out\_i}$ is the direct solar radiation incident on exterior surface of wall i [W/m^2]

$I_{diff\_abs\_out\_i}$ is the portion of the diffuse solar radiation incident on the exterior surface of wall i that is absorbed by the surface [W/m^2]

$abs_{dir\_out\_i}$ is the diffuse absorption coefficient of wall i

$I_{diff\_out\_i}$ is the diffuse solar radiation incident on the exterior surface of wall i [W/m^2].

The wall is considered to be opaque, so the solar radiation transmitted through the wall is zero.

7.2.4 Interior surface radiant heat balance for a wall with thermal mass

In this section the radiant heat balance is defined for the interior (room-exposed) surface temperature node of the wall (see Figure 42). The heat fluxes that enter the heat balance equation are shown in Figure 46.

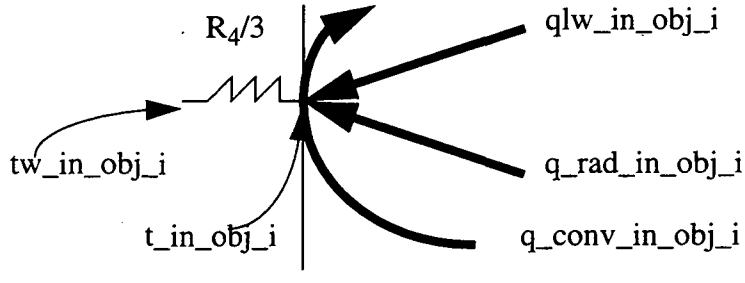

Figure 46. The heat flux balance at the interior surface temperature node

Incoming heat fluxes at a node are taken as positive. The variable names in this object have the suffix `obj_in_i` to emphasize the reference to the surface of wall i. The heat balance is given by:

$$q_{conv-in-obj-i} + q_{lw-in-obj-i} + q_{rad-in-obj-i} = \frac{t_{in-obj-i} - t_{w-in-obj-i}}{\frac{R_4}{3}} \quad (35)$$

where

$q_{conv\_in\_obj\_i}$ is the convective heat flux at the interior surface of wall i [W/m^2]

$q_{lw\_in\_obj\_i}$ is the net long wave (IR) radiation flux gain from the radiative exchange between wall i and the other walls in the room [W/m^2]

$q_{rad\_in\_obj\_i}$ is the radiation incident on surface of wall i from the sources inside the room, and the solar radiation that enters the room through the window [W/m^2]

The right-hand side of equation (22) is the conduction flux through the first interior sub-layer of wall i (refer to Figure 42 and equation (17)).

7.2.4.1 The convective heat flux on the interior surface of a wall

The convective heat flux on the interior surface of the wall is given by equation (23).

The same problems as in Section 7.2.3.1 arise in the calculation of the convective heat flux. For most applications, the room air temperature and the convective heat coefficient be averaged over the surface. As an example, Figure 47 shows the surface temperature of a vertical wall and the air temperature near the surface as a function of height. At the "neutral level" both temperatures are the same. The heat flux is from the wall towards the air at locations under the "neutral level", and from the air to the wall above the "neutral level". To use one node per wall surface, an expression for the heat must be found.

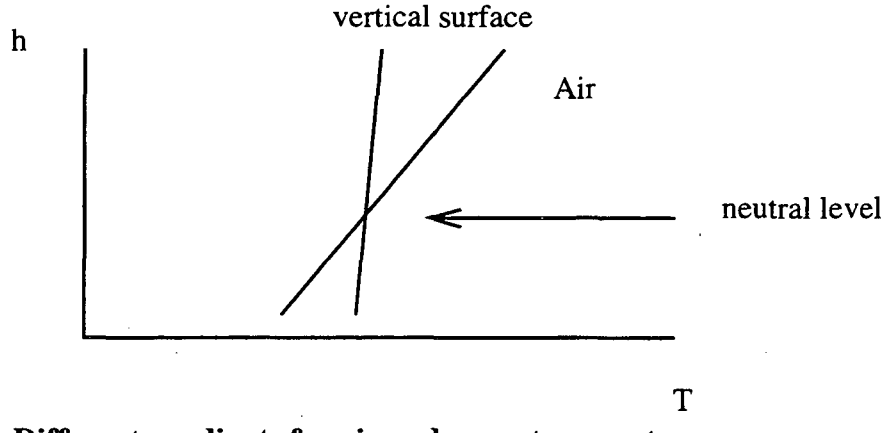

Figure 47. Different gradients for air and room temperatures

The interior convective film coefficient, h_conv_in_i, depends on the properties of the air, the wall surface roughness, and the stream field of the air. There are several levels of simplification for calculating this variable.

- constant value: as a first approximation, h_conv_in_i may be assumed constant. The value is in the range 1 – 3.5 W/m^2 K.

- a function of temperature difference; there are several such expressions. See, for example [52]

$$h_{conv-in-i} = C_1 (\Delta t)^{C2} \qquad (36)$$

where C_1 and C_2 can be constant, or depend on the properties of the fluid and/or the surface

- a function of the physical properties of the fluid and the surface: this calculation is time consuming because in order to compute air flow patterns it needs to access a database of airflow patterns.

In RADCOOL the constant convection film coefficient value approach was considered adequate.

7.2.4.2 The IR radiative exchange between a wall and the other room surfaces

Consider an enclosure composed of N discrete surfaces that have each a determined temperature T_i. A complex IR radiative exchange occurs inside the enclosure as radiation is emitted by a surface, travels to the other surfaces, is partly reflected and re-reflected many times within the enclosure with partial absorption at each contact with a surface.

There are several approaches for the calculation of the net long wave flux gain on a surface due to this radiative exchange. The two approaches that will be presented are the *mean radiant temperature* approach and the *net-radiation* approach.

The mean radiant temperature approach

This approach considers the interior surfaces with which the wall interacts as concentrated at a single node. The equation governing the radiative exchange is the grey body equation for two surface elements. The mean radiant temperature is defined as the temperature of a half space that results in the same heat flux as the real room interior.

The long wave radiation that falls on the surface is

$$q_{long-wave-in-i} = \varepsilon_{in-i}\varepsilon_{sphere-in-i}\alpha_{rad-in-i}(T_{MRT-in-i} - T_{in-i}) \qquad (37)$$

where

ε_{in_i} is the emissivity of surface i

$\varepsilon_{sphere\_in\_i}$ is the average emissivity of the non-i room surfaces.

$\alpha_{rad\_in\_i}$ is the radiative heat transfer coefficient defined in analogy to the convective heat transfer coefficient. If both emissivities and shape factors are unity, the radiative heat transfer between surfaces 1 and 2 is:

$$q_{12} = \sigma(T_1^4 - T_2^4) = \alpha_{rad-in-i}(T_1 - T_2) \qquad (38)$$

with

$$\alpha_{rad-in-i} = \sigma(T_1^3 + T_1^2T_2 + T_1T_2^2 + T_2^3) \qquad (39)$$

where

σ is the Stefan-Boltzmann constant (5.67×10^{-8} W/m^{2}K^4)

For the usual temperature differences that occur in buildings, $\alpha_{rad\_in\_i}$ is 5 - 7 W/m^2 K.

T_MRT_in_i is the temperature of a "sphere" which would exchange the same amount of heat with the surface i as the real non-i surfaces do.

Raber and Hutchinson [53] mention the influence of reflectance; they claim that the reflectance may be neglected if emissivities are higher than 0.9. Assuming that $\alpha_{rad\_in\_i}$ is constant, they derive:

$$MRT = F_{i1}T_1 + F_{i2}T_2 + \ldots + F_{ij}T_j \tag{40}$$

T_i,...,T_j are the temperatures of the other surfaces

and

Fij is the shape factor (or view factor) of surface j to surface i (the fraction of the total long wave radiation emitted by surface j that is absorbed by surface i). The calculation of the shape factors is relatively simple in the case of flat surfaces (see [55]), but rather complicated in the case of rounded surfaces.

T_in_i is the temperature of surface i.

The net-radiation approach

It is obvious that the mean radiant temperature approach has limitations. The net-radiation approach [55] provides a method to calculate the net (equilibrium) radiation incident on each surface of the enclosure, if the surface temperatures are known. This approach is well-suited to RADCOOL, where only one temperature node is defined for each surface.

Consider the area A_i of the enclosure. Let q^i_{out} and q^i_{in} be the radiant flux leaving from, and incident on, surface i. A flux balance at the surface gives:

$$q^i_{net} = q^i_{in} - q^i_{out} \tag{41}$$

where

$$q^i_{out} = \varepsilon_{in-i}\sigma T^4_{in-i} + (1 - \varepsilon_{in-i})\, q^i_{in} \tag{42}$$

Since the incoming radiant flux is a combination of outgoing radiant flux from the other surfaces, we obtain a second equation:

$$q^i_{in} = \sum_{j=1}^{N} F_{ij} q^j_{out} \tag{43}$$

By solving the system of equations (41) - (43), the net radiant gain for each surface can be determined.

7.2.4.3 Solar and people/equipment radiation incident on the interior surface of a wall

Two other sources of radiation on the interior surface of a wall are short-wave (solar) radiation entering the window and long-wave (IR) radiation from people and equipment.

Short wave radiation in a space

In a typical building short wave solar radiation enters a space through the windows and other transparent surfaces (transparent walls, skylights, etc.). The radiation is then directed to the different surfaces in the space according to the position of the windows with respect to the sun, and of the surfaces with respect to the window. A thorough calculation of this effect would determine the position of the sun at each moment, and, based on the position of the windows in the space, the fraction of the solar radiation entering the space that is incident on each surface. This calculation is not only time consuming, but also needs a follow-up in which the multiple reflections between the different surfaces are determined.

To avoid lengthy calculations and complicated distribution functions for the transmitted solar radiation, RADCOOL does solar calculations in the preliminary data processing. Paragraph 7.8.2.1 shows the calculations in detail. RADCOOL also precalculates the amount of the total solar radiation entering the space at each moment that is incident on the different surfaces.

The general equation (44) that describes this approach in RADCOOL allows for a certain fraction of the incoming solar radiation to be directed on a given combination of surfaces. Assuming that each surface of a combination receives the same radiation per unit area, the "overall" fraction for each surface is determined:

$$q_{short-wave-in-i} = fraction_{in-i} \frac{\sum_{windows} A_{window-i} q_{short-wave-window-i}}{A_{surfaces-in-i}} \qquad (44)$$

q_short_wave_in_i is the amount of transmitted solar radiation that is incident on wall i [W/m^2] and all the other walls in the combination with area ***A_surfaces_in_i.***

fraction_in_i is the fraction of the total short wave radiation entering the room that is incident on the surface combination with the total area ***A_surfaces_in_i***

A_surfaces_in_i: the area of a surface combination on which ***fraction_in_i*** of the total solar radiation is incident [m^2]; each surface of the combination receives in this case the same amount of radiation per unit area.

A_window_i is the area of window i [m^2].

q_short_wave_window_i is the solar radiation flux entering the room through window i [W/m^2].

The RADCOOL approximation is similar to the default DOE-2 approximation: 60% of the transmitted short wave radiation represents the fraction absorbed by the floor and 40% by the vertical walls, windows and ceiling of the room.

Occupants and equipment inside a space

The occupants and equipment in a space are internal heat sources. In RADCOOL the occupants and the equipment are grey bodies that participate in the long wave radiation exchange in the space (see section 7.2.4.2) and are sources of sensible and latent heat for the heat and moisture balances in the room air module (Section 7.6). A module simulating the heat balances at the occupants and equipment will be implemented later in RADCOOL.

Equations (41) - (43) describe the long wave exchange among the room surfaces and between the surfaces and the occupants/equipment. Equations (116) - (124) describe the heat generated by occupants and equipment that enters the room heat and moisture balances. The convective heat fluxes from occupants and equipment are included in the room air heat balance.

In these circumstances, the equation that gives the long wave radiation incident on the interior surface of a wall is

$$q_{rad-in-i} = q_{lw-in-i} \tag{45}$$

7.2.5 The 4-layer passive underground floor with thermal mass

7.2.5.1 Comparison between the floor and the wall with thermal mass

The main difference between a floor and a vertical wall is that the exterior of the floor is in contact with the ground, as opposed to a vertical wall, which is in contact with the outside air. A floor will then participate in conductive heat exchange with the ground, but will not undergo convective or radiative heat exchange. Based on these considerations, the case of a floor can easily be modeled based on the vertical wall (or ceiling) model:

- the heat conduction/storage for the 4-layer floor with thermal mass is the same as for a vertical wall
- the interior surface radiant heat balance of a floor is the same as that for a vertical wall
- the heat balance for the exterior surface node of a floor has only conduction terms.

7.2.5.2 Exterior surface radiant heat balance for an underground floor with thermal mass

The heat balance for the exterior surface of a floor is determined by the contact between the floor and the ground. The equivalent of equation (17) for this case is

$$q_{ground-out-i} = \frac{t_{out-obj-i} - t_{w-out-obj-i}}{\frac{R_1}{3}} \tag{46}$$

In RADCOO a resistance is modeled between the floor and the ground temperature nodes:

$$q_{gound-out-i} = U_{floor-ground-obj-i}(t_{ground-out} - t_{out-obj-i}) \quad (47)$$

where

U_floor_ground_obj_i is the inverse of the floor-ground resistance [W/m^2 K]

t_ground_out is the ground temperature from the weather file [C]

t_out_obj_i is the temperature of the exterior surface of the floor [C].

7.2.6 The double-pane window with thermal mass

To model a window in SPARK the same approach was taken as in the case of a floor: determine the differences between a window and a passive wall and then modify the wall module to reflect these differences.

7.2.6.1 Comparison between a window pane and a wall

With the exception of solar radiation effects, a multi-pane window behaves like a multi-layer wall where one or more of the layers are air or other gas.If a temperature difference is created between two window surfaces, or thermal radiation is directed on one surface of a glass pane, the glass will experience heat conduction and storage. A window and wall have different thermal behavior due to the numerical values of their thermal properties. In a wall the conduction and storage are usually both important, resulting in a significant temperature difference between inside and outside. In a window pane temperature difference between the two surfaces is small because of the high conductivity of the glass. Also, glass panes are usually thin (3 - 6 mm) so their thermal storage is small. However, in a multi-pane window, the overall temperature difference across the window can be significant, especially if the glass has low emissivity coating or the between-panes spaces are filled with a low-conductivity gas.

7.2.6.2 Heat conduction/storage for a double-pane window

The RC SPARK model for a two-pane window was designed based on the above considerations. Because of the high conductivity and low heat capacity of a glass pane, a model of one resistance and one capacity was adopted for each pane. A resistance was added between the panes to account for the thermal resistance of the gas fill. Figure 48 shows the RC model for a double-pane window.

Two temperature nodes were modeled for each of the two panes, one on the exterior surface and one on the interior (gap) surface.

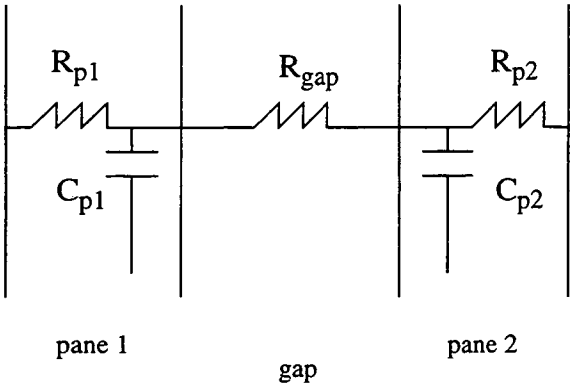

Figure 48. The RC circuit of a double-pane window

The equations that describe the heat balance for the two panes are as follows:

- for the exterior (weather-exposed) temperature node, the equivalent of equation (17) with R_{p1} instead of $R_1/3$ gives

$$q_{rad-out} = \frac{T_{out} - T_{w1}}{R_{p1}} \tag{48}$$

where

T_{out} is the ambient temperature [°C]

T_{w1} is the temperature of the exterior pane [°C]

R_{p1} is the thermal resistance of the exterior pane [m^2-K/W]

q_{rad_out} is the overall radiative heat incident on the exterior pane [W/m^2].

- for the gap-exposed temperature node of the exterior pane:

$$\frac{T_{out} - T_{w1}}{R_{p1}} + C_{p1}\frac{\partial T_{w1}}{\partial t} = U_{gap}(T_{w1} - T_{w2}) \tag{49}$$

where

C_{p1} is the thermal capacity of the exterior pane

U_{gap} is the reciprocal of the thermal resistance of the gas fill [W/m^2-K]

T_{w2} is the temperature of the second pane [°C].

- for the gap-exposed temperature node of the interior pane:

$$U_{gap}(T_{w1} - T_{w2}) = C_{p2}\frac{\partial T_{w2}}{\partial t} + \frac{T_{w2} - T_{in}}{R_{p2}} \tag{50}$$

where

R_{p2} is the thermal resistance of the interior pane [m^2-K/W]

T_{in} is the inside air temperature [°C].

- for the interior (room-exposed) temperature node, the equivalent of equation (17), with R_{p2} instead of $R_4/3$ gives

$$\frac{T_{w2} - T_{in}}{R_{p2}} = q_{rad} \tag{51}$$

where

q_{rad} is the total incident radiation on the interior pane [W/m^2].

The notation q_{rad} was chosen for the right-hand side of equation (51) rather than $q_{\_rad\_in}$ to emphasize that the heat balance for the second pane of a window also includes solar radiation transmitted the first pane and absorbed in the second pane.

7.2.6.3 The heat balance for the exterior pane of a double-pane window

The heat balance for the exterior pane of a 2-pane window is the same as that for the exterior surface of a wall. The equation that applies is therefore:

$$q_{conv-out} + q_{lw-out} + q_{solar-1} = q_{rad-out} \tag{52}$$

The left-hand terms of equation (52) are calculated as in sections 7.2.3.1 through 7.2.3.3.

7.2.6.4 The heat balance for the interior pane of a double-pane window

The heat balance for the interior pane of a 2-pane window is similar to that of a wall, except that solar radiation (transmitted through the first pane) also contributes to the balance. Also, the transmitted solar radiation is calculated in this module and will contribute to the overall short wave radiation inside the space. The heat balance equation is:

$$q_{conv-in} + q_{lw-in} + q_{rad-in} + q_{solar-2} = q_{rad} \tag{53}$$

The first three left-hand terms of equation (53) are calculated as in sections 7.2.4.1 through 7.2.4.3.The last left-hand term is calculated as in section 7.2.3.3, with the absorption coefficients corresponding to the overall coefficients for the solar radiation transmitted by the exterior pane.

The solar radiation transmitted through the two-pane window is calculated using the DOE-2 method: an overall transmissivity coefficient is calculated for the window and the radiation transmitted is

$$q_{solar-interior} = I_{trans-dir-win-i} + I_{trans-diff-win-i} \tag{54}$$

where

$$I_{trans-dir-win-i} = trans_{dir-win-i} I_{dir-out-win-i} \tag{55}$$

$$I_{trans-diff-win-i} = trans_{diff-win-i} I_{diff-out-win-i} \tag{56}$$

where

$I_{trans\_dir\_win\_i}$ is the portion of the direct solar radiation incident on the exterior surface of window i that is transmitted through the window [W/m^2]

$I_{trans\_diff\_win\_i}$ is the portion of the diffuse solar radiation incident on the exterior surface of window i that is transmitted through the window [W/m^2]

$trans_{dir\_out\_i}$ is the direct transmission coefficient of window i

$trans_{diff\_out\_i}$ is the diffuse transmission coefficient of window i

$I_{dir\_out\_win\_i}$ is the direct solar radiation incident on exterior surface of window i [W/m^2]

$I_{diff\_out\ win\_i}$ is the diffuse solar radiation incident on the exterior surface of window i [W/m^2].

The overall short wave radiation inside the space is therefore calculated as

$$q_{short-wave-tot-in} = \sum_i I_{trans-win-i} \tag{57}$$

7.3 The core cooling ceiling

7.3.1 Two-dimensional heat transfer analysis

The one-dimensional heat transfer method presented in Section 7.2.1 cannot yield good results for building components that represent a heat sources or sinks.In this case a two-dimensional heat transfer required that describes the variation of the ceiling temperature in both "main directions" of the ceiling cross-section.

7.3.1.1 The two-dimensional heat conduction/storage equations

Consider a solid ceiling with homogeneous and isotropic material properties. Assume that the temperature is a function of only two dimensions of the ceiling, and is constant in the third dimension (e.g. the temperature varies over a cross section of the ceiling, but cross sections parallel to each other have the same temperature profile).

In analogy with Section 7.2.1.1, the temperature in the cross section can be considered a function of space and time, $T = T(x, y, t)$.

Consider a volume element of this slab and a one-dimensional heat flux at one surface, as in Figure 39. The 2-D Fourier equation for heat transfer in one direction is analogous to equation (1) and has the form

$$Q(x, t) = -k\Delta A\frac{\partial}{\partial x}T(x, y, t) \tag{58}$$

where

Q is the total heat flux at the surface [W]

k is the thermal conductivity of the ceiling material [W/m-K]

ΔA is the area of the face of the volume element normal to the heat flux [m^2].

The same type of reasoning as in Section 7.2.1.1 yields a two-dimensional diffusion equation of the form

$$\frac{\partial T}{\partial t} = \alpha\left(\frac{\partial^2 T}{\partial x^2} + \frac{\partial^2 T}{\partial y^2}\right) \tag{59}$$

where

α is the thermal diffusivity given by equation (9) [m^2/s].

7.3.1.2 The RC solution to the two-dimensional heat conduction/storage equations

The approach of Section 7.2.1.2 was used to express the space and time dependence of the temperature using differences. The ceiling is described as a collection of parallel boxes, and the discretization is done in a plane normal to the surface of the ceiling. The boxes have one dimension equal to the length of the ceiling while the other two dimensions are normal to this direction and much smaller.

In an analogy to electrical circuits, a lumped thermal resistance can be defined in relation to the heat conduction through each box in a given direction, as

$$Q_\xi = \frac{\Delta T_\xi}{R_\xi} \tag{60}$$

where ξ denotes the direction in 3-D space. Similarly, a lumped thermal capacity can be defined in relation to the heat stored inside each box, as

$$Q = C\frac{\partial T}{\partial t} \tag{61}$$

The resistance and capacity are calculated by the thermal properties of the ceiling material as

$$R_\xi = \frac{\Delta \xi}{k \Delta A_\xi} \tag{62}$$

$$C = \rho c_t \Delta V \tag{63}$$

where

ΔA_ξ is the area of the box surface normal to the direction ξ [m^2]

ΔV is the box volume [m^3]

ρ is the density of the ceiling material [kg/m^3]

c_t is the heat capacity of the ceiling material

k is the conductivity of the ceiling material [W/m-K].

7.3.1.3 The two-dimensional model of the ceiling in SPARK

SPARK programs were written in order to simulate the two-dimensional heat transfer. Figures 49 and 50 show two alternative RC circuits, the one in Figure 50 displaying a "finer" box structure than the one in Figure 49.

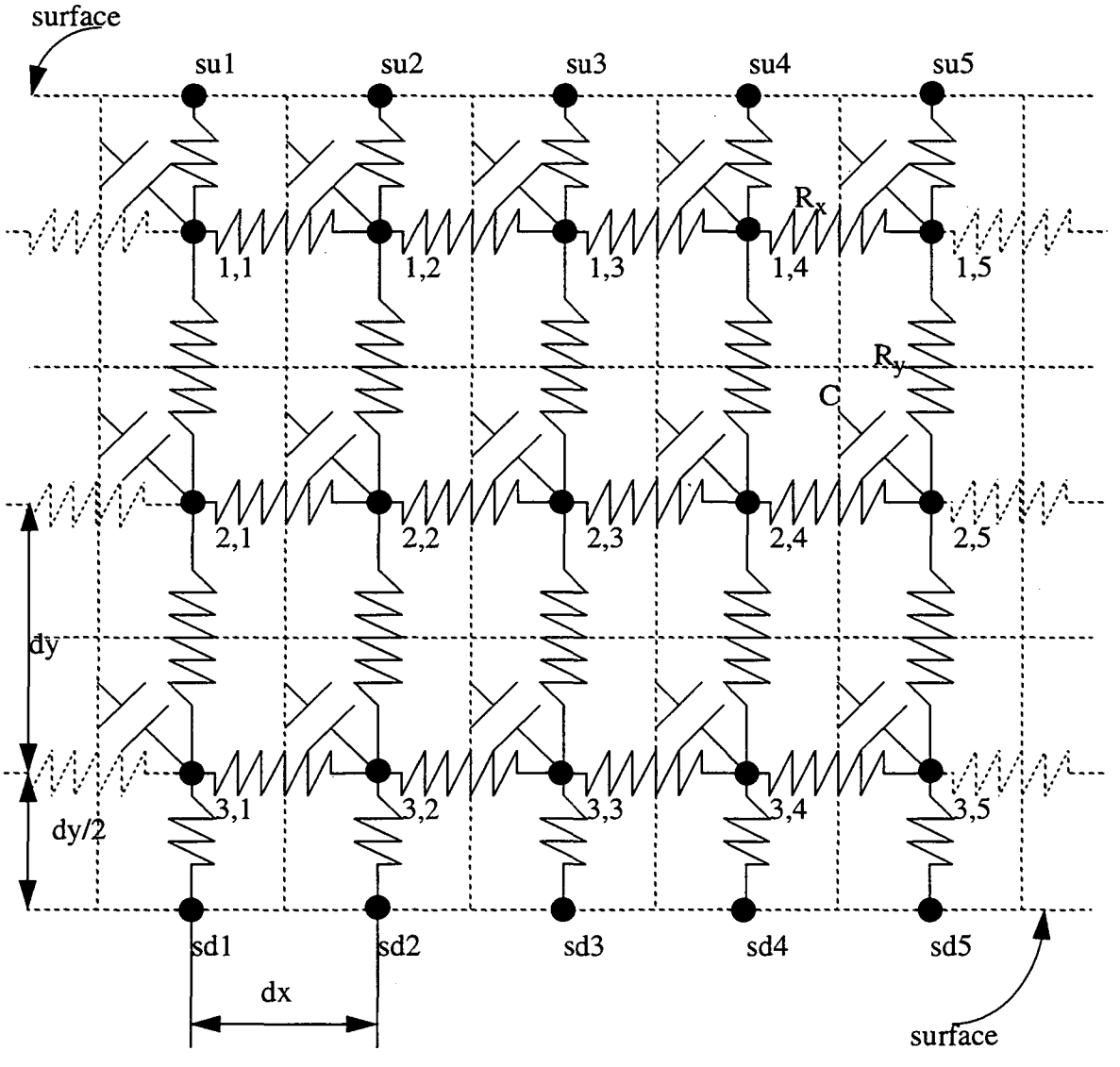

Figure 49. The 3 x 5 - node RC circuit of the wall

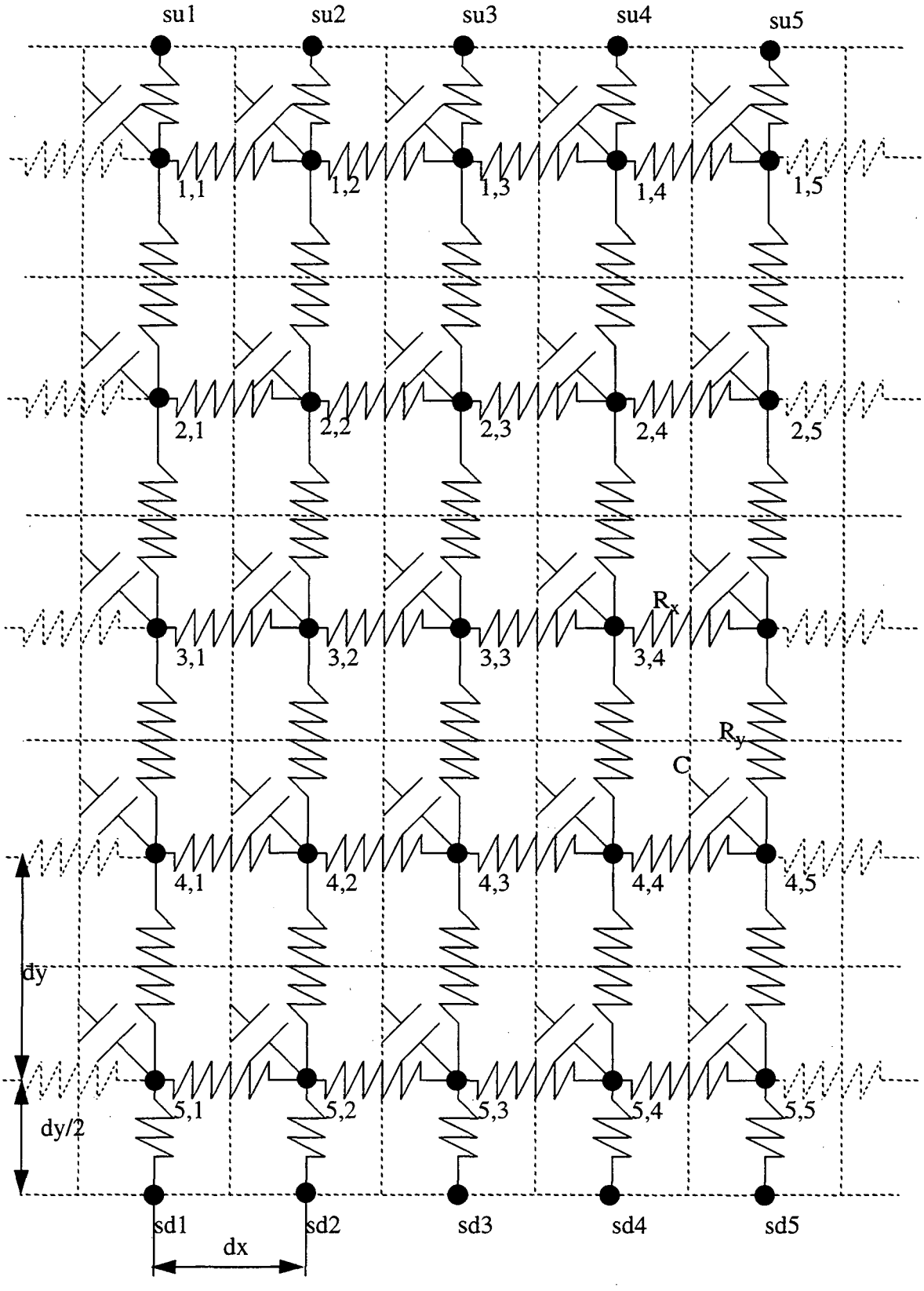

Figure 50. The 5 x 5 - node RC circuit of the wall

Both these models assume that there is some periodicity over the slab cross section, so that the analysis of a "sample" (in these cases, the sample has a thickness of 4 dx) correctly describes the temperature profile of the whole ceiling. Examples of periodicity of the temperature over the cross section of the ceiling are the case in which the isotherms are parallel to each other (passive ceiling) and the case in which there are heating or cooling sources in the ceiling, that are normal to the cross-section and periodically spaced as in a hydronically cooled or heated ceiling.

The resistances and capacities in the figures are calculated as

$$R_x = \frac{dx}{kdydz} \tag{64}$$

$$R_y = \frac{dy}{kdxdz} \tag{65}$$

$$C = \rho c_t \Delta V \tag{66}$$

and

$$dx = \frac{distance - between - pipes}{n_x} \tag{67}$$

$$dy = \frac{thickness - of - wall}{n_y} \tag{68}$$

$$\Delta V = dxdy \times z \tag{69}$$

where dz = z is the length of the ceiling. For the case in Figure 49, the number of "cells" in the x direction is $n_x = 5$, and the number of cells in the y direction is $n_y = 3$. For the case in Figure 50, $n_x = 5$, $n_y = 5$.

The heat balance at the temperature nodes can be derived by analogy with the 1-D situation (equations (15)-(17)). The heat balance for the interior node (i,j) is

$$\frac{T_{i-1,j} - T_{i,j}}{R_{x,i-1}} + \frac{T - T}{R_{y,i-1}} = C_i \frac{dT_{i,j}}{dt} + \frac{T_{i,j} - T_{i+1,j}}{R_{x,i+1}} + \frac{T_{i,j} - T_{i,j+1}}{R_{y,j+1}} \tag{70}$$

where $R_{x,k}$ and $R_{y,k}$ are thermal resistances connecting the node (i,j) with the rest of the network, in the x and y directions, respectively, and C_i is the capacitance of a cell in row i.

The heat balance for the surface node (i,j) is

$$Q_{i,j} = \frac{T_{i,j-1} - T_{i,j}}{R_{y,j-1}} \tag{71}$$

7.3.1.4 Test to determine the accuracy of the RC model

The same problem as in Section 7.2.2.2 was solved for both two-dimensional ceiling models. It was found that the results from the 2-D model with the dimensions dx = 2.5 cm (x=10 cm), dy = 4 cm (y=20 cm) and z = 3 m agree with the analytical solution.

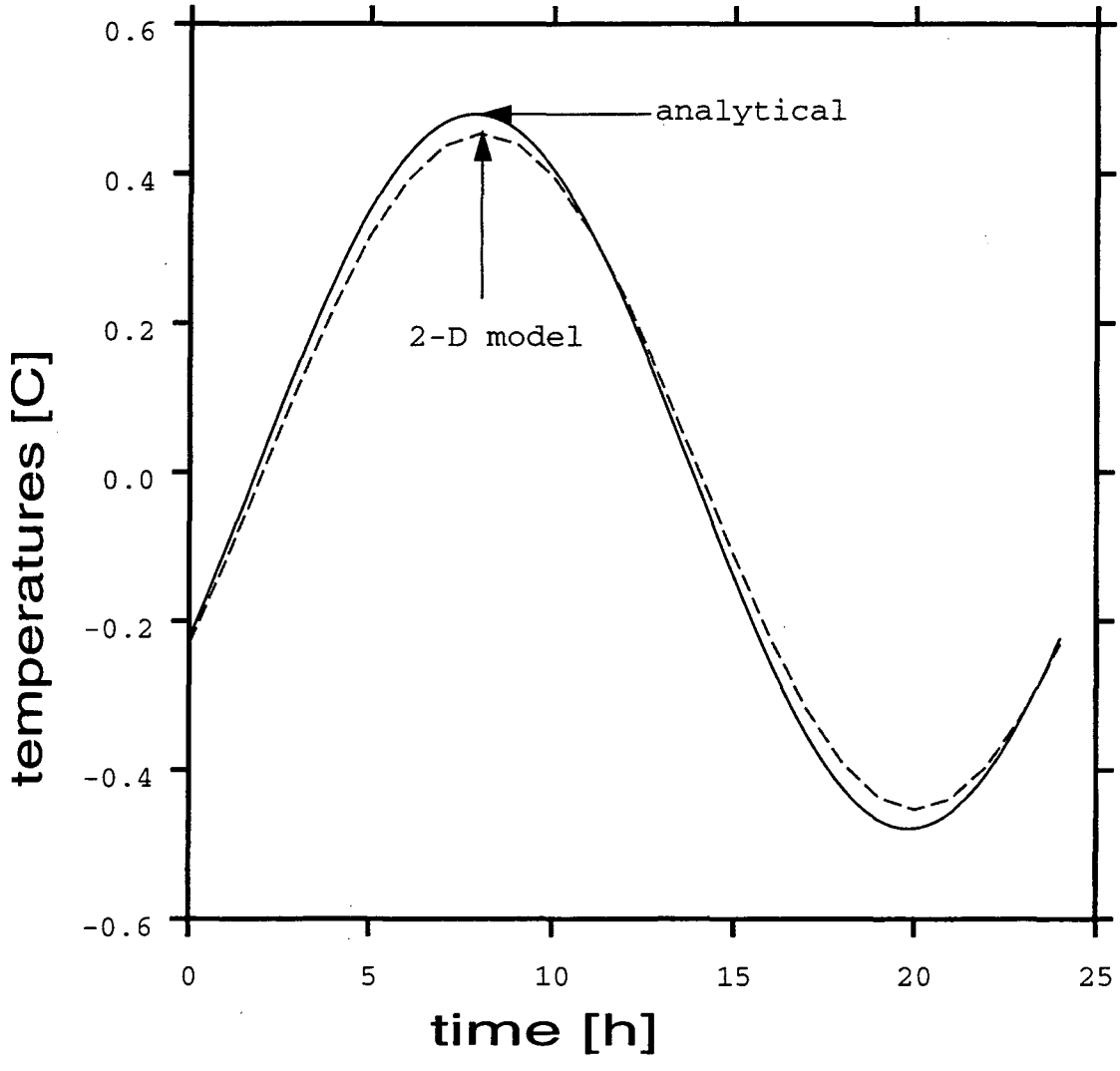

Figure 51. Temperature at the midpoint of a ceiling: comparison between the SPARK 3 x 5 - node two-dimensional model and the analytical solution

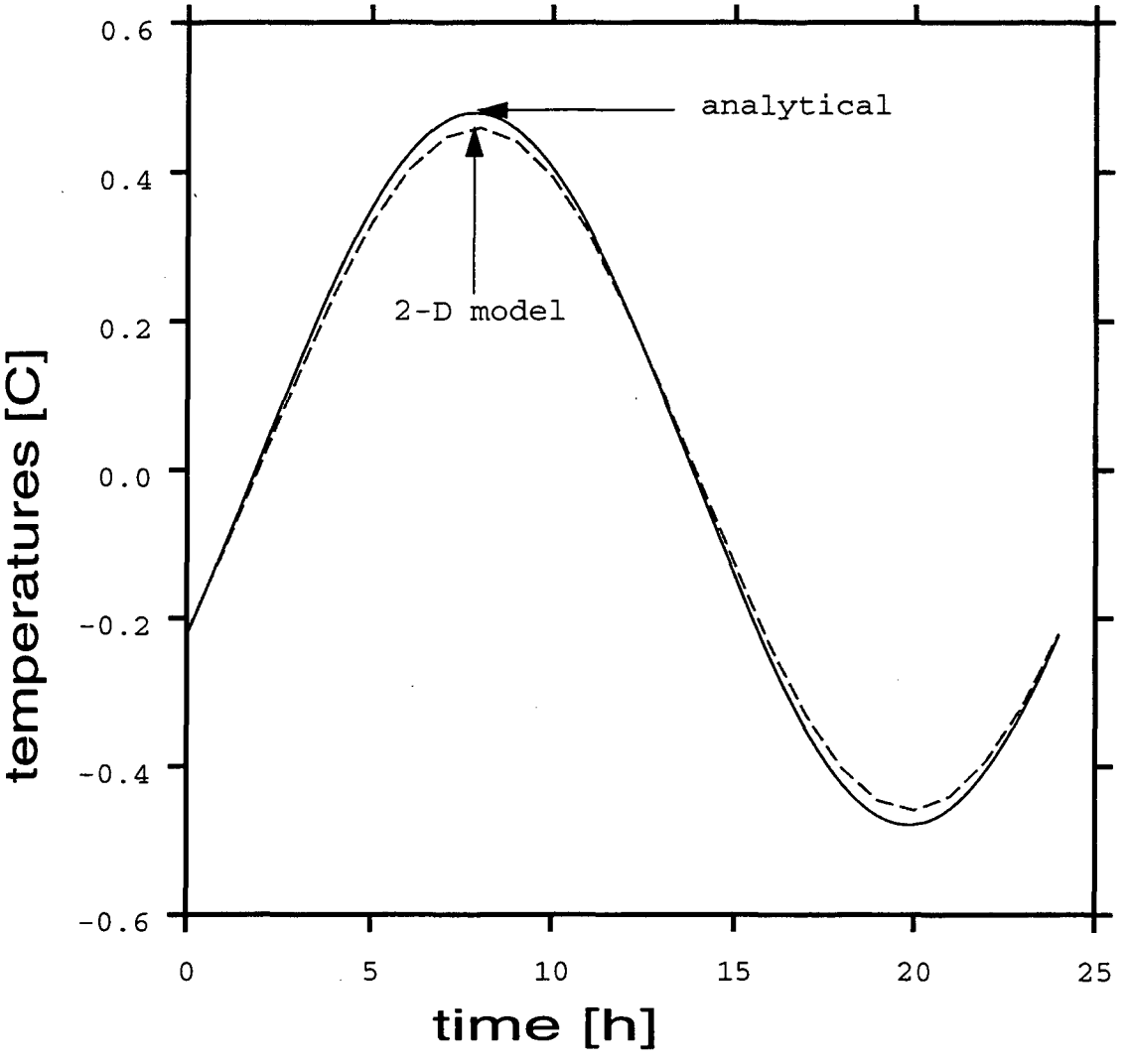

Figure 52. Temperature at the mid point of a ceiling: comparison between the SPARK 5 x 5 - node two-dimensional model and the analytical solution

7.3.2 The SPARK model of the core cooling ceiling

If pipes imbedded in a concrete or plaster ceiling are parallel to each other and form a "layer" parallel to the ceiling surface, and if cold water is circulated through the pipes, the cooling equivalent of a radiant heater is obtained. Figure 53 shows such a structure. The periodicity of the isotherms referred to in section 7.3.1.3 is obvious in this case.

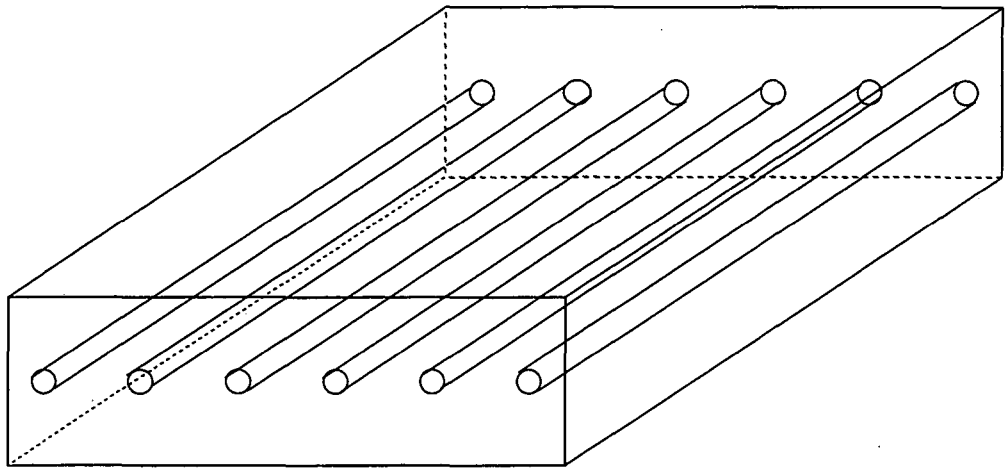

Figure 53. Structure of a cooled ceiling with imbedded pipes

7.3.2.1 Forced heat convection transfer between water and the pipe walls

If water is circulated through a pipe the temperature of the water changes if its initial temperature is different from the pipe temperature. The total heat transfer can be expressed as

$$Q_{convected-water} = hA\,(t_{pipe} - t_{water-average}) \tag{72}$$

where

h is the convection heat transfer coefficient [W/m^{2}K]

A is the total surface area for the heat transfer [m^2]

t_{pipe} is the pipe temperature [°C]

$t_{water\_average}$ is the water bulk temperature (defined as the temperature of the water in the pipe if it were well mixed), averaged between the water inlet and outlet [°C]

The convection heat transfer coefficient can be expressed in terms of the fluid and flow characteristics as follows [56]:

$$h = \frac{k}{d}Nu \tag{73}$$

where

k is the conductivity of the fluid [W/mK]

d is the pipe diameter [m]

Nu is the Nusselt number for the flow.

In the case of fully developed turbulent flow in a smooth pipe, the Nusselt number has the following empirical expression (Dittus and Boelter):

$$Nu = 0.023 Re^{0.8} Pr^{n} \tag{74}$$

where

Re is the Reynolds number for the flow

$$Re = \frac{4}{\pi} \frac{\dot{m}}{\mu d} \tag{75}$$

and

m is the mass flow [kg/s]

μ is the dynamic viscosity of the fluid [kg/m-s]

d is the pipe diameter [m]

Pr is the Prandtl number of the fluid

n is 0.4 if the fluid is heated by convection and 0.3 if the fluid is cooled by convection.

The heat convected from the pipe is stored in the water, so

$$Q_{stored-water} = \dot{m} c_p (t_{bulk-exhaust} - t_{bulk-inlet}) \tag{76}$$

and the mean bulk temperature of the water in equation (72) is

$$t_{water-average} = \frac{t_{bulk-exhaust} - t_{bulk-inlet}}{2} \tag{77}$$

7.3.2.2 Heat conduction from the pipe to the water, when the water is recirculated

To achieve comfort inside a radiatively cooled room the system needs to have some kind of control. Depending on the inlet water temperature, thermal mass of the ceiling, and room loads, running the water all the time might cool the room too much making it uncomfortable. If, however, the water flow is discontinued or the temperature of the inlet water is raised, the room is not cooled as fast and the chances of creating discomfort are reduced.

When the heat transfer between the room and the water is a small fraction of the cooling power, recirculation of the water in the pipes is a convenient way of saving chiller power. The cold water from the chiller is mixed with warmer return water, with the obvious result that the inlet ceiling water temperature becomes higher than that of the cold water produced by the chiller. The recirculation of water also provides a way in which the cooling system adjusts its output to meet the room cooling loads.

Consider that two quantities of water m_{cold} and m_{warm}, at different temperatures t_{low} and t_{high}, are mixed together. This process will result in a quantity of water $m_{total} = m_{cold} + m_{warm}$, with a temperature t_{mix} given by

$$m_{warm} c_{water} (t_{high} - t_{mix}) = m_{cold} c_{water} (t_{mix} - t_{low}) \quad (78)$$

where c_{water} is the specific heat of water. The temperature of the water after the mixing process is

$$t_{mix} = \frac{m_{cold} t_{low} + m_{warm} t_{high}}{m_{total}} \quad (79)$$

or,

$$t_{mix} = x t_{low} + (1 - x)\, t_{high} \quad (80)$$

with the "mix ratio" $x = \frac{m_{cold}}{m_{total}}$

In the case in which water is mixed from two streams, $\dot{m}_{total} = \dot{m}_{cold} + \dot{m}_{warm}$ and

$x = \frac{\dot{m}_{cold}}{\dot{m}_{total}}$.

For the cooled ceiling the two water streams consist of cold water from the chiller and warm return water. The quantity that is known is the total mass flow; the cold and warm water mass flows have to be adjusted to the room conditions. The most efficient way the adjustment can be done is based on knowing the response of the room to a change in inlet water temperature. This type of calibration curve provides the inlet water temperature, at a given room temperature, in order to have the room loads removed. However, measurements are necessary to determine the calibration curve. An alternative is to substitute the calibration curve with the "opening characteristic" method, which is not as efficient as the calibration curve method, but requires less effort.

Assume that the room air temperature range that provides occupant comfort is known. The low end, t_{low_end}, of this range corresponds to the temperature at which the cooling ceiling starts to function, and the high end, t_{high_end} to a temperature above which only unmixed cold water running through the ceiling can remove the room loads. The mix ratio is determined in this case as follows:

- a switch stops the water flow when the room air temperature falls below t_{low_end}; the mix ratio is zero

- for room air temperatures above t_{high_end} only unmixed cold water is circulated; the mix ratio is 1

- for room temperatures between t_{low_end} and t_{high_end} a mixture of cold water and warm return water is circulated; the mix ratio is between 0 and 1.

In general, if the room air temperature is known, and the opening characteristic is linear between t_{low_end} and t_{high_end}, the formula that gives the mix ratio is

$$x = \frac{t - t_{low-end}}{t_{high-end} - t_{low-end}} \tag{81}$$

where t is equal to

- t_{low_end} if $t_{room\_air} < t_{low\_end}$
- t_{room_air} if $t_{low\_end} < t_{room\_air} < t_{high\_end}$
- t_{high_end} if $t_{room\_air} > t_{high\_end}$.

7.3.2.3 Heat conduction from the pipe walls to the water, when the water is not flowing

In the case when the water flow is discontinued, the heat from the ceiling is conducted through, and stored in, the water. The heat conducted from the ceiling of a cylindrical pipe to a cylinder of water is

$$Q_{conducted-water} = U_{water}(t_{pipe} - t_{water}) \tag{82}$$

where

$U_{water} = 2\pi kz$ is the U-value of a water cylinder [W/K]

z is the total length of the water cylinder [m]

k is the conductivity of the water [W/m]

t_{pipe} is the pipe ceiling temperature [°C]

t_{water} is the temperature of the water cylinder [°C].

The heat conducted from the pipe into the water warms the water, giving

$$Q_{stored-water} = m_{water} c_{water} \frac{\partial t_{water}}{\partial t} \tag{83}$$

where

$m_{water} = \rho_{water} V_{water-cylinder}$ is the mass of the cylinder of water.

7.3.2.4 The two-dimensional model application in the case of a cooled ceiling

The theoretical model from section 7.3.1.3 can be applied to determine the heat transfer between a cooled ceiling and its surroundings. Figure 50 shows a 5x5 node RC circuit in which each horizontal layer can have a different material structure. The nodes vj_i,i+1 are interface nodes between two layers. Only vertical heat flow is modeled at the interfaces, so the heat balance for node vj_i,i+1 is

$$\frac{T_{i-1,j} - T_{vj-i-1,i}}{\frac{R_{y,i-1,j}}{2}} = \frac{T_{vj-i-1,i} - T_{i,j}}{\frac{R_{y,i,j}}{2}} \tag{84}$$

where

$R_{y,i,j}$ is the vertical thermal resistance on vertical j and in row i.

To model the thermal contact between the ceiling nodes and the water the exterior of the pipe is considered as having the temperature of the adjacent ceiling node, while the interior of the pipe is considered as having the temperature of the water (mean bulk temperature). Between these two nodes an additional horizontal resistance was modeled which is a function of the conductivity of the pipe material and reflects the cylindrical symmetry of the pipes:

$$R_{x-pipe-water} = \frac{\Delta r}{k\pi rl} \tag{85}$$

When the water is flowing, the heat balance at the pipe surface is

$$Q_{conducted-pipe} = Q_{convected-water} = Q_{stored-water} \tag{86}$$

where

$$Q_{conducted-pipe} = \frac{T_{wall-node} - T_{pipe}}{R_{x-pipe-water}} \tag{87}$$

$Q_{convected\_water}$ is given by equation (72)

Q_{stored_water} is given by equation (76).

In the case the water flow is zero, the heat balance at the pipe surface is

$$Q_{conducted-pipe} = Q_{convected-water} = Q_{stored-water} \tag{88}$$

where

$Q_{conducted\_water}$ is given by equation (82)

Q_{stored_water} is given by equation (83).

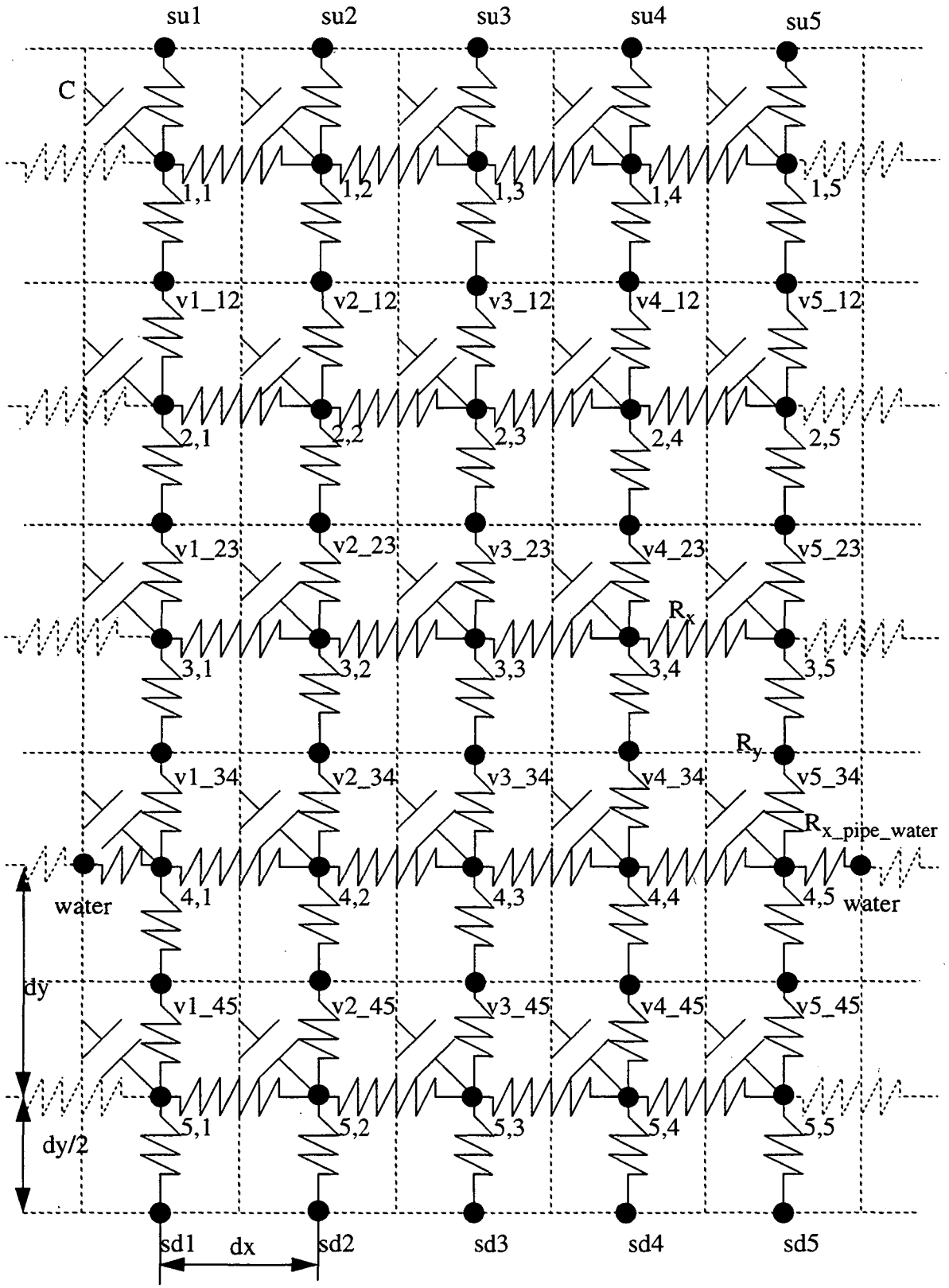

Figure 54. The 5 x 5 - node RC circuit of the cooled ceiling

7.4 The cooling panel

A different strategy to obtain a cooling ceiling is to suspend cold panels between a room and its plenum, similar to the way acoustical panels are suspended. The difference from acoustical panels is that the system is made out of aluminum, with metal pipes connected to the rear of the panel. When cold water is circulated through the pipes the good thermal contact between the pipes and the panel provides very low resistance to heat conduction. As a result the panel temperature is virtually equal to the water temperature, and this cold room surface can be maintained, at a given room temperature, by circulating water at a given rate. This system is more efficient than concrete core cooling if associated with an appropriate control strategy that adjusts the water flow to the cooling load requirements. This higher efficiency results from a lower time constant (time elapsed between the moment when an extra load is created and the moment when the ceiling temperature is optimally adjusted to the load), but also because the panel interacts with both the room and the plenum by means of convection.

7.4.1 The model of the cooling panel

7.4.1.1 Cooling panel heat transfer

Consider a room with a cooling panel system. Figure 55 shows the placement of the different components.

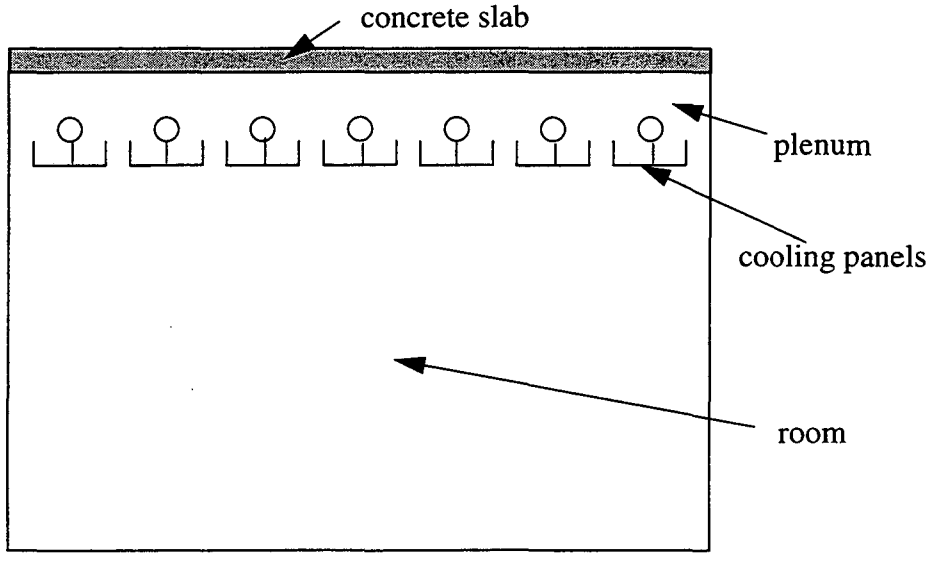

Figure 55. Room layout in the case of panel cooling.

The cooling panel exchanges radiation with the other surfaces in the room and with the concrete slab above the plenum. As a result, the room walls, floor, and the plenum slab are cooled. These surfaces will therefore IR radiation from sources inside the room and will convectively cool the room air. An additional cooling effect is achieved when the plenum

and room air are exchanged through the panels. In this case, rising room air will be convectively cooled by the top side of the panels and the plenum ceiling.

7.4.1.2 Cooling panel heat balance

The overall heat balance for the cooling panel is shown in Figure 56.

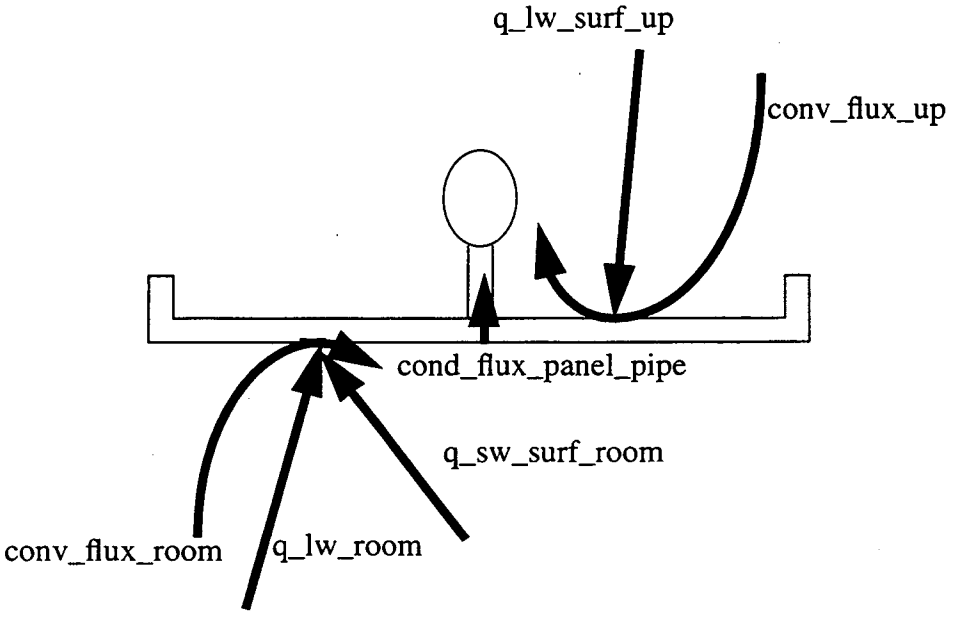

Figure 56. The heat balance in the case of the cooling panel

The balance equation is

$$sum-fluxes-room = conv-flux-room + q-lw-room + q-sw-room \quad (89)$$

$$sum-fluxes-up = conv-flux-up + q-lw-surf-up \quad (90)$$

$$cond-flux-panel-pipe = sum-fluxes-room + sum-fluxes-up \quad (91)$$

where

conv_flux_room is the convective flux on the room side of the panel [W/m^2]

q_lw_room is the long wave flux on the room side of the panel [W/m^2]

q_sw_room is the short wave flux on the room side of the panel [W/m^2]

sum_fluxes_room is the overall flux on the room side of the panel [W/m^2]

conv_flux_up is the convective flux on the plenum side of the panel [W/m^2]

q_lw_flux_up is the long wave flux on the plenum side of the panel [W/m^2]

sum_fluxes_up is the overall flux on the plenum side of the panel [W/m^2]

cond_heat_panel_pipe is the conductive heat flux from the panel to the pipe [W/m^2].

The heat transfer from the pipe to the water is given by

$$Q-cond-pipe-water = A\text{–}panel \times cond-heat-pane-pipe \quad (92)$$

where

Q_cond_pipe_water is the heat conducted into the water [W]

A_panel is the area of the panel [m^2].

The mechanisms by which the heat conducted into the water is removed are the same as those for the concrete core cooling (see paragraphs 7.3.2.1 - 7.3.2.3).

7.5 Radiant cooling system controls

As previously stated (e.g. in Section 7.3.2.2) it is possible to maintain comfort conditions by controlling the water flow in the ceiling of a room conditioned by radiant cooling. However, due to the time constant of the heat transfer process, the response of the room to a change in the water flow might be relatively slow. Therefore, a control mechanism is needed that allows the occupant to modify the response of the radiant system to specific building loads.

7.5.1 Thermostat-based control

The most common control of an air-conditioning system is thermostat based. The air temperature of the room air or the return air is measured. When the room temperature drops below a predetermined setpoint cooling is stopped. When the loads cause the temperature to rise above the setpoint, cooling is started.

For radiant cooling thermostat-based control is used to start or stop the flow of cold water as shown in Figure 57. The functioning control is based on the following algorithm:

$$\dot{m}_{water} = \dot{m}_{design} \text{ if } t_{room-air} \geq t_{setpoint}$$

$$\dot{m}_{water} = 0 \text{ if } t_{room-air} < t_{setpoint} \quad (93)$$

Although thermostat-based control mechanism is easy to implement it does not address the problem of delay in system response. Thermostat-based control is therefore more suitable for cooling panel systems, which have low thermal mass, than for concrete core cooling systems, which have high thermal mass.

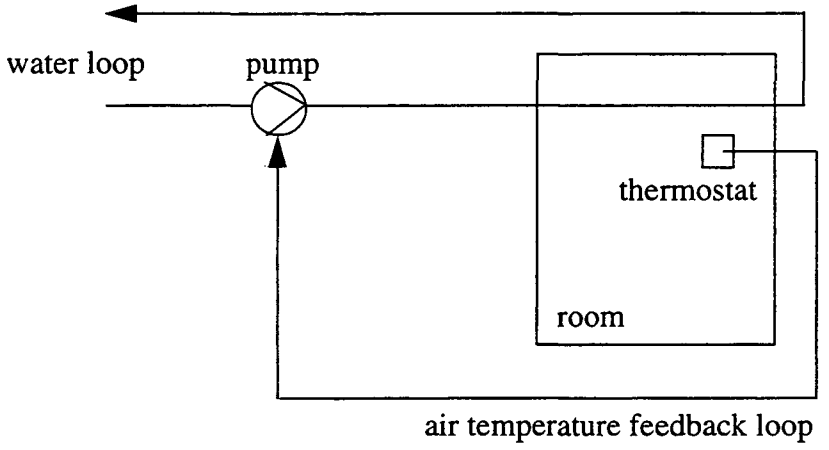

Figure 57. Thermostat-based control strategy

7.5.2 The timer-based control

Another type of control is time based. The system provides cooling according to a pre-set schedule. In some cases this control strategy is equivalent to achieving "distributed cold storage", which in turn can lead to a shift of the peak load away from its "natural" time of occurrence.

If the cooling is done overnight the time of occurrence of the peak load can be shifted to the evening or even nighttime hours. Figure 57 shows a schematic of timer-based control.

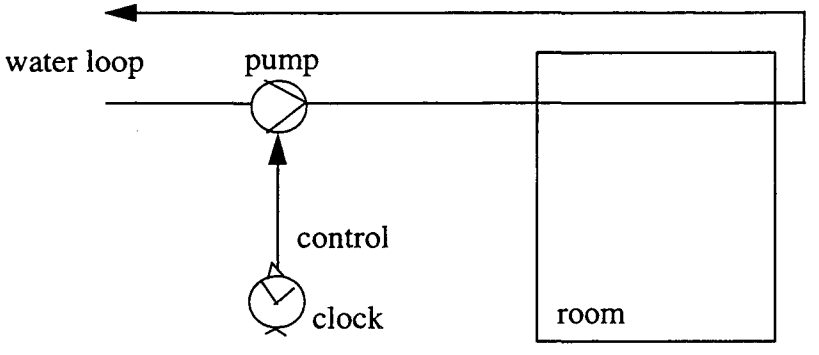

Figure 58. Timer-based control strategy

The timer-based strategy will not, however, respond to loads during the day, which makes it appropriate only for certain building types (those with large thermal mass) and certain climates (those with stable daily temperature amplitudes over a long period of time).

7.5.3 Hybrid control

Hybrid control is based on varying the water flow and temperature according to predetermined system information. If the response of the room to changes in the operation of the system is known the system can be operated so as to meet the cooling load. If the response of the room is not known, an "opening characteristic" can be used instead.

One type of a hybrid control strategy for radiant cooling is based on adjusting the water inlet temperature according to the room load. This can be achieved by using recirculation. The ratio of recirculated to total flow is controlled by the room conditions. The schematic of this control strategy is shown in Figure 57.

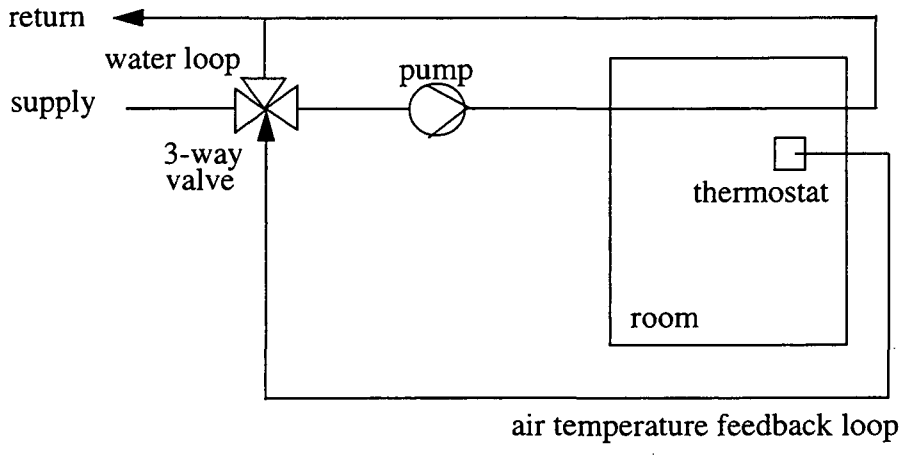

Figure 59. Hybrid control strategy

The hybrid control system used in the RADCOOL simulations in Chapter 5 is based on the following algorithm:

$$\dot{m}_{inlet} = \dot{m}_{cold} + \dot{m}_{return} \;,\; t_{inlet} = \frac{\dot{m}_{cold} t_{cold} + \dot{m}_{return} t_{return}}{\dot{m}_{inlet}},$$

with

$$\dot{m}_{cold} = x\dot{m}_{inlet} \;,\; \dot{m}_{return} = (1-x)\,\dot{m}_{inlet},$$

and

$$x = max\left[\frac{t_{room-air} - t_{setpoint-low}}{t_{setpoint-high} - t_{setpoint-low}}, 1\right] \text{, if } t_{room-air} \geq t_{setpoint-low}$$

$$\dot{m}_{inlet} = 0 \text{ if } t_{room-air} < t_{setpoint-low} \qquad (94)$$

The temperature interval [$t_{setpoint-low}$, $t_{setpoint-high}$] is input by the user.

7.6 The room air

7.6.1 The air temperature

The room air temperature is a function of many variables. Assuming constant air thermal properties and constant pressure, the room air temperature can be expressed as a function of time and position:

$$T_{air} = T_{air}(x, y, z, t) \tag{95}$$

Determining the space-time air temperature is complicated. It is difficult to find a closed form for T_{air} in SPARK, but approximate solutions for the temperature at discrete points can be determined. To that end, the room needs to be discretized and the mass and heat flows between the subdomains calculated. This procedure is, however, very time consuming (CPU time on the order of magnitude of 10 minutes on a mainframe for a steady state calculation [57]). Also, for RADCOOL, the interest is not so much in knowing the air temperature at a large number of nodes but in determining it at only a few points (Figure 60).

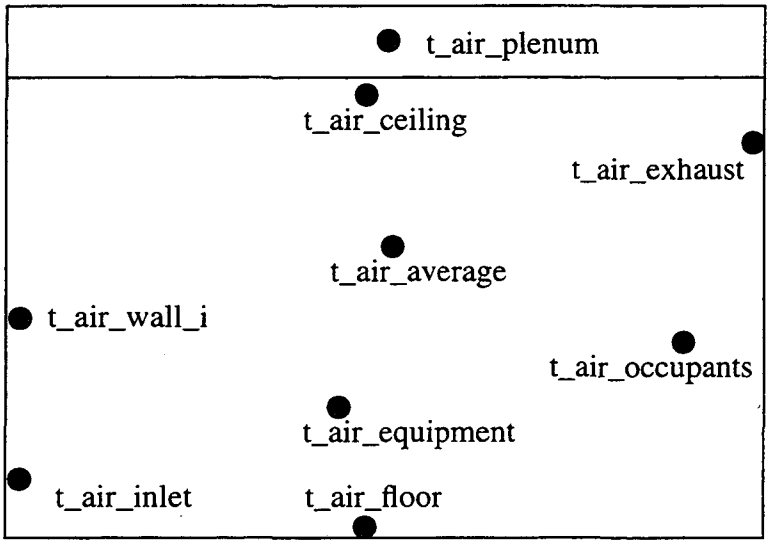

Figure 60. Air temperatures of interest in a room

The air temperatures shown in Figure 60 are the following:

t_air_inlet is the temperature of the incoming air. It constitutes a boundary condition for the other air temperatures

t_air_average is the air temperature in a room with fully mixed air

t_air_exhaust is the temperature of the air exhausted from the room

t_air_wall_i is the air temperature near wall i

t_air_floor is the air temperature near the floor

t_air_ceiling is the air temperature near the ceiling

t_air_occupants is the air temperature near the occupants

t_air_equipment is the air temperature near the equipment

t_air_plenum is the air temperature in the plenum.

7.6.2 Discretization of the room air domain in SPARK

In order to discretize the room air domain in SPARK simplifying assumptions for the different air temperatures need to be made. In RADCOOL the different air temperatures are expressed as a sum of the average air temperature and a temperature increment:

$$t_{air-wall-i} = t_{air-average} + t_{increment-wall-i} \quad (96)$$

$$t_{air-floor} = t_{air-average} + t_{increment-floor} \quad (97)$$

$$t_{air-ceiling} = t_{air-average} + t_{increment-ceiling} \quad (98)$$

$$t_{air-occupants} = t_{air-average} + t_{increment-occupants} \quad (99)$$

$$t_{air-equipment} = t_{air-average} + t_{increment-equipment} \quad (100)$$

where ***t_increment_...*** may be constant or proportional to the cooling load (see [58]).

In the current version of RADCOOL all the increments are zero, which corresponds to a one-zone model. Finding appropriate constants or functions for the increments is a subject of future research.

The calculations done in SPARK to determine the room air temperature involve heat and moisture balances.

7.6.3 Room air heat balance

The room air interacts with the wall and window surfaces, people, and equipment, and can be heated/cooled by the air that infiltrates or is brought into the room for ventilation. The room can also lose heat to the plenum, if it is cooler than the room. The heat balance equation for the room air is written in terms of the total heat per unit time that is absorbed or lost by the air in the room according to the equation

$$Q_{cap-air} + Q_{conv-in-tot} = Q_{vent-air-room} + Q_{infil-air-room} - Q_{from-room} + Q_{people} \quad (101)$$

where

Q_cap_air is the heat stored in the room air as a result of heat generated inside the room boundaries [W]

Q_conv_in_tot is the total convective heat absorbed by the room surfaces [W]

Q_vent_air_room is the heat brought into the room by the air conditioning equipment [W]

Q_infil_air_room is the heat brought into the room by air infiltration [W]

Q_conv_from_room is the heat lost by the room to the colder plenum [W]

Q_people is the heat generated by room occupants [W].

Equation (101) corresponds to Figure 61.

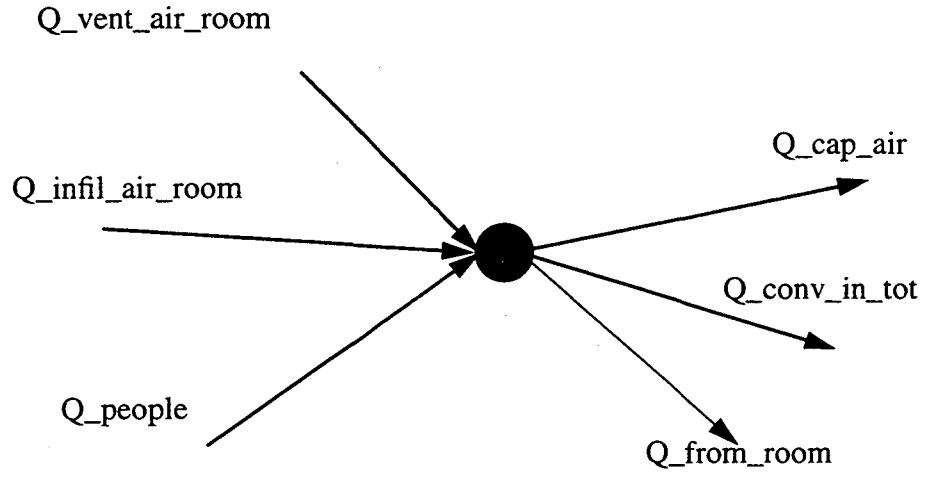

Figure 61. Heat balance for the room air

The heat balance is applied to a control volume whose boundary is identical with the interior surfaces of the room. The algorithms to calculate the heat terms in equation (101) are as follows:

Q_cap_air_room

This term represents the heat stored in the room air as a result of the room air temperature change:

$$Q_{cap-air-room} = \rho_{air} V_{room} c_{p-air} \frac{\partial T_{air-average}}{\partial t} \tag{102}$$

where

ρ_{room_air} is the room air density [kg/m^3], calculated as

$$\rho_{room-air} = \frac{0.62\,(1 + w_{room-air})\,p_{air}}{287.5\,(0.62 + w_{room-air})\,T_{air-average}} \tag{103}$$

and

p_{air} is the air pressure inside the room (considered equal to the outside air pressure [N/m^2]

$T_{air\_average}$ is the absolute temperature of the room air [K]

w_{room_air} is the room air moisture expressed in terms of the humidity ratio [kg of vapor/ kg of dry air]

V_{room} is the room volume.

c_p_air is the heat capacity of the room air, [J/kg K], calculated as

$$c_{p-air} = c_{p-dry-air} + w_{room-air} c_{p-vapor} \quad (104)$$

where

$c_{p\_dry\_air}$ and c_{p_vapor} are considered constant for RADCOOL purposes (see [59]):

$$c_{p-dry-air} = 1006 \frac{J}{kgK} \quad (105)$$

$$c_{p-vapor} = 1805 \frac{J}{kgK} \quad (106)$$

Q_conv_in_tot

This term represents the heat exchanged between the air and the surfaces by convection. The convective heat flux at each of the room surfaces are described in section 7.2.3.1. To conveniently use the fluxes (23), the convective heat for the room air is expressed as heat lost by the room air (and therefore appears in the left-hand side of equation (102)). It is calculated as the sum of all the heat flows Q_conv_in_i at the wall surfaces (see section 7.2.3.1), multiplied by the respective surface areas, plus the components for the occupants and the equipment:

$$Q_{conv-in-tot} = \sum_i A_{in-i} q_{conv-in-i} + Q_{conv-occupants} + Q_{conv-equipment} \quad (107)$$

Q_vent_air_room

This term corresponds to the heat added to the room air by air conditioning. Considering the density and pressure of the air constant at a given moment, and neglecting the influences of differences in velocities and potential energy of the air flow domain, the ventilation heat term in the room air heat balance is expressed as [60]:

$$Q_{vent-air-room} = \dot{m}_{vent-air-flow} c_{p-air} (t_{inlet} - t_{air-average}) \quad (108)$$

where

$m_{vent\_air\_flow}$ is the mass flux of the ventilation air [kg/s]

Q_infil_air_room

This term corresponds to the heat added by air infiltration. Based on the same consideration as in the section about ventilation heat, the infiltration term in the room heat balance is:

$$Q_{infil-air-room} = \dot{m}_{infil-air-flow} c_{p-air} (t_{air-out} - t_{air-average}) \quad (109)$$

where

$m_{infil\_air\_flow}$ is the mass flux of the infiltration air [kg/s].

It is generally rather difficult to obtain correct infiltration data. There are infiltration programs such as COMIS [61] that deal with this problem. Although there are several straightforward approaches, it is questionable whether the results obtained are accurate. The following is a summary of some different ways to calculate infiltration:

Proportional To Air Change Rate: this method assumes that the mass flow due to infiltration is proportional to the mass flow from ventilation. Although this is a very convenient approach it may be a little too rough and definitely fails for residential buildings.

DOE-2 Methodology: in DOE-2 three different approaches may be selected [62]: the air change method, the building method, and the crack method.

From A Database: this is the method with the highest accuracy if the database is based on calculations with an infiltration modeling program such as COMIS.

Q_conv_from_room

This term represents the heat transferred from the room to the plenum.

Consider the case when the room and plenum air have different temperatures (and therefore densities). If the two spaces communicate there will be air and heat exchange between them. The situation is analogous to Epstein's "air flow through horizontal openings"[54] which identifies four different regimes that depend on $\frac{L}{D}$, where L is the (vertical) thickness of the opening and D is the diameter of the opening.

For a cooled panel, the opening area through which this air exchange takes place is the total "crack" area in the panel-covered ceiling. The cracks are due to imperfect coverage, or are intentional, in order to augment the cooling effect of the ceiling.

Consider a room with a 4m x 5 m ceiling. If the panels are 20 cm thick and 5 m long in order to completely cover the ceiling, the total crack length will be

$$length_{crack} = \left(1 + \frac{width_{ceiling}}{width_{panel}}\right) length_{ceiling} = 105m \tag{110}$$

For 3 mm wide cracks, the total crack area is

$$area_{crack} = length_{crack} width_{crack} = 0.32m^2 \tag{111}$$

which gives a "lumped diameter"

$$D = \sqrt{\frac{4}{\pi} area_{crack}} = 0.63m \tag{112}$$

If the vertical thickness of the crack is L = 1 cm, the ratio $\frac{L}{D} = 0.015$. This corresponds to Epstein's Regime I, $\frac{L}{D} < 0.1$. This regime is governed by Taylor instability where the two fluids intrude into each other and an oscillatory exchange is observed. The regime is characterized by a constant dimensionless Froude number, meaning that the flow rate between the two fluids depends only on the densities (or the temperatures) of the two fluids. According to Epstein, a fluid exchange in Regime I is governed by the equation

$$\dot{V} = 0.04 D^{\frac{5}{2}} \left(g \frac{\Delta\rho}{\bar{\rho}}\right)^{\frac{1}{2}} \tag{113}$$

where

g is the acceleration due to gravity, 9.81 m/s^2

$\Delta\rho$ is the difference in density between the two fluids

$\bar{\rho}$ is the average density of the two fluids.

Assuming that the fluid exchange takes place at constant pressure (a good approximation for the case of room-plenum air exchange), equation (113) is equivalent to

$$\dot{V} = 0.04 D^{\frac{5}{2}} \left(g \frac{-\Delta T}{\bar{T}}\right) \tag{114}$$

where

ΔT is the temperature difference between the two fluids. The minus sign indicates that the flow occurs from the colder to the warmer fluid.

$\bar{T}$ is the average of the temperatures of the two fluids.

Equation (114) can be used to determine the heat flow between the room and the plenum due to the air exchange, given by

$$Q_{conv-heat-from-room} = \rho_{air} \dot{V} c_{air} (t_{room} - t_{plenum}) \ , \ t_{room} \geq t_{plenum},$$

$$C_{conv-heat-from-room} = 0, \ t_{room} < t_{plenum} \tag{115}$$

Q_people

This term represents the heat generated by the occupants in the room. It depends on the metabolic rate of the occupants, the radiative heat transfer between occupants and the environment and other factors:

(116)

$$Q_{people} = Q_{sensible} + Q_{latent} + \{Respiration, Conduction, Transpiration\}$$

$Q_{sensible}$ and Q_{latent} are calculated as in DOE-2 [61]:

$$Q_{sensible} = 0.293 \{A_s + \left[B_s \left(\frac{9}{5} t_{dry-air} + 32\right)\right]\} \tag{117}$$

where A_s and B_s are given by

$$A_s = 28 + 909.6Q_m - 119.5Q_m^2 \quad (118)$$

$$B_s = 1.2 - 100.48Q_m + 1.49Q_m^2 \quad (119)$$

$t_{dry\text{-}air}$ is the dry-bulb temperature of the room air (denoted so far by $t_{air\_average}$) and Q_m is the metabolic rate of all the people in the room [W]:

$$Q_{met} = number_{occupants} \bar{A}_{occupant} (metabolic - rate) \quad (120)$$

In equation (120)

$A_{occupant}$ is the average body area given by the Dubois empirical equation:

$$\bar{A}_{occupant} = 0.203 W^{0.425} H^{0.725} \quad (121)$$

where

W is the weight of the person [kg]

H is the height of the person [m].

The metabolic rate is usually expressed in *met* units (1 met = 58.15 W/m^2). It depends on the air temperature around a person, on the person's clothing and on the type of activity that the person performs [52]:

$$Q_{latent} = 0.293 \{A_l + \left[B_l (\frac{9}{5} t_{dry-air} + 32) \right]\} \quad (122)$$

with

$$A_l = 206 - 733.8Q_m + 160.9Q_m^2 \quad (123)$$

$$B_l = -6.7 + 15.16Q_m - 2.558Q_m^2 \quad (124)$$

Equations (117) and (122) give $Q_{sensible}$ and Q_{latent} in units of [W]. The respiration, conduction and transpiration terms are small and so are neglected in RADCOOL.

7.6.4 Plenum air heat balance

The plenum air interacts with the dropped ceiling and slab surfaces and can be heated/ cooled by the air that infiltrates from the room. The heat balance equation for the plenum air is analogous to that for the room air:

$$Q_{from-room} = Q_{cap-air-plenum} + Q_{conv-plenum-air} \quad (125)$$

where

Qcap_air_plenum is the heat stored in the plenum air as a result of heat generated inside the plenum boundaries [W]

Qconv_plenum_air is the total convective heat absorbed by the plenum surfaces [W]

Q_conv_from_room is the heat lost by the room to the colder plenum [W].

Equation (125) corresponds to Figure 62.

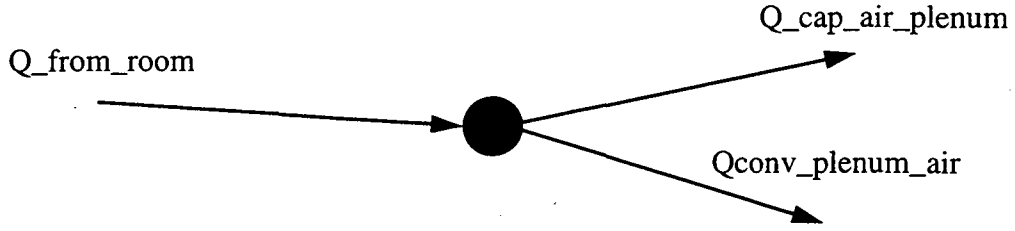

Figure 62. Heat balance for the plenum air

The heat balance is applied to a control volume whose boundary corresponds to the interior surfaces of the plenum. The algorithms to calculate the heat terms in equation (125) are similar to the ones described in paragraph 7.6.3. The term representing the heat infiltrated from the room is the same (equations (102) - (106)). In the case of the heat storage term the only difference is that instead of room air quantities, equations (110) - (115) should be based on quantities specific to the plenum air. The convection term in the plenum air balance can be calculated with

$$Q_{conv-plenum-air} = \sum_i A_{in-i} q_{conv-in-i} \tag{126}$$

where the products in the right-hand side are calculated for all the plenum surfaces.

7.6.5 Room air moisture balance

In addition to the heat balance for the room air, RADCOOL performs a moisture balance. Moisture enters the room by ventilation and infiltration, or comes from the occupants. The moisture balance has the form

$$V_{room} \frac{\partial w_{room-air}}{\partial t} = \dot{m}_{vent-air-flow} \Delta w_{vent} + \dot{m}_{infil-air-flow} \Delta w_{infil} + P \tag{127}$$

with

$$\Delta w_{vent} = w_{inlet-air} - w_{room-air} \tag{128}$$

$$\Delta w_{infil} = w_{air-out} - w_{room-air} \tag{129}$$

and

w_inlet_air the humidity ratio of the supply air [kg vapor/kg dry air]

w_air_out the humidity ratio of the outside air [kg vapor/kg dry air]

The people term P is given by

$$P = Q_{latent} \frac{q_{latent-specific}}{\rho_{room-air}} \tag{130}$$

where

Q_{latent} is calculated with equation (122).

7.7 Link objects

Link objects can be considered as the "glue" that connects the other classes of components. Link objects have to be written for each particular model of a room. For this reason these objects do not belong to a library but are created in the preliminary data processing phase of RADCOOL.

Currently in RADCOOL only a few quantities need to be calculated depending on the number and position of surfaces in the room. These are the total convective heat for the air heat balance, the air temperatures in the vicinity of the room surfaces, the total short wave radiation entering the room through transparent surfaces (windows, transparent walls), and the long wave radiation between the interior room surfaces.

The total convective heat for the air transfer balance is calculated from equation (107). The air temperatures in the vicinity of the room surfaces are calculated from equations (96) - (100). The entering short wave radiation is calculated from equation (44).

The long wave radiation exchange is calculated with equations (41) - (43).

7.8 Preliminary data processing

7.8.1 Introduction

We describe here the calculations that provide data for the SPARK program.

The first task is to collect information from the user that specifies the building to be modeled. Relevant data include:

- the characteristics of the building: number and type of walls (passive, radiant), number of windows, whether the building has an underground floor, etc.
- the characteristics of the building site: location of building, solar radiation, outside air temperature, ground temperature, wind, etc.
- the occupancy and equipment schedules of the building: number of occupants, type of activities performed, type of equipment, etc.
- the air flow characteristics (ventilation, infiltration)
- the HVAC system characteristics (thermostat setpoints, etc.)

- the desired output quantities from the calculation.

The second task is to convert these data for use in SPARK. Some of the data, such as thermal properties of building materials, hourly weather, etc. may be available in databases. Other inputs include shape factors the long wave radiation exchange and weather-dependent thermal properties. FORTRAN or C programs be used at this stage.

The third task is to create the SPARK model of the building which involves linking the different building components and creating the input files. This task is described in Appendix B for the RADCOOL test room.

7.8.2 Weather-related data

Weather-related quantities that need to be determined include primary weather data (such as ambient drybulb and dewpoint temperatures), soil temperature, and cloud cover. These quantities can usually be found in the weather file for a particular site. Also needed is the following weather-dependent information:

- the outside surface convective film coefficient h_{conv_out} (based on [50]), which depends on outside temperature, surface temperature, wind speed and wind direction. This value is currently obtained from DOE-2 hourly output.
- the sky emissivity ε_{sky},which depends on dewpoint temperature and sky cover (equation (25)).
- the direct and diffuse solar radiation incident on each surface, which depend on the position of the sun, cloud cover, and orientation of the surface
- the solar absorptivity of each glazing layer and the overall solar transmittance of each window, which depend on glazing type, sun position, and window orientation.

The next sections offer the algorithm for the calculation of the direct and solar radiation on a surface.

7.8.2.1 Algorithms to calculate the direct and diffuse solar radiation on a surface

A weather file may include measured direct and diffuse solar radiation on a horizontal plane and on a plane normal to the sun's rays. The heat balance equation for outside surfaces involve irradiance on tilted surfaces. We describe here the algorithms used to transform the measured solar quantities to those needed for the SPARK calculations. The methods are taken from [22]. The required irradiance values are calculated by DOE-2 and imported into RADCOOL.

Weather file quantities

The main solar quantities of interest are the direct normal irradiance I_{DN} and the total horizontal irradiance I_{tH} .

Solar position-related quantities

The calculation of direct and diffuse irradiance on a surface of arbitrary orientation involves the following sun-related quantities.

a. Apparent solar time

The apparent solar time depends on the local civil time, the geographical position of the building site and the fluctuations in the velocity of the earth [22], according to

$$AST = LST + ET + 4\,(LSM - LON) \tag{131}$$

where

AST is the apparent solar time

LST is the local standard time

ET is the value of the equation of time for the day of the year when the calculation is made

LSM is the local standard time meridian in degrees of an arc

LON is the local longitude in degrees

4 is the number of minutes it takes the Earth to rotate 1°.

According to [61] ET can be developed in a Fourier series as a function of the day of the year, n:

$$ET = A_0 + A_1 \cos W + A_2 \cos 2W + A_3 \cos 3W + B_1 \sin W + B_2 \sin 2W + B_3 \sin 3W \tag{132}$$

with

$$W = (\frac{2\Pi}{365})\, n \tag{133}$$

The coefficients in (133) are given in Table 6.

TABLE 6. Coefficients for Equation (132)

A_0	A_1	A_2	A_3	B_1	B_2	B_3
0.000696	0.00706	-0.0533	-0.00157	-0.122	-0.156	-0.00556

b. Solar angles

The position of the sun with respect to the site is usually described by the solar altitude, β, and solar azimuth, ϕ, measured from the south. The solar azimuth is positive for afternoon hours and negative for morning hours. Both these angles depend on the solar declination, δ, the hour angle, H, and the latitude L, according to:

$$\sin\beta = \cos L \cos\delta \cos H + \sin H \sin\delta \tag{134}$$

$$\cos\phi = \frac{\sin\beta \sin L - \sin\delta}{\cos\beta \cos L} \tag{135}$$

Consider a surface with azimuth Ψ measured from south and a tilt angle Σ. The surface solar azimuth, γ, is defined as:

$$\gamma = \phi - \Psi \tag{136}$$

If $90° < \gamma < 270°$, the surface is in shadow.

The angle of incidence, ϑ, of direct radiation on the surface is defined as the angle between the normal to the surface and the ray from the surface to the sun. The angle ϑ is given by

$$\cos\vartheta = \cos\beta\cos\gamma\sin\Sigma + \sin\beta\cos\Sigma \tag{137}$$

Direct irradiance

The direct solar irradiance I_D, incident on a surface depends on the direct normal irradiance, I_{DN}, and the angle of incidence, ϑ:

$$I_D = I_{DN}\cos\vartheta, \text{ if } \cos\vartheta > 0$$

$$I_D = 0, \text{ if } \cos\vartheta \leq 0 \tag{138}$$

Diffuse irradiance

The diffuse irradiance I_d, is composed of diffuse ground reflected irradiance, I_{dg}, and diffuse sky irradiance, I_{ds}.

$$I_d = I_{dg} + I_{ds} \tag{139}$$

A simple expression for I_{ds} is

$$I_{ds} = CI_{DN}F_{sky} \tag{140}$$

where

C is the sky diffuse factor

F_{sky} is the sky form factor (26), with $\Phi_{wall} = \Sigma$.

Similarly, I_{dg} is given by

$$I_{dg} = I_{th}\rho_g F_{ground} \tag{141}$$

where

ρ_g is the ground reflectance

F_{ground} is the ground form factor (29), with $\Phi_{wall} = \Sigma$.

C can be developed in a series as:

$$C = A_0 + A_1\cos W + A_2\cos 2W + A_3\cos 3W + B_1\sin W + B_2\sin 2W + B_3\sin 3W \tag{142}$$

with

$$W = (\frac{2\Pi}{365})n \tag{143}$$

The coefficients in (142) are given in Table 7.

TABLE 7. Coefficients for Equation (142)

A_0	A_1	A_2	A_3	B_1	B_2	B_3
0.0905	-0.041	0.0073	0.0015	-0.0034	0.0004	-0.0006

For vertical surfaces it is possible to express the diffuse radiation in terms of the total horizontal irradiance I_{tH}:

$$I_d = YI_{tH} \tag{144}$$

where the factor Y can be written as:

$$Y = 0.55 + 0.437\cos\vartheta + 0.313(\cos\vartheta)^2 \qquad \text{if } \cos(\vartheta) > -0.2$$

$$Y = 0.45 \qquad \text{if } \cos\vartheta \leq -0.2 \tag{145}$$

The direct and diffuse irradiances are presently input into RADCOOL from an output DOE-2 file.

7.8.3 Shape factors

7.8.3.1 Surface-to-surface shape factors

As stated in section 7.2.4.2, a surface in a room exchanges long wave (IR) radiation with the other surfaces in the room. The net long wave radiation absorbed by surface i in an N-surface enclosure is given by equations (41) - (43). In this section we show how the shape factors F_{ij}, are calculated.

The shape factor F_{ij} between surface i and surface j represents the fraction of the total long wave radiation emitted by surface j that is incident on surface i. In an N-surface enclosure the shape factor depends only on the geometry of the surfaces. The general equation for F_{ij} for surfaces i and j having the areas A_i and A_j respectively, is [55]:

$$F_{ij} = \frac{1}{A_i}\int_{A_i}\int_{A_j}\frac{\cos\theta_i\cos\theta_j}{\pi S^2}dA_i dA_j \tag{146}$$

where

S is the distance between a point on i and a point on j

θ_i is the angle between the surface normal on i and the line connecting i and j

θ_j is the angle between the surface normal on i and the line connecting i and j.

The integral on the right hand side of (146) is not always easy to calculate. In the case of rectangular surfaces the shape factors can be calculated by shape factor algebra [55]. Shape factor algebra provides relationships between analytically calculated shape factors corresponding to a given relative position of two surfaces, and shape factors corresponding to another given relative position of two surfaces. The basic relationship between the shape factor F_{ji} and the shape factor F_{ij} is

$$F_{ji} = \frac{A_i}{A_j} F_{ij} \tag{147}$$

To calculate the shape factors between arbitrarily located rectangles both integration and shape factor algebra are necessary.

In RADCOOL, the shape factor calculations are based on a library of FORTRAN programs. Each program calculates the shape factor for a given relative position of two surfaces in a rectangular room. To calculate the shape factor for a pair of surfaces the user selects the program corresponding to the surface pair, and then runs the program with input data corresponding to the dimensions of the surfaces.

The FORTRAN library for shape factor calculations

This library allows the user to calculate the shape factor between two walls, a wall and a window, or two windows.

The first two programs of the library contain two formulas that represent (exact) analytical solutions of the integral in (146). These formulas calculate the shape factors between two finite rectangular surfaces in the cases that:

- the surfaces have a common edge

- the surfaces are parallel and have the same dimensions (see Figure 63):

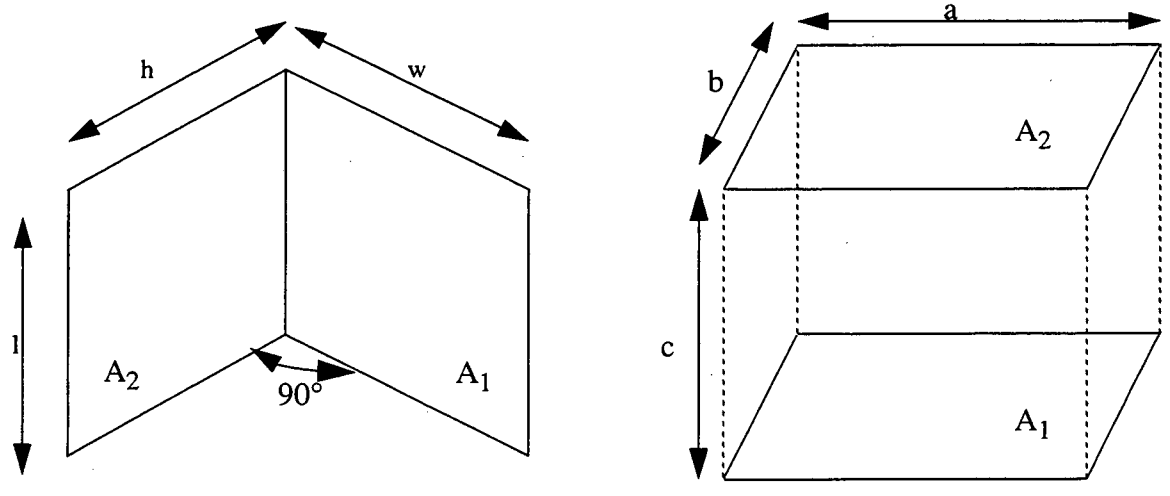

Figure 63. Relative positions of two rectangular surfaces that give exact solutions for the shape factors

The formulas are [55]:

$$F_{1-2-shape1} = \frac{1}{\pi W}(term_{1-shape1} - term_{2-shape1}) \tag{148}$$

where

$$term_{1-shape1} = W\operatorname{atan}\frac{1}{W} + H\operatorname{atan}\frac{1}{H} - \sqrt{H^2+W^2}\operatorname{atan}\frac{1}{\sqrt{H^2+W^2}} \tag{149}$$

$$term_{2-shape1} = \frac{1}{4}ln\{\frac{(1+W^2)\ (1+H^2)}{1+W^2+H^2}term_{3-shape1}\} \tag{150}$$

$$term_{3-shape1} = \left[\frac{W^2(1+W^2+H^2)}{(1+W^2)\ (W^2+H^2)}\right]^{W^2}\left[\frac{H^2(1+H^2+W^2)}{(1+H^2)\ (H^2+W^2)}\right]^{H^2} \tag{151}$$

$$H = \frac{h}{l} \tag{152}$$

$$W = \frac{w}{l} \tag{153}$$

and

$$F_{1-2-shape2} = \frac{2}{\pi XY}(term_{1-shape2} + term_{2-shape2}) \tag{154}$$

where

$$term_{1-shape2} = ln\left[\frac{(1+X^2)\ (1+Y^2)}{1+X^2+Y^2}\right]^{\frac{1}{2}} - X\operatorname{atan}X - Y\operatorname{atan}Y \tag{155}$$

$$term_{2-shape2} = X\sqrt{1+Y^2}\operatorname{atan}\frac{X}{\sqrt{1+Y^2}} + Y\sqrt{1+X^2}\operatorname{atan}\frac{Y}{\sqrt{1+X^2}} \tag{156}$$

$$X = \frac{a}{b} \tag{157}$$

$$Y = \frac{c}{b} \tag{158}$$

The other programs in the library use the first two and the following general relationship [55]: consider an arbitrary area A_1 exchanging radiation with a second area A_2. The shape factor F_{1-2} is the fraction of the total radiation emitted by A_1 that is incident on A_2. If A_2 is divided into two parts A_3 and A_4, the fraction of the total energy leaving A_1 that is incident on A_3 and the fraction incident on A_4 must total to F_{1-2} (see Figure 64).

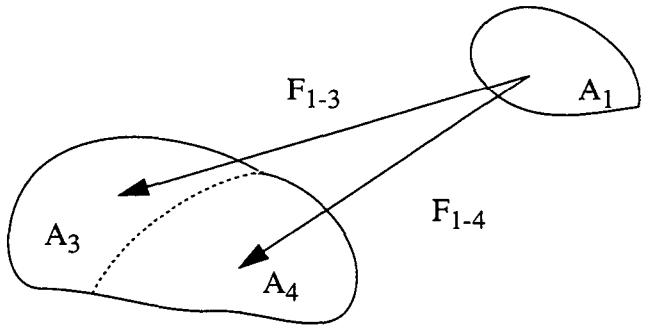

Figure 64. Energy exchange between finite areas with one area subdivided

Therefore

$$F_{1-2} = F_{1-(3+4)} = F_{1-3} + F_{1-4} \tag{159}$$

The calculation of shape factors in the other programs uses an algorithm that applies the analytical formulas (148)-(153) or (154)-(158), together with (159), to the specific case of a pair of surfaces. The relative positioning of the possible surface pairs in a rectangular enclosure is shown in Figures 65 - 68 (Appendix A). Each relative position corresponds to a FORTRAN program that calculates the shape factor between the shaded surface and the unshaded surfaces. Equation (147) can then be used to calculate the reciprocal shape factor.

7.8.3.2 Occupant-to-surface shape factors

The shape factor between an occupant and a surface can be obtained from (146) but the intergral is difficult because of the complexity of human geometry. Fanger [52] used a photographic method to find occupant-to-surface shape factors for standing and sitting persons. The results are contained in charts. However, using the charts is cumbersome, and can lead to errors in the program. An alternative solution was proposed by Summers et al. [63].

Currently, no long wave calculations involving occupants are done in RADCOOL.

7.9 Output data processing

A set of programs is available that extracts and plots user-selected, time-dependent output variables from a RADCOOL run. These variables include air temperature, surface temperatures, water flow, and water temperature. Thermal comfort can be determined from the air and surface temperatures is an indoor humidity level, currently not calculated in RADCOOL, is assumed. Chilled water use can be calculated from the water flow and temperature. Adding a chiller model to RADCOOL would allow calculating the energy needed to produce the chilled water.

8. Acknowledgments

We thank Meierhans and Partner AG and the Swiss National Energy Fund (NEFF) for providing the measurements described in section 4.2.2. We also thank Hans-Peter Graenicher, Hans-Georg Kula and Jan Maurer for their help in different stages of the project, and Brian Smith for producing most of the figures in sections 1 and 2.

We thank our CIEE program manager, Karl Brown, for his helpful comments on this report.

9. References

1. Usibelli,A., Greenberg, S., Meal, M., Mitchell, A., Johnson, R., Sweitzer, G., Rubinstein, F. and Arasteh, D., *Commercial-Sector Conservation Technologies*, Lawrence Berkeley Laboratory Report LBL-18543, 1985.
2. Simulation Research Group (LBL), *DOE-2 Basics*, LBL-29140, 1991.
3. Feustel, H.E., *Economizer Rating*. Report prepared for Southern California Edison Company, 1989.
4. 1991 ASHRAE Handbook, *Heating, Ventilating, and Air-Conditioning Systems and Applications*, American Society of Heating, Refrigerating and Air-Conditioning Engineers, Inc., Atlanta, GA, 1987.
5. Kroeling, P., *Gesundheits- und Befindensstoerungen in klimatisierten Gebaeuden*, Zuckschwerdt Verlag, Muenchen 1985.
6. Fanger, P.O., *Strategies to Avoid Indoor Climate Complaints*, Proc. Third International Congress on Building Energy Management, ICBEM '87, Volume I, Presses Polytechnique Romandes, Lausanne, 1987.
7. Mandell, M. and Smith, A.H., *Consistent Pattern of Elevated Symptoms in Air-Conditioned Office Buildings: A Reanalysis of Epidemiologic Studies*, American Journal of Public Health, 80 (1990), No. 10.
8. Esdorn, H., Knabl H. and Kuelpmann R., *Air-Conditioning, New Horizons - New Opportunities*, Proc. Indoor Air '87, Berlin, 1987.
9. Mayer, E., *Thermische Behaglichkeit und Zugfreiheit, physiologische und physikalische Erkenntnisse*, Proc. XXII. Internationaler Kongress fuer Technische Gebaeudeausruestung, Berlin, 1988.
10. Keller, G.M., *Energieaufwand fuer den Lufttransport mindern*, Clima Commerce International, Vol. 21, No. 2, 1988.
11. Skaret, E., *Displacement Ventilation*. Proc. Roomvent '87, Stockholm, June 1987.
12. Sutcliff, H., *A Guide to Air Change Efficiency*, Technical Note AIVC TN 28, Air Infiltration and Ventilation Centre, Coventry, (1990).
13. Mathisen, H.M., *Analysis and Evaluation of Displacement Ventilation*, Division of Heating and Ventilation, NTH, NTH-Report No. 1989:31, Ph.D. Thesis, 1989.
14. Cox, C.W.J., Ham, P.J., Koppers, J.M. and Van Schijndel, L.L.M., *Displacement Ventilation Systems in Office Rooms - A Field Study*, Proc. Room Vent '90, Oslo, June 1990.
15. Baker, M., *Improved Comfort through Radiant Heating and Cooling*, ASHRAE Journal 2 (1960), No. 2.
16. Fanger, P.O., *Thermal Comfort Analysis and Applications in Environmental Engineering*, Mc.Graw Hill, Inc., New York, NY, 1972.
17. McNall, P.E. and Biddison, R.E., *Thermal and Comfort Sensations of Sedentary Persons Exposed to Asymmetric Radiant Fields*; ASHRAE Transactions, Vol. 76, pp. 123-136, 1970.

18. Schlegel, J.C. and McNall, P.E., *The Effect of Asymmetric Radiation on the Thermal and Comfort Sensations of Sedentary Subjects*; ASHRAE-Transactions, Vol. 74, pp. 144-154, 1968.

19. Mayer, E., *Auch die Turbulenzen sind wichtig*, Clima Commerce International 19 (1985), No. 10, p. 20.

20. Mayer, E., *Air Velocity and Thermal Comfort*, Proc. Indoor Air '87, Berlin, 1987.

21. ASHRAE Standard 55-1992, *Thermal Environmental Conditions for Human Occupancy*, American Society for Heating, Refrigeration and Air-Conditioning Engineers, Inc., 1992

22. ASHRAE Handbook, *Fundamentals*, American Society for Heating, Refrigeration and Air-Conditioning Engineers, Inc., 1993.

23. ISO 7730. 1984. *Moderate Thermal Environments - Determination of the PMV and PPD Indices and Specification of the Conditions for Thermal Comfort.*

24. Kollmar, A., *Die zulaessige Kuehldeckentemperatur aus waermephysiologischer Sicht*, Gesundheits-Ingenieur 88 (1967), No. 5, pp. 137-140.

25. Trogisch, A., *Kuehldecke und Lueftung*, Clima Commerce International 4(1991), p.50.

26. Glueck, *Leistung von Kuehldecken*, Kuehldecke und Raumluft, Fachinstitut Gebaeude-Klima, Stuttgart, 1990.

27. Anon., *Marktuebersicht Kuehldecken*, KI Klima-Kaelte-Heizung, No. 1/2, 1993.

28. Anon.,*Radiant Metal Ceiling Panels - A Method of Testing Performance*, Department of Veterans Affairs (Date unknown).

29. Anon., *SPC 138P, MOT for Rating Hydronic Radiant Ceiling Panels*, Handout at the SPC138P-meeting on June 24, 1991, Indianapolis.

30. FGK Vorschrift KD 1, *Vorschriften des Fachinstituts Gebaeude-Klima e.V. fuer: Waermetechnische Messungen an Kuehldeckenelementen*, Fachinstitut Gebaeude-Klima e.V., Bissingen-Bietigtheim, December 1992.

31. DIN 4715 Entwurf, *Raumkuehlflaechen; Leistungsmessung bei freier Stroemung; Pruefregeln*, Beuth Verlag GmbH Berlin, April 1993.

32. Kuelpmann, R., *Thermal Comfort and Air Quality in Rooms with Cooled Ceilings - Results from Scientific Investigations*, ASHRAE Transactions 1993, Vol. 99, Pt. 2, 1993.

33. Fanger, P.O., Ipsen, B.M., Langkilde, G., Olesen, B.W., Christensen, N.K. and Tanabe, S., *Comfort Limits for Asymmetric Thermal Radiation*, Energy and Buildings, 8 (1985), pp. 225-236.

34. Esdorn, H.and Ittner, M., *Betriebsverhalten vo8n Deckenkuehlsystemen*, HLH Heizung- Lueftung- Haustechnik 41 (1990), pp. 598-601.

35. Feil, K., *Wirtschaftliche Betrachtungen zu Kuehldecken in Bueroraeumen*, In: Kuehldecke und Raumlueftung, Fachinstitut Gebaeude-Klima e.V., Bietigheim-Bissingen, F.R.G., 1991.

36. Hoenmann, W.and Nuessle F., *Kuehldecken verbessern Raumklima*, In: Kuehldecke und Raumlueftung, Fachinstitut Gebaeude-Klima e.V., Bietigheim-Bissingen, F.R.G., 1991.

37. Meierhans, R. *DOW Europe S.A., Horgen*, NEFF Project 464, 1994, unpublished.

38. Graeff, B., *Kuehldecke und Raumklima*, In: Kuehldecke und Raumlueftung, Fachinstitut Gebaeude-Klima e.V., Bietigheim-Bissingen, F.R.G., 1991.

39. Anon., *The KA.RO Air Conditioning System from Herbst*, Product Information Herbst Technik, Berlin, F.R.G., 1991.

40. Meierhans, R. and Zimmermann M., *Slab Cooling and Earth Coupling*, Proceedings to "Innovative Cooling Systems", International Energy Agency, Energy Conservation in Buildings and Community Systems, Solihull, U.K., May 1992.

41. Anon., *Advanced Hydronic Heating and Cooling Technology*, Leaflet, eht-Siegmund, Inc., Tustin, CA.

42. Feustel, H.E., *Reduktion der elektrischen Spitzenlast durch Strahlungskuehlung*, Clima Commerce International, 1991.

43. Feustel, H.E., *Hydronic Radiant Cooling, Overview and Preliminary Assessment*, LBL-33194 UC 350, 1992.

44. Feustel,H.E., De Almeida,H., Blumstein, C., *Alternatives to Compressor Cooling in California Climates - Review and Outlook*, CIEE Research Report Series, LBL-30041, 1991.

45. Zweifel, G., *Simulation of Displacement Ventilation and Radiative Cooling with DOE-2*, ASHRAE Transactions 1993, Vol. 99, Pt. 2, 1993.

46. Sowell, E.F., Buhl, W.F., Erdem, A.E. and Winkelmann, F.C.: *A Prototype Object-based System for HVAC Simulation*, Proc. Second International Conference on System Simulation in Buildings, Liege, Belgium, December 1986. LBL-22106.

47. El Daisty, R., Fazio, P. and Budaiwi, I., *Modelling of Indoor Air Humidity: the Dynamic Behavior Within an Enclosure*, in Energy and Buildings 19 (1992), pp. 61-73.

48. Sowell, E.F. and Moshier, A.M., *HVAC Component Model Library for Equation-Based Solvers*, Proc. Building Simulation '85..

49. Carslaw,H.S. and Jaeger, J.C., *Conduction of Heat in Solids*, Clarendon Press, Second edition, 1978.

50. Klems, J.H.,*U-Values, Solar Heat Gain and Thermal Performance: Recent Studies Using the MoWiTT*, LBL-25487 Revised, Mo-254, 1989.

51. TARP Reference Manual, NBSIR 83-2655, 1981, p.21.

52. Fanger, P.O., *Thermal Comfort*, McGraw-Hill,1970.

53. Raber, B.F. and Hutchinson, F.W., *Panel Heating and Cooling Analysis*, John Wiley, New York, 1947.

54. Epstein, M., *Buoyancy-Driven Exchange Flow Through Small Openings in Horizontal Partitions*, Trans. of the ASME, Journal of Heat Transfer Vol. 110, pp. 885-892.

55. Siegel, R. and Howell, J.R., *Thermal Radiation Heat Transfer*, Second Edition, Hemisphere Publishing Corporation, 1981, pp.172-198 and 236-238.

56. Holman, J.P., *Heat Transfer*, Sixth Edition, McGraw-Hill, 1986.

57. Shoemaker, R.W., *Radiant Heating*, McGraw-Hill, Second Edition, 1954.

58. Chen,C.Q. and Van der Kooi, J., *Accuracy - a Program for Combined Problems of Energy Analysis, Indoor Air Flow and Air Quality*, ASHRAE Transactions, 94(1988).

59. Brandemuehl, R., Gabel, S. and Andresen, I., *A Toolkit for Secondary HVAC System Energy Calculations*, Prepared for ASHRAE, University of Colorado at Boulder, 1993.

60. Baehr, H. D., *Thermodynamik*, Springer Verlag, 1989 (7th Edition).

61. Feustel, H.E. and Rayner-Hooson, A. (editors), *COMIS Fundamentals*, LBL-28560, 1990.

62. Simulation Research Group (LBL) and Group Q-11 (LANL), *DOE-2 Engineering Manual,* LBL-11353, 1982.

63. Summers, L.H. and Kalisperis, L.N., *Expanded Research on Human Shape Factors for Inclined Surfaces,* Energy and Buildings, 17 (1991) 283-295.

Appendix A. The shape factor calculation in the case of rectangular surfaces

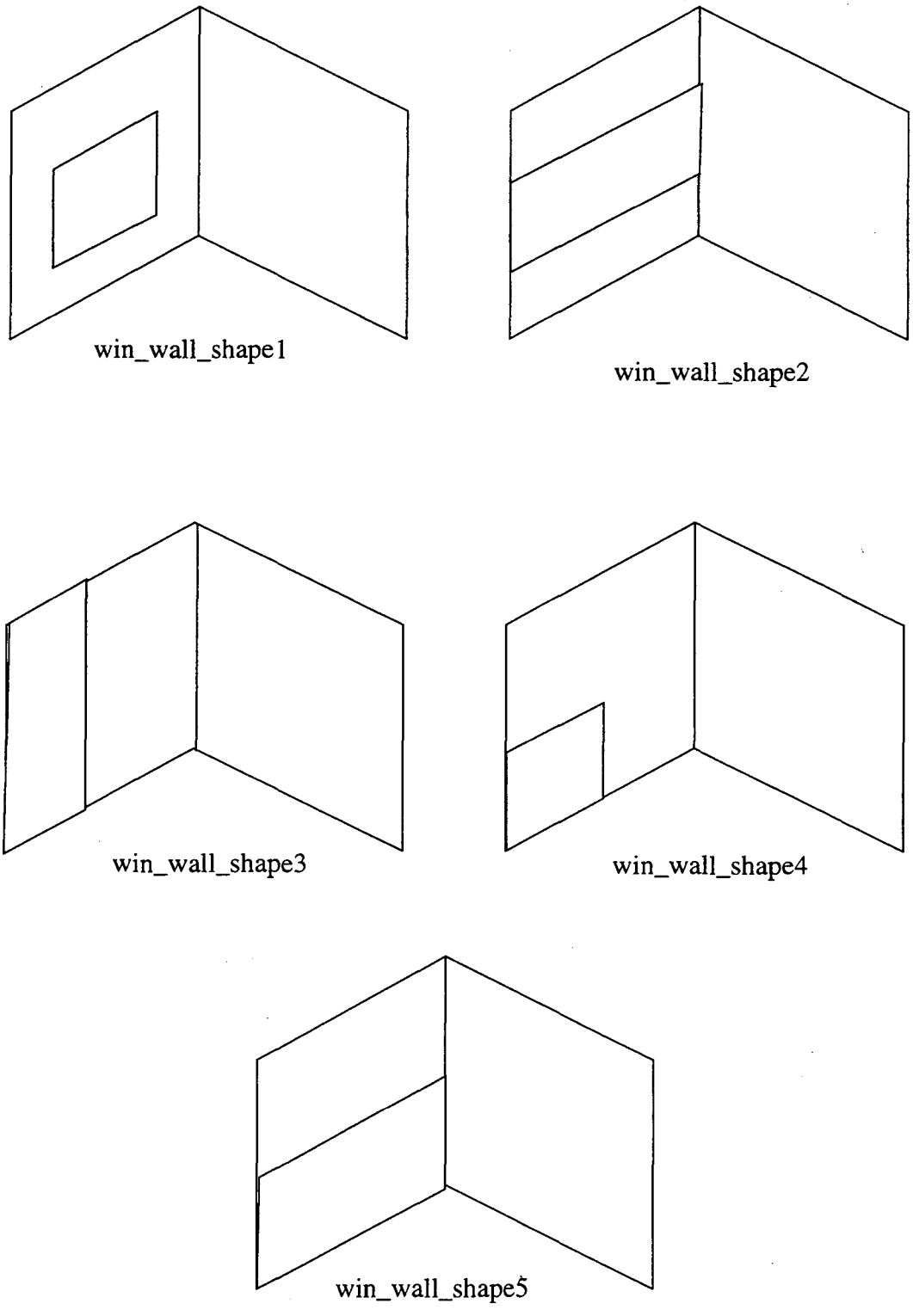

Figure 65. The relative positioning of adjacent window and wall surfaces at an angle of 90°.

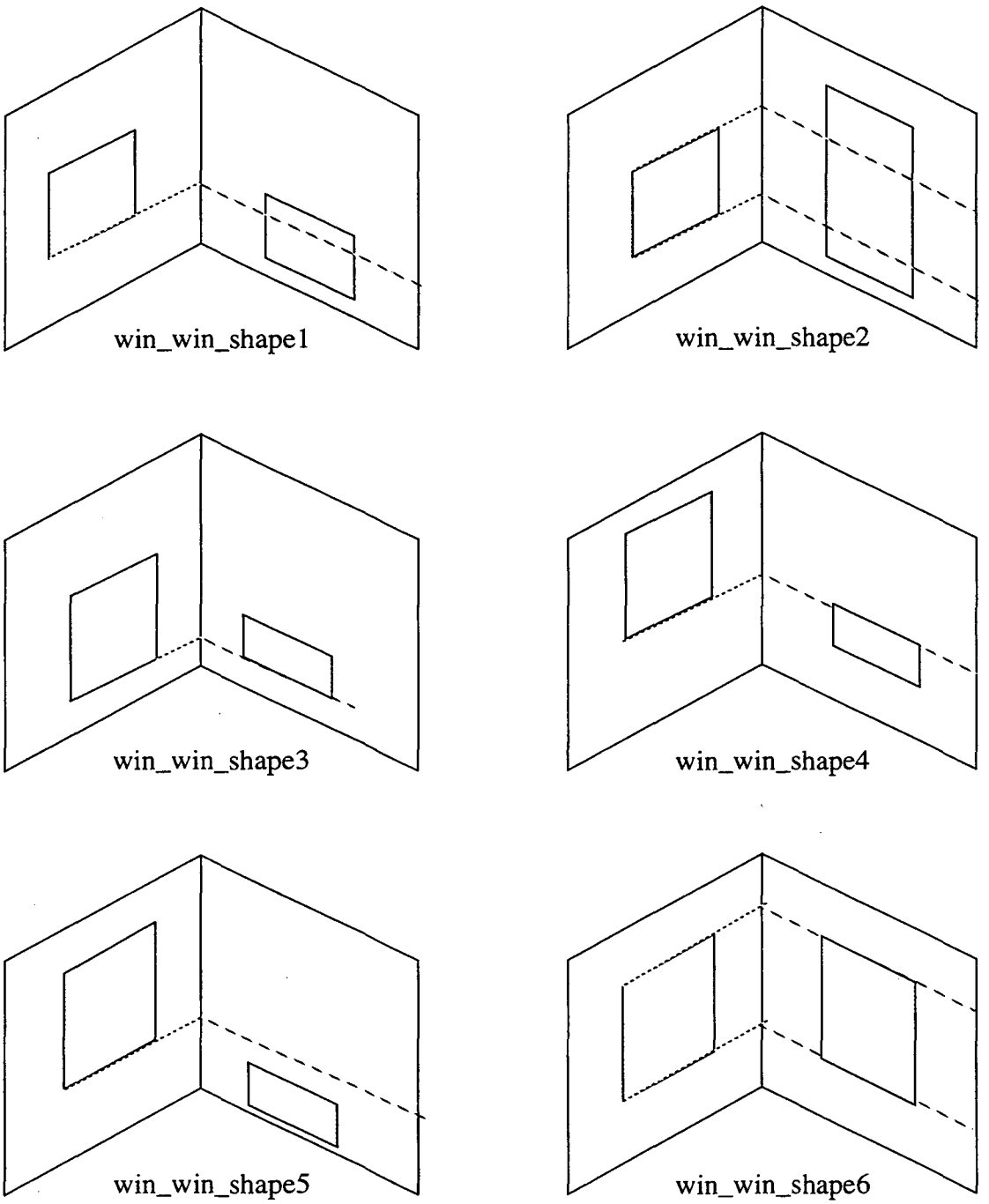

Figure 66. The relative positioning of two adjacent window surfaces at an angle of 90°.

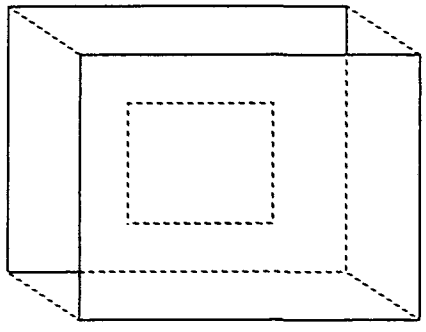

win_opp_shape1

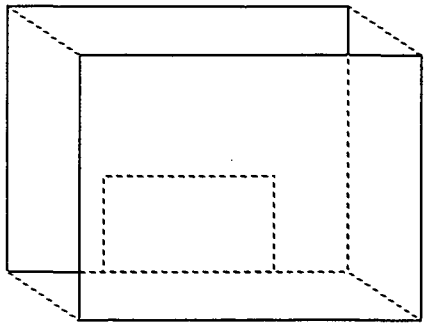

win_opp_shape2

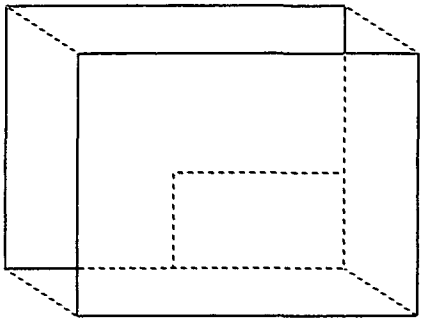

win_opp_shape3

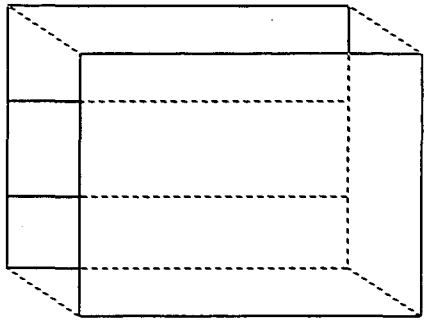

win_opp_shape4

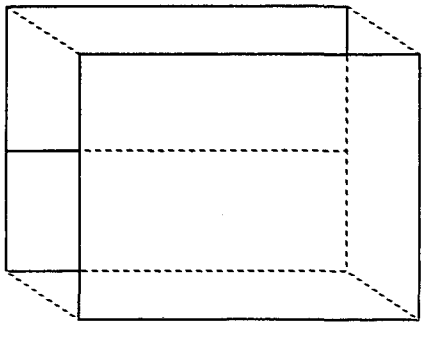

win_opp_shape5

Figure 67. The relative positioning of parallel window and wall surfaces

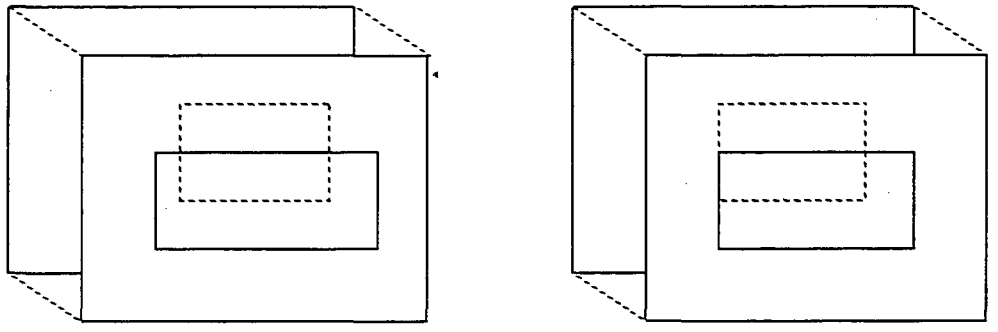

win_win_opp1

win_win_opp2

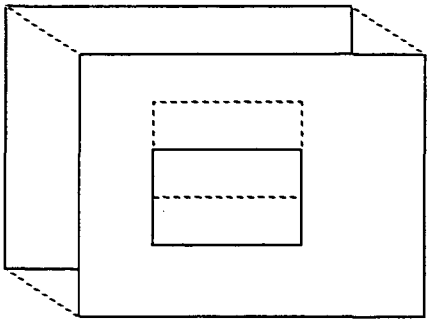

win_win_opp3

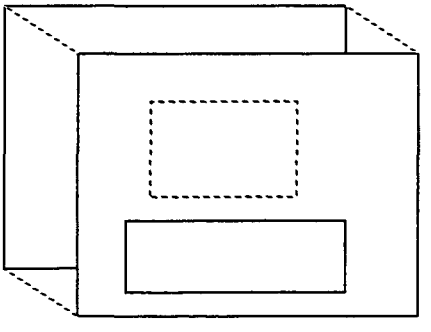

win_win_opp4

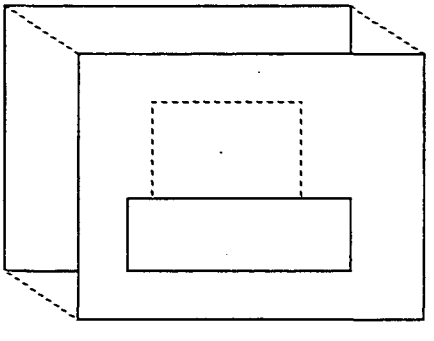

win_win_opp5

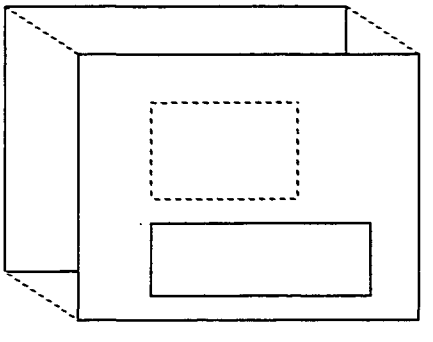

win_win_opp6

Figure 68. The relative positioning of two parallel windows. The shaded window is located on the back wall.

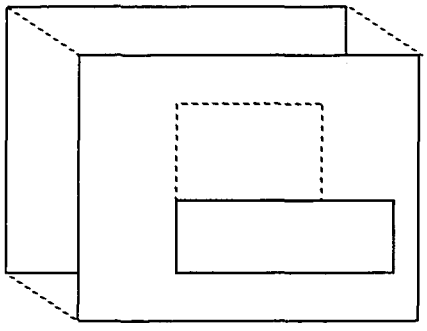

win_win_opp7

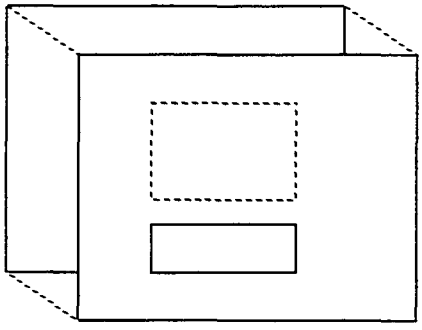

win_win_opp8

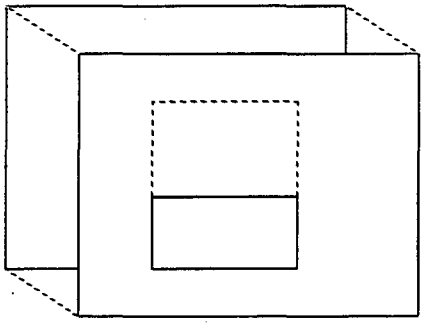

win_win_opp9

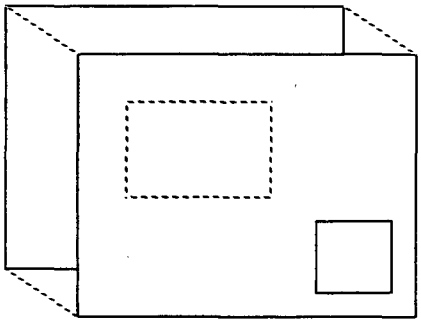

win_win_opp10

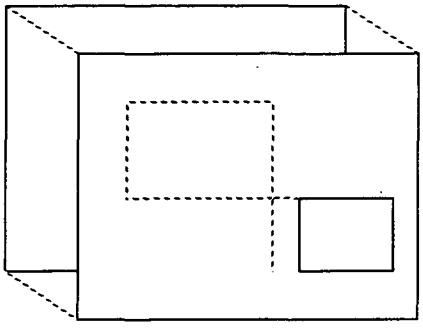

win_win_opp11

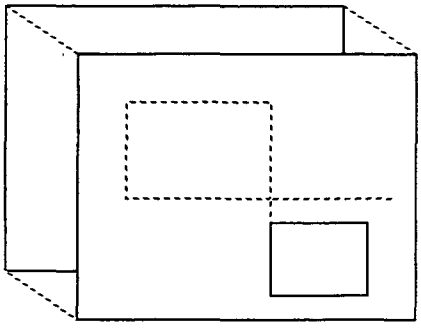

win_win_opp12

Figure 68. (continued)

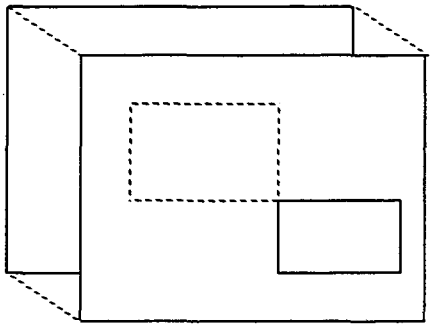

win_win_opp13

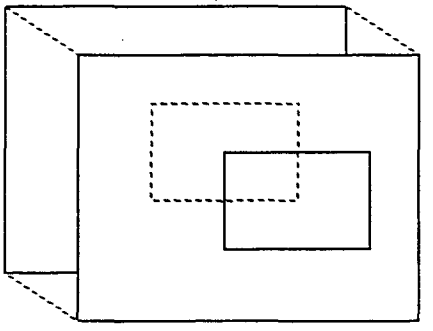

win_win_opp14

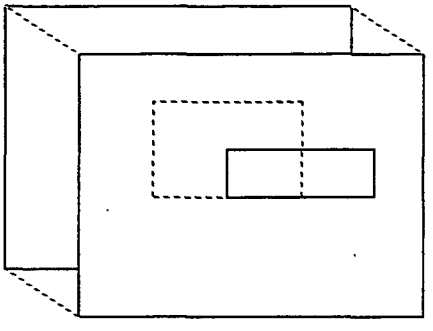

win_win_opp15

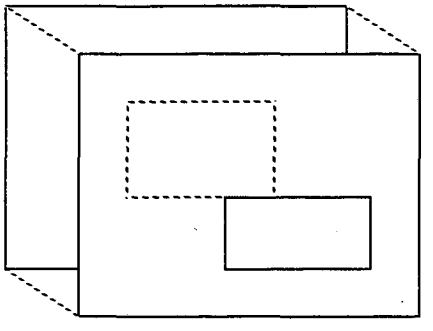

win_win_opp16

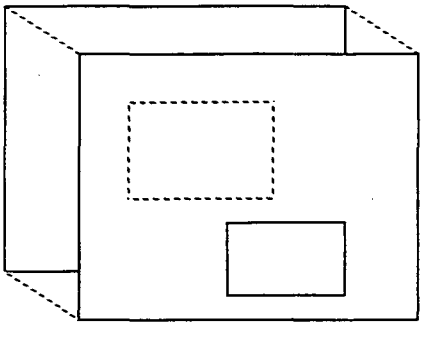

win_win_opp17

Figure 68. (continued)

Appendix B. Guide to setting up a SPARK file for a test room

B.1 Introduction

In this section we describe how to set up the SPARK program to simulate a test room with 4 vertical walls (of which one has a window), an underground floor and an exterior ceiling. Each surface is rectangular.

There are many ways to create a SPARK problem specification (`.ps`) file for such a problem. For clarity a step-by-step approach was chosen. The problem has been divided into subproblems such as the 4-layer passive wall for which stand-alone modules exist in the SPARK library or need to be created to suit each problem.

A consistent nomenclature is crucial for a SPARK simulation. We have numbered each component of the room in order to make the identification of variables easier. The vertical walls of the room are numbered from 1 to 4 1 = west, 2 = north, 3 = east, 4 = south. The ceiling is number 5. The floor is number 6. The window is number 1_w1 to show that it is located on wall number 1 (facing west) and that it is the first window to be modeled.

In the following we describe the steps involved in constructing a RADCOOL model for the test room.

B.2 First step: surfaces

Surfaces in RADCOOL separate the interior of the room from the outside. Examples of surfaces are walls and windows.

We define [k] to be a counting variable for the surfaces, with [kmax] equal to the total number of surfaces.

B.2.1 Read in the `.ps` files

The process described below is performed for each surface.

Read in the surface modules

Read in the file `four_layer_wall_generic.ps`;

change the surface object names from `_o` to `_[k]_o`;

change variable names from `_i` to `_[k]`;

write 'declare' line on top of the file.

Repeat for all the five vertical walls.

Read in the file `four_layer_floor_generic.ps`;

change the surface object names from `floor_o` to `floor_6_o`;

change variable names from `_i` to `_6`;

write 'declare' line on top of the file.

Read in the file `two_pane_window_generic.ps`;

change the surface object names from `win_o` to `win_1_w1_o`;

change variable names from `_i` to `_1_w1`;

write 'declare' line on top of the file.

B.2.2 Connect the surface modules together

Some variables and constants such as outside air temperature, cloud cover fraction, time step, are used by all surfaces. These variables are handled by inputting them once for the first surface and then referring to them for the other surfaces. The procedure for doing this is the subject of this section.

Connect the time step

In the line for dt, after

`four_layer_wall_1_o.dt,`

write all the other

`,four_layer_wall_[k]_o.dt`, with $2 \leq k \leq 5$;

write

`,four_layer_floor_6_o.dt`

`,two_pane_window_1_w1_o.dt.`

Delete all other lines for 'dt' in the other wall modules.

Connect the outside air drybulb temperature

In the line for `t_air_out`, after

`four_layer_wall_1_o.t_air_out,`

write all the other

`,four_layer_wall_[k]_o.t_air_out`, with $2 \leq k \leq 5$ (the floor is not in contact with the outside air);

write

`,two_pane_window_1_w1_o.t_air_out.`

Delete the lines for `t_air_out` in the surface modules.

Connect the outside air dewpoint temperature

In the line for `td_air_out`, after

`four_layer_wall_1_o.td_air_out,`

write all the other

`,four_layer_wall_[k]_o.td_air_out`, with $2 \leq k \leq 5$ (the floor does not exchange infrared radiation with the building surroundings);

write

`,two_pane_window_1_w1_o.td_air_out.`

Delete the lines for `td_air_out` in the other modules.

Connect the sky cover coefficient

In the line for `N`, after

`four_layer_wall_1_o.N,`

write all the other

`,four_layer_wall_[k]_o.N`, with $2 \leq k \leq 5$ (the floor does not exchange infrared radiation exchange with the building surroundings);

write

`,two_pane_window_1_w1_o.N.`

Delete the lines for `N` in the surface modules.

Connect the total interior short wave radiation

In the line for `Q_short_wave_tot`, after

`four_layer_wall_1_o.Q_short_wave_tot_in_i,`

write all other

`,four_layer_wall_[k]_o.Q_short_wave_tot_in_i` with $2 \leq k \leq 5$;

write

`,four_layer_floor_6_o.Q_short_wave_tot_in_i;`

write

`,two_pane_window_1_w1_o.Q_short_wave_tot_in_i.`

Delete the lines for `Q_short_wave_tot` from the surface modules.

Note: included in the two-pane window is the statement that the total short wave radiation entering the room equals the transmitted solar radiation through the window. For a room with more than one window, the total short wave radiation is the sum of the solar radiation transmitted through all of the windows.

B.3 Second step: the room air

The room air is represented by the `.ps` file `room_air_generic.ps`.

B.3.1 Read in the `.ps` file

Read in `room_air_generic.ps`;

write the declare line after 'declare equal q_sw_in;'

B.3.2 Connect the room air module with the surface modules

Connect the time step

In the line for dt, after

two_pane_window_1_w1_o.dt,

write

,room_air_o.dt.

Delete the line for dt from the room air module.

Connect the outside air drybulb temperature

In the line for t_air_out, after

two_pane_window_1_w1_o.t_air_out_i,

write

,room_air_o.t_air_out.

Delete the line for t_air_out from the air balance module.

Move the other weather-related quantities to the top of the file

Move the lines for

p_air_out,

w_air_out,

w_inlet_air,

c_dry_air,

c_vapor,

after the line for the cloud cover 'N'. This assures that all of the non-room dependent variables will be at the top of the SPARK input file.

B.4 Third step: the links between room components

The links between room components are SPARK modules that depend on the room layout, i.e., the number and type of surfaces. In the current version of RADCOOL, the two existing link modules are the room air and the long wave radiation.

B.4.1 The connection between the room air module and the room surfaces

This linking module is represented by the file link_air_generic.ps. The file was created to calculate the convective term for the room air heat balance. This module also calculates the air temperature near each surface.

Read in the .ps file

Read in the `link_air_generic.ps` file.

Write the declare line after '`declare room_air room_air_o;`'

Connect the quantities

Connect the convection heat fluxes

Starting with the first surface module, in the line for `qconv_in_obj_1`, after

`four_layer_wall_1_o.qconv_in_obj_i,`

write

`,link_air_o.qconv_wall_1.`

Repeat for `qconv_in_obj_[k]`, for $2 \leq k \leq 5$.

Delete the lines for `qconv_in_wall_[k]` from the link module.

In the floor module, in the line for `qconv_in_obj_6`, after

`four_layer_floor_6_o.qconv_in_obj_i,`

write

`,link_air_o.qconv_floor_6.`

Delete the line for `qconv_in_floor_6` from the link module.

In the window module, in the line for `qconv_in_win_1_w1`, after

`two_pane_window_1_w1_o.qconv_in_win_i,`

write

`,link_air_o.qconv_win_1_w1.`

Delete the line for `qconv_in_win_1_w1` from the link module.

Connect the total convective heat term in the room air module

In the link module, in the line for `Qconv_air_room`, after

`link_air_o.Qconv_air_room,`

write

`,room_air_o.Qconv_air_room.`

Delete the line for `Qconv_air_room` from the room air module.

Connect the average air temperature

In the air module, in the line for the average air temperature `t_air_average`, after

`room_air_o.t_air_average,`

write

,link_air_o.t_air_room.

Delete the line for t_air_room from the link module.

Connect the interior air temperatures on which the convection calculation is based

In the link module, in the line for t_air_wall_1, after

link_air_o.t_air_wall_1,

write

,four_layer_wall_1_o.t_air_in_i.

Repeat for the lines corresponding to t_air_wall_[k]_o for $2 \leq k \leq 4$.

Delete the lines for t_air_in_[k] from the vertical wall modules.

In the link module, in the line for t_air_ceiling, after

link_air_module.t_air_ceiling,

write

,four_layer_wall_5_o.t_air_in_i.

Delete the line for t_air_in_5 from the ceiling module.

In the link module, in the line for t_air_floor, after

link_air_module.t_air_floor,

write

,four_layer_floor_6_o.t_air_in_i.

Delete the line for t_air_in_6 from the floor module.

In the link module, in the line for t_air_win_1_w1, after

link_air_module.t_air_win_1_w1,

write

,two_pane_window_1_w1_o.t_air_in_i.

Delete the line for t_air_in_1_w1from the window module.

B.4.2 The total short wave radiation entering the room through transparent surfaces

This linking module is represented by the file link_sw_generic.ps. The file was created to calculate the total short wave radiation that enters the room.

Read in the .ps file

Read in the link_sw_generic.ps file.

Write 'declare' line on top of the file.

Connect the quantities:

Connect the window area

In the air link module, in the line for `A_in_win_1_w1`, after

```
link_air_module.A_in_win_1_w1,
```

write

```
,link_sw_o.A_in_win_1_w1.
```

Delete the line for `A_in_win_1_w1` from the short wave radiation link module.

Connect the short wave radiation transmitted through the window surface

In the window module, in the line for `q_sw_win_1_w1`, after

```
two_pane_window_1_w1.q_sw_win_1_w1,
```

write

```
,link_sw_o.q_solar_win_1_w1.
```

Delete the line for `q_solar_win_1_w1` from the short wave radiation link module.

Connect the total interior short wave radiation

In the short wave radiation link module, in the line for `Q_solar_win_1_w1`, after

```
link_sw_o.Q_solar_win_1_w1,
```

write

```
,total_sw.a.
```

In the general input data section, in the line for `Q_short_wave_tot_in`, after

```
Q_short_wave_tot_in(
```

write

```
,total_sw.b.
```

In the declare section, after the declare line for the short wave radiation link module, write

```
declare equal    total_sw;
```

B.4.3 The long wave radiation connection among the room surfaces

This linking module is represented by the file `lw_rad_in_generic.ps`. The file was created to calculate the net long wave radiation at each of the 7 room surfaces and at effective surfaces representing occupants and equipment.

Read in the `.ps` file

Read in the `lw_rad_in_generic.ps` file.

Write 'declare' line on top of the file.

Connect the quantities

Connect the interior surface emissivities

Starting with the first surface module, in the line for `eps_in_1`, after

`four_layer_wall_1_o.eps_in_i,`

write

`,lw_rad_in_o.eps_surface_1.`

Repeat for all the other `eps_in_[k]`, with $2 \leq k \leq 5$.

Delete the lines for `eps_in_surface_[k]` from the long wave radiation module.

In the floor module, in the line for `eps_in_6`, after

`four_layer_floor_6_o.eps_in_i,`

write

`,lw_rad_in_o.eps_surface_floor.`

Delete the line for `eps_surface_floor` from the long wave radiation module.

In the window module, in the line for `eps_in_1_w1`, after

`two_pane_window_1_w1_o.eps_in_i,`

write

`,lw_rad_in_o.eps_surface_win.`

Delete the line for `eps_surface_win` from the long wave radiation module.

Connect the grey body radiation of the interior surfaces

Starting with the first surface module, in the line for `qstar_in_1`, after

`four_layer_wall_1_o.qstar_in_i,`

write

`,lw_rad_in_o.qstar_surface_1.`

Repeat for all the other `qstar_in_[k]`, with $2 \leq k \leq 5$.

Delete the lines for `qstar_in_surface_[k]` from the long wave radiation module.

In the floor module, in the line for `qstar_in_6`, after

`four_layer_floor_6_o.qstar_in_i,`

write

`,lw_rad_in_o.qstar_surface_floor.`

Delete the line for `qstar_surface_floor` from the long wave radiation module.

In the window module, in the line for `eps_in_1_w1`, after

`two_pane_window_1_w1_o.qstar_in_i,`

write

`,lw_rad_in_o.qstar_surface_win.`

Delete the line for `qstar_surface_win` from the long wave radiation module.

Connect the net long wave radiation gain of the interior surfaces

In the long wave radiation module, in the line for `qnet_1`, after

`lw_rad_in_o.qnet_1,`

write

`,four_layer_wall_1_o.qlw_in_obj_i.`

Repeat for the `qnet_[k]` with $2 \leq k \leq 5$.

Delete the lines for `qlw_in_obj_[k]` from the surface modules.

In the long wave radiation module, in the line for `qnet_floor`, after

`lw_rad_in_o.qnet_floor,`

write

`,four_layer_floor_6_o.qlw_in_obj_i.`

delete the line for `qlw_in_obj_6` from the floor module.

In the long wave radiation module, in the line for `qnet_win`, after

`lw_rad_in_o.qnet_win,`

write

`,two_pane_window_1_w1_o.qlw_in_obj_i.`

Delete the line for `qlw_in_obj_1_w1` from the window module.

Appendix C. Cooling Power

Radiant cooling elements extract heat from a room by cooling the air and by cooling the surfaces of the room envelope. The two effects can be described by a convection term

$$q_c = \alpha_c (t_{air} - t_{surface}) \tag{160}$$

and a radiation term

$$q_r = \sigma F_a F_e \left[\left(\frac{T_r}{100}\right)^4 - \left(\frac{T_p}{100}\right)^4 \right] \tag{161}$$

where

q_c is the heat transfer by convection [W/m^2]

α_c is the convective coefficient [W/m^2 K]

t_{air} is the room air temperature [°C]

$t_{surface}$ is the surface temperature [°C]

q_r is the heat transfer by radiation [W/m^2]

σ is the Stefan-Boltzmann constant [W/m^{2}K^4]

T_r is the mean radiant temperature of unconditioned surface [K]

T_p is the mean radiant temperature of cooled surface [K]

F_a is the configuration factor

F_e is the emissivity factor.

This shows that the overall heat extraction is a function of the temperature difference between the cooling panel and the room air and the temperature difference between the cooling panel and the other room surfaces.

Both the convection and radiation can be expressed by means of heat transfer coefficients. The combined heat transfer coefficient can be calculated using Glueck's empirical equation [26] based on measurements of cooled ceilings:

$$\alpha_{tot} = 8.92 (t_{air} - t_{surface})^{0.1} \tag{162}$$

where

α_{tot} is the sum of convective and radiant heat coefficient [W/m^2 K].

This equation assumes that the mean surface temperature of the room is close to the air temperature. With this assumption, the specific cooling power (per square meter) of a cooled ceiling becomes:

$$q_{tot} = 8.92 (t_{air} - t_{surface})^{1.1} \tag{163}$$

where

q_{tot} is the sum of convective and radiant heat transfer [W/m^2].

LAWRENCE BERKELEY LABORATORY
UNIVERSITY OF CALIFORNIA
TECHNICAL AND ELECTRONIC
INFORMATION DEPARTMENT
BERKELEY, CALIFORNIA 94720